Université d'Ottawa · University of Ottawa

The Effects of Heat-shock and Differentiation on Nuclear Structure / Functions in Mammalian Cellular Systems

Nisrine Haddad

Thesis submitted to the
Faculty of Graduate and Postdoctoral Studies
University of Ottawa
In partial fulfillment of the requirements for the
M.Sc. degree in the

Ottawa-Carleton Institute of Biology

Thèse soumise à
la Faculté des Études Supérieures et Posdoctorales
Université d'Ottawa
en vue de l'obtention de la maitrise ès sciences à

l'Institut de Biologie d'Ottawa-Carleton

Acknowledgements

I would like to thank my supervisor Dr. M. Paulin-Levasseur for her support and endless patience throughout this research project and throughout our acquaintance. I would also like to thank members of my committee, Dr. D. Johnson, Dr. M. McBurney and Dr. J. Vierula for always giving me advice when I needed it.

I acknowledge Dr. David Currie and Dr. Jeff Houlahan, as well as Cosette Choueiri for their indispensable help with statistical analysis. Also, I would like to thank Andrew Ochalski for his help with computer programs relating to my figures. Siba Haykal and Marie-France Rollin are University of Ottawa undergraduate students who worked in the lab of Dr. Paulin-Levasseur. They helped me with Western blotting. Siba Haykal also helped me with cell counts. Sébastien Clément, an Honours student in the lab of Dr. Paulin-Levasseur helped me with the analysis of the differentiation system using L6E9 cells.

I thank my colleagues in the department, past and present, for their advice and their sense of humor: Mehrdad, Parisa, Nicole, Sandra, Haude and especially Ariane Beauvais for all the time we spend together working or laughing. I would also like to thank my special friend Rani Gebara for his wonderful help and for his concern.

I appreciate enormously that Dr. M. McBurney permitted me to use his lab facilities to conduct analysis with the flow cytometer. I also thank endlessly Meena Abrol (ORCC), Irena Frenkel (ORCC) and Leigh Miller (ORCC) regarding the use of the flow cytometer: without them I could never do it.

Finally, I thank my family, both my parents and my brothers for their endless support, patience and love so I can accomplish my work to the best of my ability.

ABSTRACT

The nucleus is the site of important functions related to gene expression such as: DNA replication, DNA transcription, RNA splicing and nucleocytoplasmic shuttling. There is accumulating evidence suggesting that these functions are facilitated by an organization of the architecture framework within the nuclear space. The work delienated in this research thesis aims to achieve advances in understanding nuclear structure-function interrelationships.

Two natural physiological processes - heat-shock and differentiation - have been used in order to provide a clearer understanding of the "big picture" that links structure and functions together. I have performed experiments using mild or severe heat-shock on HeLa S3 cells and I differentiated L6E9 myoblasts into skeletal muscle fibers. Microscopic and biochemical analysis were used in order to assess the effects of heat-shock and differentiation on nuclear morphology. A series of antibodies specific to the nuclear periphery such as: lamin-associated-polypeptides, emerin, lamins A/C and lamin B were used to analyze structural changes that occurs at the nuclear periphery. Similarly, nuclear matrix antigens such as the proliferating cell nuclear antigen or PCNA, the nucleocytoplasmic shuttling protein 2A7, 2H12 and fibrillarin, two nucleolar proteins, were used as tools to assess structural changes that occur in the nuclear morphology.

The first step was to validate the heat-shock and differentiation systems. The effects of heat-shock, mild and severe, on HeLa S3 cellular growth and

survival was assayed. I observed cellular proliferation to be arrested. I also studied the effect of heat-shock on DNA replication using BrdU incorporation and observed this function to be drastically inhibited due to heat-shock. The effects of mild or severe heat-shock on the organization and the expression of nuclear proteins was assessed using immunofluorescence microscopy and quantitative analysis. I observed that mild or severe stress do not change the organization of antigens located at the nuclear periphery. However, a change in the distribution of internal nuclear antigens was observed. Mild and severe heat-shocks induced remarkable changes in the organization of 2A7 which may suggest a change in nucleocytoplasmic transport. A severe treatment also had an effect of the 2H12 antigen and reorganized the distribution of fibrillarin, which may indicate that the nucleolar structrure and functions are affected. The effect of a severe shock was also observed when a component of the splicing machinery was studied. The number of speckles characterizing this antibody diminished considerably in severely treated cells. This may indicate an effect on mRNA splicing. Quantitative analysis showed that the levels of LAP2β increase following mild and severe heat-shock. It was shown to be the only antigen at the nuclear periphery to undergo such changes. Quantitative analysis obtained for the other antigens indicated that the levels of 2A7 are reduced prominently following a severe shock. A mild treatment induces a reduction in the expression of 2H12. Thus, the effects of mild and severe heat-shocks on nuclear architecture are not always similar, indicating that possibly

there are at least two pathways by which these stresses function and affect nuclear morphology. This research also provides further evidence that nuclear structure and function are interconnected. For instance, HeLa S3 cellular proliferation and DNA replication are deeply affected by hyperthermia. However, qualitative and quantitative changes are not observed with all the antigens observed.

I also studied the effect of differentiation of L6E9 myoblasts into myotubes on nuclear structure. My data indicated that this differentiation system does not induce any reorganization in the proteins of the nuclear periphery. However, a redistribution of 1B4 is observed. This antigen reorganizes from its speckled distribution and spreads throughout the nucleoplasm excluding the nucleoli. Quantitative changes were observed for all antigens studied. All antigens of the nuclear periphery had a reduced level of expression.

TABLE OF CONTENTS

LIST OF ABBREVIATIONS

ATTC	American Type Culture Collection
BAF	Barrier-to-Autointegration Factor
BrdU	5-Bromo-2'-deoxy-Uridine
BSA	bovine serum albumin
CLN	cyclin
cs	coverslip
CY3	indocarbocyanine
ddH_2O	double distilled water
DFC	dense fibrillar component
DNase	deoxyribonuclease
DRB	5,6-dichloro-1-β-D-ribofuranosylbenzimidazole
DTT	dithiothreitol
ECL	enhanced chemiluminescence
EDMD	Emery-Dreifuss muscular dystrophy
EDTA	ethylene diamine tetra-acetic acid
ER	endoplasmic reticulum
FCS	fetal calf serum
FC	fibrillar centers
FITC	fluorescein isothiocyanate
GC	granular component
hnRNA	heterogeneous nuclear ribonucleic acid
hnRNP	heterogeneous nuclear ribonucleoprotein
HS	horse serum
Hsp	heat-shock protein
IMP	integral membrane protein
INM	inner nuclear membrane
LAP	lamin-associated protein
LMB	low magnesium buffer
mAB	monoclonal antibody
MEM	minimal essential medium
MHC	myosin heavy chain
MW	molecular weight
NM	nuclear matrix
NMP	nuclear matrix protein
NUMA	nuclear mitotic apparatus protein
ONM	outer nuclear membrane
pAB	polyclonal antibody
PAGE	polyacrylamide gel electrophoresis
PARP	poly (ADP-ribose) polymerase
PBS	phosphate buffer saline
PCNA	proliferating cell nuclear antigen
PI	propidium iodide

PMSF	phenylmethylsulfonylfluoride
rDNA	ribosomal DNA
rRNA	ribosomal RNA
RNase	ribonuclease
RNP	ribonucleoprotein
RPI	RNA pol I
RT	room temperature
SDS	sodium dodecyl sulfate
snRNA	small nuclear ribonucleic acid
snRNP	small nuclear ribonuceleoprotein particle
STM	sucrose-Tris-magnesium buffer
TT	thermotolerant
TCA	trichloroacetic acid

LIST OF FIGURES

LIST OF TABLES

I. INTRODUCTION

1. THE NUCLEAR COMPARTMENT

The nuclear compartment is the control center of the eukaryotic cell. It is comprised of an amalgam of chromatin-containing and chromatin-depleted domains, which together form a structural partnership essential for many nuclear functions. These include DNA replication, DNA transcription, RNA splicing, and nucleocytoplasmic transport of macromolecules.

The nucleus secures the genetic material and it is spatially separated from the cytoplasm. The nuclear envelope delimits the nuclear boundary and maintains the nuclear shape. It includes the inner nuclear membrane (INM) and the outer nuclear membrane (ONM), which are separated by the perinuclear space. Both membranes are joined together at the nuclear pore complexes. These macromolecular structures may be found in higher eukaryotic cells at numbers varying from 2000-4000 protein complexes per cell nucleus according to cell type (Gerace and Burke, 1988); they are responsible for the trafficking of macromolecules between the nucleus and the cytoplasm (Paine *et al.*, 1975; reviewed by: Stoffler *et al.* 1999). The outer nuclear membrane is continuous with the endoplasmic reticulum (ER) and is covered with ribosomes; its composition is similar to that of the ER. In contrast, the inner nuclear membrane has a distinct composition and is closely associated with the nuclear lamina and chromatin (reviewed by: Worman and Courvalin, 2000; Gruenbaum *et al.*, 2000).

The cell nucleus contains distinct substructures characterized by the absence of delimiting membranes; they are called nuclear compartments for three main reasons: A) each substructure is inhabited by defined "resident" proteins; B) they can be

identified by both light and electron microscopy; C) some substructures can be biochemically isolated in an enriched form (reviewed by: Dundr and Misteli, 2001). The discovery of these distinct nuclear dynamic compartments and the difficult question regarding the functional organization of nuclear space led to the hypothesis that a nuclear matrix defines nuclear architecture.

2. THE NUCLEAR MATRIX AND ITS STRUCTURAL COMPONENTS

The nuclear matrix, a universal feature of eukaryotic nuclei, is a dynamic proteinaceous structure that is associated with the functional organization of DNA into specific domains (reviewed by: Nelson *et al.*, 1986). When intact nuclei are subjected to a series of sequential extractions with nonionic detergents such as Triton X-100, followed by hypotonic (0.2 mM $MgCl_2$) and hypertonic (2 M NaCl) salt treatments, as well as DNase I and RNase I digestion, an insoluble residual proteinaceous structure termed the nuclear matrix or karyoskeleton is obtained (Berezney and Coffey, 1974, 1976, 1977; reviewed by: Pederson, 1998; Nelson *et al.*, 1986). Its content varies between 85-95% proteins and 5-15% nucleic acids (reviewed by Bosman, 1999). The nuclear matrix resembles the nucleus in size and shape. It is also composed of the nuclear lamina, the nucleolar remnants and an internal fibrillogranular network. Berezney and Coffey (1974, 1975) were the first to predict that the nuclear matrix facilitates nuclear functions and, thus, to recognize it as a functional entity. Since then, it has been a persistent suggestion that the nuclear matrix is implicated in replication and transcription of DNA, as well as processing of RNA molecules and their transport into the cytoplasm (reviewed by: Berezney, 1991; Nickerson, 1998; Pederson, 1998; Marshall *et al.*, 1997).

2.1. The nuclear lamina

The nuclear lamina is an insoluble filamentous meshwork apposed to the inner nuclear membrane (Dessev, 1992; Gerace and Burke, 1988; reviewed by: Worman and Courvalin, 2000; Gruenbaum *et al.*, 2000). This proteinaceous structure may provide an architectural framework to the nuclear envelope. The major proteins constituting the nuclear lamina are the nuclear lamins; they are type V intermediate filaments. In vertebrate cells, nuclear lamins are divided into two types: type A and type B, based on the differences in their biochemical properties, primary sequence and expression patterns. Type A lamins have a developmentally regulated and cell type-specific expression pattern (Fisher *et al.*, 1986; McKeon *et al.*, 1986; reviewed by: Franke, 1987; Bosman, 1999) while type B lamins are widespread in every cell (reviewed by: Bosman, 1999). These two types also possess different localization in the cell during mitosis. While type A lamins become completely soluble in the cytoplasm, type B lamins remain associated with nuclear membranes. In vertebrate genomes, there is one lamin A gene that codes for 4 known proteins by alternative splicing: lamins A, AΔ10, C_1, and C_2. There are two lamin B genes coding for 3 known proteins: lamin B_1, B_2 and B_3, the latter being a splice variant of the B_2 gene. Lamins B_3 and C_2 are specific to germ cells (Furukawa and Hotta, 1993; Furukawa *et al.*, 1994; reviewed by Gruenbaum *et al.*, 2000). Lamins bind directly to DNA and evidence suggests that the nuclear lamina acts as an anchoring site for interphase chromosomes (Nigg, 1992; Benavente and Krohne, 1986; Gerace and Burke, 1988; Ulitzur *et al.*, 1992). Lamins are peripheral proteins and lack membrane-integrated domains (Dessev, 1992). The interaction between the nuclear lamina and the inner nuclear membrane could be mediated by

post-translational modifications of lamin isotypes or by non-lamin integral membrane proteins. Most lamins, such as lamin A, lamins B1 and B2 are post-translationally modified by farnesylation of a carboxyl-terminal "CaaX"motif and this lipid moiety is crucial for membrane association of these proteins (reviewed by: McKeon, 1991; Worman and Courvalin, 2000). Integral membrane proteins (IMPs) include lamin-B receptor (LBR), lamin-associated proteins (LAPs)1, LAPs2/thymopoietins (TPs), emerin, MAN1 antigen (reviewed by: Chu *et al.*, 1998; Lin *et al.*, 2000), nurim and UNC-84 (reviewed by: Gruenbaum *et al.*, 2000; Wilson *et al.*, 2000) (figure 1). Protein sequence analysis showed that LAP2/TPβ, emerin and MAN1 share a conserved globular domain that has been termed the LEM module - for LAP2, emerin and MAN1. All these proteins therefore are now known to be members of the LEM family (Lin *et al.*, 2000).

LBR was the first integral inner nuclear membrane protein to be identified; it has a nucleoplasmic amino-terminal domain of 200 amino acids. It has been shown to bind B-type lamins and chromatin proteins (reviewed by: Wilson, 2000). Its amino-terminal domain is followed by a hydrophobic region with 8 putative transmembrane segments (figure 1).

Two different monoclonal antibodies contributed in identifying two other protein families of the inner nuclear membrane. Senior and Gerace (1988) discovered the existence of lamina associated polypeptides: LAP1A, 1B and 1C. In 1993, Foisner and Gerace showed that both LAP1A and LAP1B bind to lamin A, C and B_1. LAP1C has a simpler structure than LBR with an amino-terminal domain followed by a single transmembrane segment (Martin *et al.*, 1995); both other LAP1 isoforms possess a similar structure. All three polypeptides arise by alternative RNA splicing (Worman and

Figure 1: Schematic representation showing a simplified version of some integral inner nuclear membrane proteins. Some polypeptides have different isotypes and may interact with chromatin and nuclear lamins. LAP2β, Emerin and MAN1 possess the conserved LEM module.

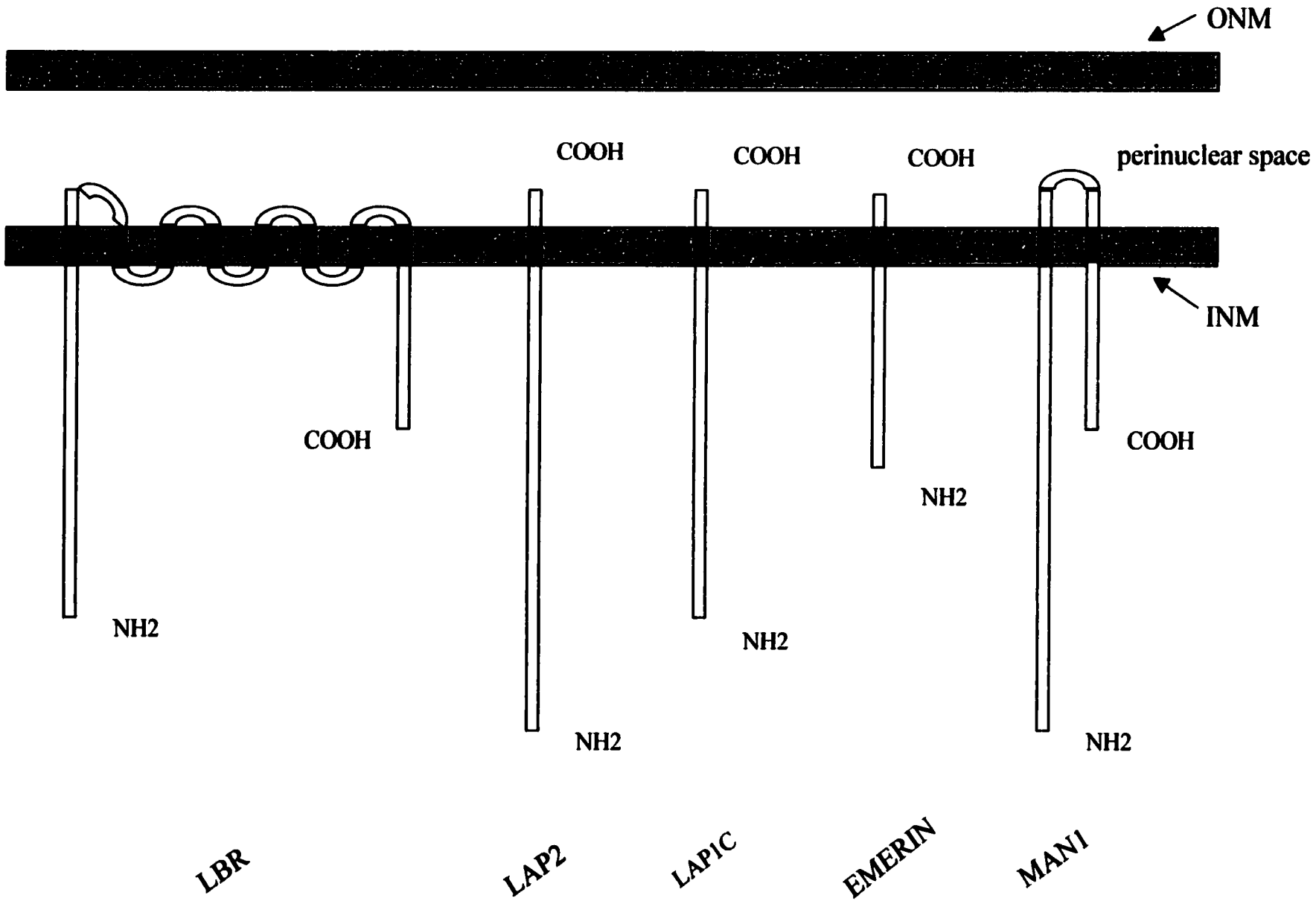
ONM
perinuclear space
INM
COOH
COOH
COOH
COOH
COOH
NH2
NH2
NH2
NH2
NH2
LBR
LAP2
LAP1C
EMERIN
MAN1

Courvalin, 2000; Martin *et al.*, 1995). The second monoclonal antibody recognized several LAP2 isoforms (Foisner and Gerace, 1993). DNA cloning and sequencing of alternatively spliced mRNAs led to the identification of three major LAP2 isoforms: α, β and γ (Furukawa *et al.*, 1995).

While all LAP1 isoforms label the inner nuclear membrane, LAP2 isoforms differ in their distribution within the nucleus. Although all three proteins possess identical amino-terminal domains, LAP2α does not contain a transmembrane segment. It diffusely stains the nucleoplasm, excluding the nucleoli (Dechat *et al.*, 1998). LAP2 β and γ are type II integral membrane proteins with one transmembrane domain (Furukawa *et al.*, 1995; reviewed by: Worman and Courvalin, 2000). LAP2β was first identified and cloned in rat (Foisner and Gerace, 1993; Furukawa *et al.* 1995). It has been shown to bind lamin B_1 and associates with chromatin in dependence with mitotic phosphorylation (Foisner and Gerace, 1993). This protein accumulates at the surface of chromosomes prior to B-type lamins during the reassembly of the nuclear envelope in late anaphase (Foisner and Gerace, 1993). Furukawa (1999) used the nucleoplasmic domain of LAP2β as a bait in a yeast two-hybrid screen. He intended to isolate a LAP2 interacting protein, which was identified as rat L2BP1 or LAP2 binding protein 1. Sequence analysis has confirmed that this protein is 98% and 97% identical to mouse and human BAF (Barrier-to-Autointegration Factor) cloned from mouse and human cells (Lee and Craigie, 1998). BAF is a cellular trans-acting factor involved in protecting the reverse-transcribed Molony murine leukemia viral DNA against autointegration. It binds DNA with no sequence specificity (Lee and Craigie, 1994; 1998). The L2BP1/BAF

binds LAP2β in the first 186 amino acids common to the LAP2 family of proteins. This binding site may have a role in the association with chromatin and chromosomes. The interaction between LAP2β and L2BP1/BAF may be required for nuclear dynamics during the mammalian cell cycle (Furukawa, 1999).

Emerin is a 34 KDa inner nuclear membrane protein responsible for the X-linked Emery-Dreifuss muscular dystrophy. It is absent from the inner nuclear membrane in most patients with this disease (Manilal *et al.*,1996; Nagano *et al.*, 1996; reviewed by: Wilson, 2000). Similar to LAP1 isoforms and LAP2β and γ, emerin has one nucleoplasmic amino-terminal domain followed by a single transmembrane segment and a short carboxyl-terminal tail in the perinuclear space and the ER lumen (reviewed by: Worman and Courvalin, 2000).

2.2. <u>The nucleolar remnants</u>

The membrane-less nucleolus is a dynamic structure. Three main nucleolar structural components are recognized by thin section electron microscopy. The roughly globular *fibrillar centers (FC)* are surrounded by the *dense fibrillar component (DFC)*, which in turn is enclosed by the *granular component (GC)*, found at the nucleolar periphery. Being the site of ribosome synthesis, the nucleolus coordinates the transcription of ribosomal RNA (rRNA) genes, the processing of their transcripts and their packaging with ribosomal proteins (reviewed by: Bosman, 1999; Scheer and Benavente, 1990; Schwarzacher and Wachtler, 1993). Several nucleolar proteins involved in ribosomal DNA (rDNA) transcription and rRNA processing, as well as in the maturation, assembly and transport of preribosomal particles have been identified in the nucleolar remnants. It seems that factors involved in the early stages of ribosomal

biosynthesis are found in the FC and/or the DFC, while ones that have roles in latter assembly stages are found in the GC. Among the proteins involved in the early stages, DNA topoisomerase I and II are required for the relaxation of the superhelical coiling of DNA; RNA polymerase I (RPI) is involved in rRNA synthesis; fibrillarin binds to U3 small ribonuclear RNA (snRNA) and is an important factor for the early steps of rRNA processing; nucleolin (C23) has roles in rDNA transcription, rRNA processing, and in the regulation of preribosome production; the upstream binding factor (UBF) to RPI has a role in rRNA transcription; ribogranulin, a 52 KDa protein associated with U3 snRNA is important for rRNA processing (reviewed by Bosman, 1999). Mostly found in the GC, B23 (also called numatrin) is essential for latter stages of ribosomal assembly; it is an RNA associated phosphoprotein found with mature preribosomal RNP and is involved in the transport of preribosomes to the cytoplasm (reviewed by Schwarzacher and Wachtler, 1993).

2.3. <u>The internal fibrillogranular network</u>

The internal nuclear matrix as revealed by electron microscopy consists of fibers known as perichromatin fibres, and of granules or interchromatin granules surrounded by chromatin-depleted regions (reviewed by: Bosman, 1999). This fibrillogranular network is composed of proteins such as the nuclear mitotic apparatus protein (NuMA), a very large molecule that may have a role in the organization of the nuclear matrix. The existence of protein kinases in this nuclear infrastructure may indicate the presence of an intranuclear regulatory signaling pathway (reviewed by: Bosman, 1999). Analyses by two-dimensional gel electrophoresis have allowed the identification of 12 members of the matrin family of proteins (Bosman, 1999; Nakayasu and Berezney, 1991). Matrin

250 is identical to a form of RNA polymerase II and evidence suggests its association with splicing complexes *in vivo*. Other internal matrix proteins involved in splicing of pre-mRNA include the splicing factor SC35 and small nuclear ribonucleoproteins or snRNPs (five types: U1, U2, U4-U6 have been identified so far). All have been shown to localize into interchromatin granules or "speckles" connected by the perichromatin fibrils; splicing would occur in parallel with transcription alongside the perichromatin fibrils where RNA polymerase II is found (Bosman, 1999; van Driel *et al.*, 1995). Labeled nascent DNA appears to be associated with the nuclear matrix. DNA replication activity seems to be organized in hundreds of small domains scattered throughout the nucleus. Wansink *et al.* (1994) studied the spatial distribution of these domains: apart from being responsible for replicating DNA, these domains also contain cyclins, DNA methyltransferase, components of the replication machinery and proliferating cell nuclear antigen (PCNA) (reviewed by: Bosman, 1999). PCNA is a nuclear protein, first identified as cyclin (Miyachi *et al.*, 1978). It has a molecular weight of 36 KDa, and its synthesis is required for cell cycle progression (Baserga, 1991). The levels of cyclin/PCNA increase during the S phase of the cell cycle (Bravo and Celis, 1980; Bravo *et al.*, 1982). It is used as a marker for replication foci. PCNA has been cloned and sequence analysis shows that it possesses homology with DNA binding proteins (Almendral *et al.*, 1987; Matsumoto *et al.*, 1987). PCNA forms a homotrimeric ring around the DNA, thus it ensures high processivity (Wyman and Botchan, 1995; Jonsson and Hubscher, 1997; Kelman and Hurwitz, 1998). It has been shown using GFP-PCNA in live cells that replication foci assemble and disassemble in an asynchronous manner throughout S phase (Leonhardt *et al.* 2000).

Another protein of the fibrillogranular network, p160, was characterized by De Graaf *et al.* (1992). p160 is associated with the internal nuclear matrix and is extranucleolar in rat, mouse and human cells. In control cells, immunoelectron microscopy showed that p160 is diffusely associated with the fibrillogranular network of the nuclear matrix. This antigen has been shown to reorganize upon heat-shock. A mild treatment at 42°C for 3 hours resulted in a spotted staining of (2-10) large clusters and a large number of relatively small spots.

3. NUCLEAR ENVELOPE AND NUCLEAR MATRIX ANTIGENS IN DISEASES

It is recognized now that nuclear proteins serve more than providing a structural framework to maintain the size and the shape of the nucleus. There is also greater evidence that nuclear envelope proteins are involved in muscular dystrophy (reviewed by Wilson, 2000). Nuclear matrix antigens cause human tumors due to their overexpression (Hughes and Cohen, 1999).

The Emery-Dreifuss muscular dystrophy (EDMD) can be X-linked recessive or autosomal dominant. The loss or the improper targeting of emerin to the nuclear membrane causes the first form. The latter is due to mutations in the gene that encodes lamins A and C (Wilson, 2000; Bonne *et al.*, 1999). Patients with EDMD suffer from a slow degeneration of cardiac and skeletal muscle, as well as early contractions of the ankles, the elbows and the neck. There is evidence that loss of lamin expression leads to growth retardation and results in the development of muscular dystrophy (Wilson, 2000; Sullivan *et al.*, 1999). This phenotype is characterized by structural changes to the nuclear envelope such as an improper localization of emerin to the inner nuclear membrane (Sullivan *et al.*, 1999). For instance, reduced lamin Dm0 expression

in *Drosophila* will cause impaired locomotion and neuromuscular defects (Lenz-Bohme *et al.*, 1997); this is the muscular dystrophy in invertebrates. The loss of this lamin isotype will result in a lack of interaction between chromatin and the nuclear envelope, the clustering of nuclear pore complexes and subsequently cell death (reviewed by: Wilson, 2000). As mentioned above, nuclear lamins, the nuclear envelope and its proteins are tightly interactive: a relationship that is essential for nuclear functions. An interesting point is that both emerin and lamins A/C are found in many tissues; however, EDMD affects muscle cells only. One of the hypotheses suggests that muscle cells are more prone to physical damage of nuclei due to contractions. Also, in contrast to other tissues, skeletal and cardiac muscle cells express lamins A/C and lamin B2 but lamin B1 is not expressed (Wilson, 2000; Manilal *et al.*, 1999). Thus lamins A/C might be indispensable tools for anchoring emerin to the nuclear envelope. A mouse model for EDMD was created by experimental knockout of the gene that encodes lamins A/C (Wilson, 2000; Sullivan *et al.*, 1999). Knockout mice start developing muscle wasting and contractures similar to EDMD by 3-4 weeks and die by 8 weeks after birth. Derived cell lines for these lamin-A/C-null mice indicated that emerin is found in the ER and not at the nuclear envelope, while lamin B2, LAP2 and pore complexes show a normal distribution. This is an indication that lamins A/C play a major role in retaining emerin at the inner membrane (reviewed by: Wilson, 2000).

Since its discovery, the concept of the nuclear matrix has been metamorphosed from a structural entity to a dynamic family of proteins. It is well established that alterations in the composition or function of nuclear matrix proteins (NMPs) results in

different disorders. The nuclear matrix protein profile undergoes metamorphogenesis during cellular differentiation, apoptosis, and cell division (reviewed by Hughes and Cohen, 1999). Khanuja *et al.* (1993) used normal human breast tissue and breast tumors to study the differences in composition in NMPs. They extracted NMPs from tumor tissues of 10 patients; they also extracted NMPs from breast cancer cell lines and from normal human breast tissue. They demonstrated that normal and tumoral proteins share many of the same proteins. However, some NMPs were exclusively found in tumors but not in normal tissue.

4. HYPOTHESIS AND OBJECTIVES

Accumulating evidence indicates that nuclear functions are facilitated by a defined organization of chromatin and nuclear space. This might be due to dynamic interactions of chromatin with components of the inner nuclear membrane and nuclear internal matrix. This has led many researchers to formulate the following hypothesis: new adaptations in the physiological state of the nucleus should be accompanied by changes in the organization and/or composition of the nuclear matrix and the nuclear envelope (Moir *et al.*, 2000).

My research project aims at deciphering such relationships. Antigens associated with the nuclear envelope such as LAPs, emerin and lamins will serve as markers for analyzing any structural change that occurs at the nuclear periphery. Similarly, nuclear matrix antigens like P160, PCNA, 2H12, 2A7 and 1B4 will serve also as markers for assessing structural changes in the organization and/or composition of the nuclear interior. Two naturally occurring processes, hyperthermia and cell differentiation, will be exploited to reach these objectives.

5. RESEARCH STRATEGY

5.1. Nuclear envelope and nuclear matrix antigens

Changes that occur in the organization of the nuclear envelope and nuclear matrix protein organization during heat shock and during differentiation will be monitored using antibodies specific to different nuclear domains (Table 1). The labeling of the nuclear periphery will require specific antibodies directed to LAP2/TPβ, LAP1C, emerin, lamins A/C and lamin B1. Likewise, the fibrillogranular protein P160, the PCNA antigen involved in cell cycle progression, the nucleolar antigens 2H12 and fibrillarin, the nucleoplasmic 2A7 shuttling protein, as well as the 1B4 antigen associated with the splicing machinery are internal nuclear matrix proteins and will be probed with specific antibodies. All these antigens are resident in different nuclear compartments and will offer a better look at the "big picture" of nuclear organization and structure. They may provide significant leads into the structure/functions relationships of the nucleus. Fibrillarin is a highly conserved protein involved in rRNA processing. It is found in mammalian cells, frogs, slime mold, yeast and plants. It is a 34 KDa protein localized in the dense fibrillar component of interphase nucleoli and in coiled bodies or Cajal bodies. In 1991, Ochs and Smetana studied the behavior of fibrillarin in the nucleolar remnants of the nuclear matrix. HeLa S3 cells were processed for *in situ* nuclear matrix preparations. Fibrillarin remained associated with residual nucleolar structures following digestion with nucleases (DNase I and RNase A) and extraction with high salt concentrations.

The 2H12, the 2A7 and the 1B4 antigens were first characterized by Paulin-Levasseur *et al* (1995; 1997; 1999). The 2H12 antigen is a non-shuttling 40 KDa

Table 1: List of the antigens studied in HeLa S3 cells and / or L6E9

Antigen	Function	Location	Cell line
Hsp70	Chaperone	Cytoplasm and Nucleoplasm	HeLa S3
Myosin	Cell motility	Cytoplasm	L6E9
Myogenin	Transcription factor	Nucleoplasm	L6E9
LAP1C	Structural	Nuclear envelope	L6E9
LAP2beta	Structural	Nuclear envelope	Both
Emerin	Structural	Nuclear envelope	Both
Lamins A/C	Structural	Nuclear envelope	Both
Lamin B	Structural	Nuclear envelope	Both
2H12	Structural	Nucleolus	HeLa S3
Fibrillarin	rRNA processing	Nucleolus	HeLa S3
PCNA	Proliferation	Nucleoplasm	Both
2A7	Nucleocytoplasmic shuttling	Nucleoplasm	HeLa S3
P160	Unknown	Nuclear matrix	HeLa S3
1B4	Structural	Speckles	Both

nuclear matrix human nucleolar protein, a phosphorylated variant of the human nucleolar protein B23 (Paulin-Levasseur *et al.*, 1995). The behavior of this antigen was monitored throughout all the steps of in *situ* nuclear matrices from HeLa cells using immunofluorescence microscopy. The antigen resisted the extraction with low and high salt solutions and the digestion with DNase I and RNase A. So it is tightly associated with the nucleolar skeleton (Paulin-Levasseur *et al.*, 1995). The 2A7 antigen is an 85 KDa human nucleocytoplasmic shuttling protein that resides throughout the nucleoplasm during interphase and becomes associated with condensed chromosomes during mitosis (Paulin-Levasseur and Julien, 1999). The authors studied the behavior of the 2A7 antigen during *in situ* isolation of nuclear matrices from HeLa cells. The nucleoplasmic fraction of this antigen was extracted after treatments with detergent and salts whereas the nucleolar fraction resisted detergent, salt extraction, and DNase digestion. The nucleolar fraction of the 2A7 antigen was rendered labile upon RNase treatment of residual nuclear matrices. These results indicated that the 2A7 antigen would be present in a labile form in the nucleoplasm; however, it is associated with the karyoskeletal framework of nucleoli through interactions with RNA moieties. The1B4 antigen is distributed throughout the nucleoplasm - excluding the nucleolus - into 20-30 distinct speckles. Its distribution resembles that of the non-snRNP SC35 factor (Luus and Paulin-Levasseur, 1997). 1B4 was identified as a component of the nuclear matrix. HeLa cells were processed for *in situ* nuclear matrix preparations with low and high salt solutions, and subsequent digestions with DNase I and RNase A. 1B4 maintained its speckled distribution (Luus and Paulin-Levasseur, 1997).

5.2. Cellular systems

HeLa S3 cells are derived from human HeLa cells. They are human cervix carcinoma epithelial cells (CCL2.2) (American Type Culture Collection, ATCC; Rockville, Md). This cell line is readily grown in culture. It can be grown in suspension or on a substrate and is universally used. Both HeLa and HeLa S3 cells have been used extensively in earlier and more recent studies relating to the stress response. For example, an early study by Blair *et al.* (1979) used flow cytometric analysis to study the effect of hyperthermia on the protein content of HeLa cell nuclei. HeLa cells were heated for 7.5, 15, or 30 minutes at 45°C; their nuclei were isolated, fixed and stained with fluorescein isothiocyanate (FITC). Flow cytometric analysis showed a higher protein content in cells exposed to heat for longer times. Another group (Chiodi et al., 2000) used HeLa cells to study the redistribution of a heterogeneous nuclear ribonucleoprotein (hnRNP) called hnRNP A1 interacting protein (HAP) (Weighardt *et al.*, 1999) upon induction of heat-stress. HAP is identical to Scaffold Attachment Factor B (SAF-B), a protein of the nuclear scaffold and to HET (for Hsp27-ERE-TATA-binding protein), a transcriptional regulator of the gene coding for heat shock protein 27 (Hsp27) (Weighardt *et al.*, 1999). HAP bodies are formed in human cell nuclei following heat-shock and are storage sites of transcripts in the form of perichromatin granules.

L6E9 myoblasts are an indispensable *in vitro* system for analyzing muscle cell proliferation and differentiation (reviewed by: Lawson and Purslow, 2000). Developmental processes leading to muscle differentiation include mechanisms leading to cell specification, differentiation and morphogenesis (reviewed by: Nay and Olson, 1999). The L6E9 cell line offers as a cultured system all of the features of muscle

myogenesis, including myoblast proliferation, migration, cell fusion, myotube formation and contraction (reviewed by: Lawson and Purslow, 2000). In our studies, L6E9 myoblasts were differentiated into multinucleated myotubes for 9 days.

5.3. Hyperthermia

Cells subjected to environmental, chemical and physiological stress respond by a rapid increase in the expression of a highly conserved group of proteins, called heat-shock proteins or Hsps. Ritossa (1962) discovered this form of cellular protection in *Drosophila melanogaster*. He observed the induction of specific chromosomal puffs in the polytene chromosomes of this organism upon exposure to elevated temperatures and chemical treatment (reviewed by: Cotto and Morimoto, 1999). The expression of Hsps is regulated by environmental stress (i.e., hyperthermia), physiological stress (i.e. ischaemia) and non-stressful conditions (i.e. differentiation) (reviewed by: Cotto and Morimoto, 1999). Some of these conditions, such as heat shock, may induce protein denaturation and/or aggregation. The cell protects itself by inducing the expression of Hsps. They have been classed into several families according to their molecular mass. Each family member plays an essential role as a molecular chaperone; their function might include protein synthesis, protein translocation to different cellular compartments, or protein folding and degradation (reviewed by: Cotto and Morimotto, 1999). DiDomenico *et al.* (1982) demonstrated that the heat shock response is self-regulated at both the transcriptional and post-transcriptional levels. This group heat-shocked Drosophila cells at 37°C and monitored the expression of the major heat-induced proteins in these cells, Hsp70. The expression of this protein is quantitatively correlated with the degree of stress. The level of protein synthesis is controlled transcriptionally

(repression of Hsp70 mRNA synthesis) and post-transcriptionally (destabilization of Hsp70 transcripts).

Heat shock affects different cellular processes. It has been shown that a mild heat shock treatment (42.5°C) causes structural changes of the nuclei and chromatin in human HeLa cells. There is an inhibition of major nuclear functions such as mRNA splicing and nucleocytoplasmic transport (Bond, 1988). There is a significant decrease in transcription and processing of non-heat shock genes, while heat shock gene expression increases (Welch and Suhan, 1986). Heat shock proteins (Hsps) are found in bacteria, plant, yeast and mammals (reviewed by Sharp *et al.*, 1999). Some of them are expressed constitutively. These molecular chaperones are involved in protein folding and their subsequent translocation across membranes (reviewed by: De Maio, 1999). Others proteins known as inducible Hsps are involved in cell protection upon protein denaturation due to stress such as hyperthermia (reviewed by: Cotto and Morimoto, 1999). It has been proven that a severe heat shock treatment (45°C) blocks the mRNA transport pathway in *Schizosaccharomyces pombe* and induces accumulation of poly(A) RNA in nucleoli (Tani *et al.*, 1995).

Earlier studies about the localization of Hsp70 demonstrated that this antigen is present in the nucleus and the cytoplasm at basal levels in untreated cells. Its expression increased upon heat shock with a noticeable accumulation in the nuclei and nucleoli (LaThangue, 1984; Pelham, 1986; Welch and Feramisco, 1984). Ohtsuka *et al.* (1986) investigated the intracellular localization of Hsp70 in HeLa cells by immunofluorescence after methanol fixation. In control cells, diffuse staining of the cytoplasm but not the nuclei was observed. When cells were heat shocked for 2-4h at

42°C, the nucleoli became stained. At 6-9 hours post-treatment, the staining became cytoplasmic again. Welch and Mizzen (1988) studied the expression of Hsp70 in non-tolerant and thermotolerant HeLa cells previously given a mild heat shocked treatment. They established a comparison of Hsp70 expression in thermotolerant and nontolerant cells before and after a severe heat shock at 45°C for 30 minutes. Their results indicated a faster migration of Hsp70 into the nucleolus of thermotolerant cells. The occurrence of cellular stress is tightly linked to the occurrence of cellular apoptosis (reviewed by Garrido *et al.*, 2001). Novel research has indicated that Hsps may serve as apoptotic modulators, or inhibitors. It seems that the Hsp27 and the Hsp70 families play a role in preventing apoptosis, and as a result cause a problem for cancer therapy (reviewed by Garrido *et al.*, 2001).

Preliminary observations by Paulin-Levasseur and Julien (1999) have indicated that, upon exposure of cells to mild heat shock treatment (42.5°C), there is redistribution of nuclear matrix antigens. For example, the 2A7 antigen, which is distributed throughout the nucleus under normal circumstances, was seen to accumulate in nucleoli. Lutz *et al.* (1988) demonstrated that two proteins associated with hnRNPs have an altered distribution upon severe heat shock treatment HeLa cells. More recently, Lavoie *et al.* (1999) have shown that heat shock caused alterations in phosphorylation of the largest subunit of RNA polymerase II in different cell types. Recent studies by Chaly and Stochaj (1999) demonstrated that circumferin, a non lamin protein that localizes at the nuclear periphery in interphase nuclei, is redistributed between the nucleoplasm and the cytoplasm in both HeLa and yeast cells upon heat shock.

5.4. Differentiation

Skeletal muscle differentiation is a multi-step process. L6E9 cycling rat myoblasts are mononucleated muscle precursor cells that fuse into postmitotic multinucleated fibers called myotubes. This cell fusion is accompanied with cessation of DNA synthesis (Yaffe, 1968). Certain studies have demonstrated a remodeling of the nuclear periphery during muscle cell differentiation *in vitro*. Chaly et al. (1996) have studied the distribution of nuclear lamins during L6E9 myogenesis. They found that the expression of both type A and type B lamins increase prior to extensive cell fusion. A review by Chaly and Stochaj (1999) discussed that statin, which localizes at the nuclear periphery, is absent from primary culture of newborn rat myogenic precursors but is present when myocytes begin to fuse (Connolly *et al.*, 1988). Statin was identified in earlier studies by Wang and Krueger (1985): this 57 KDa protein stains the nuclei and is specific to non-cycling cells. This protein disappears in cells re-entering the cell cycle (Wang and Krueger, 1985). Wang and Krueger (1985) also demonstrated that statin is absent from proliferating populations, but is present in nonreplicating differentiated cells such as cardiomyocytes. The same group showed that the disappearance of a cyclin-like protein and the appearance of statin are correlated with the onset of differentiation during myogenesis (Connolly *et al.*, 1988).

II. MATERIALS AND METHODS

1. TISSUE CULTURE

HeLa S3 cells were obtained from the American Type Culture Collection (ATCC: CCL2.2; Manassas, VA, USA). L6E9 cells were kindly provided by Dr. Michael McBurney (Cancer Research Laboratories, Faculty of Medicine, University of Ottawa). Both cell lines were cultured in α-modified Eagle's minimal essential medium (α-MEM; GIBCO BRL, Burlington, Ontario, Canada) supplemented with 10% fetal calf serum (FCS; GIBCO BRL), and 1% antibiotics (50U/ml penicillin and 50 µg/ml streptomycin; GIBCO BRL). Cells were grown in a humidified incubator at 37°C and 5% CO_2 and passaged every two days. HeLa S3 cells were grown at a density of $1X10^6$ per $100mm^2$ dish (Corning; Fisher Scientific Limited, Nepean, ON, Canada).

To differentiate L6E9 cells into myotubes, cells were plated at a density of $4X10^5$ per $100mm^2$ dish and grown for 24 hours. The medium was then changed and replaced with one containing 10% heat inactivated horse serum (HS; GIBCO BRL) for 9 days. Cells were nourished every two days with 2ml of this medium.

2. HYPERTHERMIA TREATMENTS AND VIABILITY TESTS

Forty-eight hours after seeding, HeLa S3 cells were subjected to mild (42°C) and severe (45°C) heat shock treatments for 90 minutes using a Haake Circulator (Fisher Scientific Limited, kindly provided by Dr. Donal Hickey, Department of Biology, Faculty of Science, University of Ottawa, Ottawa). Prior to heat-shock, the old medium was replaced by new medium (pre-warmed at 37°C in all dishes). Petri dishes were then surrounded with parafilm and placed to float in the water bath at the appropriate temperature. Viability of control and heat-shocked cells was assayed using Trypan blue

exclusion (Celis, 1990). This series of tests was also performed on cells allowed to recover from heat-shock treatments at 37°C for different time lengths. In all cases, cells suspended in the cultured medium and cells attached to the petri dishes were harvested together and used in the count.

3. FLOW CYTOMETRY

3.1. PI staining and flow cytometry

Control HeLa S3 cells, cells subjected to mild (42°C) or severe (45°C) heat shock treatments for 90 minutes, and cells allowed to recover at 37°C were collected and assayed using Trypan blue exclusion as described above. Cells were then washed twice with phosphate buffer saline (PBS; 1.3 mM NaCl, 50 mM Na_2HPO_4, 15 mM KH_2PO_4, pH 7.0) and resuspended in 500 µl of this buffer. To fix cells, 5 ml of cold ethanol were added slowly to the suspension while vortexing, to prevent clumping. Cells remained in the fixative until used. When needed, cells were collected by low speed centrifugation twice in PBS containing 1% bovine serum albumin (BSA) and resuspended in 800 µl of this solution. To each sample, 100 µl of a 10X propidium iodide (PI) solution (500 µg/ml in $3.8X10^{-2}$ M sodium citrate, pH 7.0) was added to the cells. Boiled RNase A (10 mg/ml prepared in 10 mM Tris-HCl, pH 7.5) (RNase A; Sigma, St Louis, Mo) was added at a quantity of 100 µl / sample. The stained cells were incubated at 37°C for 30 minutes prior to analysis.

Cell cycle distribution was then measured using a LSR flow cytometer (Becton Dickinson, Franklin Lakes, New Jersey, USA). For DNA analysis, a 488 nm Argon laser and a F12 detector equipped with 575/26 BP filter was used. For acquisition of analysis, CellQuest software was used.

3.2. BrdU labeling, PI staining and flow cytometry

5-Bromo-2'-deoxy-Uridine (BrdU, labeling and detection kit 1) (Roche Diagnostic Inc., Indianapolis, IN, USA) was added directly to the medium of the cell population at a final concentration of 10 µM. The plate was rocked gently and incubated at 37°C for 30 minutes. Afterwards, the cells were rinsed twice with PBS and collected at the appropriate times by trypsinization. The culture was then resuspended in 5 ml of medium and centrifuged for 5 minutes at 500g in a refrigerated centrifuge at 5°C. The cell pellet was then resuspended in BSA (1% in PBS) at room temperature (RT) and centrifuged for 5 minutes. The pellet was then resuspended in PBS on ice, added dropwise to 5 ml of 70% ethanol pre-cooled at –20°C, and kept on ice for 30 min before another spin. The supernatant was aspirated carefully and the pellet was loosened by vortexing. One ml of 2N HCL/Triton X-100 (0.5%) (BDH, Ville St-Laurent, Quebec, Canada) was added to the fixed cells while vortexing, and the cell suspension was incubated at R.T. for 30 minutes. Following centrifugation, the pellet was resuspended in 1 ml of 0.1M $Na_2B_4O_7$ to neutralize the acid. The cell suspension was centrifuged again and mixed well in 1 ml of cold ethanol, stored at –20°C until ready to be labeled and to run flow cytometry.

When needed, cells were centrifuged and resuspended in 50 µl of Tween 20/BSA/PBS (0.5% and 1% respectively). Twenty µl of anti-BrdU (BrdU labeling and detection kit 1) used at 1:50 were added to the cell populations and incubated for 30 minutes at room temperature. Cells were then incubated with a FITC-conjugated polyclonal goat anti-mouse IgG (Jackson Immunoresearch, West Grove, Pa. USA) at 1:150 for 30 minutes and kept in the dark. Cells were then centrifuged for 5 min. at R.T.

and resuspended in 1 ml of PBS containing 5 µg/ml of propidium iodide. Samples were then run through in the flow cytometer. RNase A was added for cells not stained with BrdU and used as controls. The other samples did not require RNase A since they were already mixed with the primary antibody (BrdU labeling and detection kit 1).

4. PROTEIN EXTRACTION

In all cases, whole cell extracts were prepared for sodium dodecyl sulfate polyacrylamide gel electrophoresis (SDS-PAGE). HeLa S3 cells were solubilized in SDS- sample buffer 2X (2XSB) (Laemmli, 1970): $1X10^6$ cells were solubilized in 250 µl 2XSB.

L6E9 myoblasts and L6E9 myotubes were collected and resuspended in 1 ml of 10% trichloroacetic acid (TCA) and incubated at 40°C for 15 minutes. The protein precipitate was collected by low-speed centrifugation and washed with 5% TCA and 99% acetone. Proteins were solubilized in 1XSB and quantified using the RC/DC assay (BIO-RAD, Hercules, California, USA).

5. SDS-PAGE AND WESTERN BLOTTING

For one-dimensional gel electrophoresis, HeLa S3 samples remained undiluted (2.4×10^4 cells per well) or were diluted further 1:5 (0.48×10^4 cells per well) in 1X SB. L6E9 protein homogenates were loaded at a concentration of 4 µg / well. All samples were boiled at 95°C for 5 minutes and were loaded onto 5% stacking and 8% or 12% resolving SDS-PAGE using the BIO-RAD minigel apparatus.

Protein profiles were visualized by Coomassie blue (0.1% Coomassie blue in 10% acetic acid and 25% methanol) staining or separated polypeptides were electrophoretically transferred from gels onto nitrocellulose membranes, and then

processed for immunoblotting as specified in the Western Blotting Kit (Amersham Canada, Oakville, Ontario, Canada).

For immunoblotting, nitrocellulose membranes were incubated in 5% Carnation milk in PBS-Tween (0.05%) to block non-specific sites, followed by incubation with the primary antibody. Immunoblots were reacted with the appropriate biotinylated secondary antibody in 5% milk in PBS-Tween and followed by incubation with streptavidin-conjugated with horseradish peroxidase (1:5000; Amersham Canada) to permit visualization of antigen-antibody complexes. Each incubation was for 1 hour; washes with PBS-Tween were performed between incubations. Finally, blots were developed using the chemiluminescence reagents (Amersham Canada) and the reactivity was visualized on hyperfilm ECL (Amersham Canada).

6. DENSITOMETRIC ANALYSIS

Scanning laser densitometry (BIO-RAD, Segrate, Milan, Italy) and image analysis (Quantity One quantitation software, Windows/McIntosh) were used to quantify protein expression on immunoblots reacted with specific probes. The values were then imported into Systat 10 for statistical analysis. Data were analyzed with a general linear model and Tukey test for multiple comparisons. Significance was assumed at $p < 0.05$.

7. IMMUNOLABELLING

Cells were fixed, permeabilized and stained as previously described (Chaly *et al.* 1984). Briefly, cells were rinsed in (PBS), fixed in 3% paraformaldehyde (BDH) for 5 minutes and rinsed again in PBS. Afterwards, cells were quenched 3X4 minutes in 1 mg / ml sodium borohydride ($NaBH_4$; BDH) and permeabilized for 20 min in 0.1% Triton

X-100. Fixed cells were then washed 3X5 min in PBS.

All antibody incubations were performed at room temperature for 1 hour in PBS and followed by 3X5 min PBS washes. Cells were counterstained for 3 min in 1 µg/ml Hoechst 33258 (Polysciences Inc., Warrington, Pennsylvania, USA) diluted 1:3000 in PBS; they were mounted in 0.1% *p*-phenylene diamine in 50% glycerol/PBS (v/v), pH 7.0.

8. NUCLEAR MATRIX PREPARATIONS

Nuclear matrices were prepared as described by Chaly *et al.* (1985). HeLa S3 cells were grown on sterile glass coverslips and heat shocked as described above.

For nuclear matrix preparations, all solutions were adjusted to pH 7.4 unless otherwise mentioned. Protease inhibitors (1mM PMSF, 1 mg/ml soybean trypsin inhibitor, 2 mM sodium tetrathionate; all from Sigma, St. Louis, MO) were included in all buffers. All steps were carried out at room temperature (RT) except where indicated otherwise.

Following heat-shock, control and treated cells were processed as follows: coverslips were submerged in 5 ml of the appropriate solution in a weight boat. First, cells were rinsed twice for 4 minutes with sucrose-Tris-magnesium buffer (STM; 0.25 M sucrose, 10 mM Tris Base, 2 mM $MgCl_2$.H2O, 25 mM KCl), pH 6.2. Cells were then permeabilized in 0.5% Triton X-100 in STM for 25 minutes, and rinsed in STM (2X4minutes). Cells were digested with deoxyribonuclease I type IV (10 µg/ml) from bovine pancreas (DNase I; Sigma) in low magnesium buffer (LMB; 0.04 mM $MgCl_2$, 2 mM Tris-Base), on ice for 30 minutes. Following this digestion, cells were rinsed with 4 ml LMB for 15 minutes on ice. Afterwards, cells were treated with 4 ml volumes of 2M

high salt buffer (HSB, 2 M NaCl in LMB) added dropwise onto each coverslip for 15 minutes. The same treatment was repeated with 4M HSB (4 M NaCl in LMB). Cells were then subjected to either of the following digestions: a) 50 µg/ml of DNase I in LMB or b) 50 µg/ml of DNase I in combination with 50 µg/ml of ribonuclease A type II A from bovine pancreas (RNase A) in LMB for 20 minutes each. Nuclear matrix preparations were then rinsed in STM (2X4 minutes) before proceeding to fixation and immunolabelling as described above, except that permeabilisation with 0.1% Triton X-100 was omitted. Immunolabelling was performed with antibodies to the Hsp70 antigen, fibrillarin and 2A7.

9. IMMUNOFLUORESCENCE MICROSCOPY

Conventional epifluorescence microscopy was carried out on a Zeiss Axiophot microscope equipped with a 50 W Hg burner. Images were recorded on Ilford 400 ASA B&W film and scanned with a CanoScan 4000 US scanner (Canon, Mississauga, Ontario, Canada). Micrographs were edited using Adobe Photoshop and mounted using PowerPoint (Microsoft).

10. ANTIBODIES

10.1. PRIMARY ANTIBODIES

The following antibodies were used against nuclear envelope antigens: anti-LAP1C is a mouse monoclonal IgG1 (clone 3) provided by Dr. Roberto Campos (Transduction Laboratories, Lexington, KY) and used at 1:250 for immunofluorescence or 1:500 for immunoblotting; anti-LAP2 is a mouse monoclonal IgG1 (clone 27) provided by Dr. Roberto Campos (Transduction Laboratories, Lexington, KY) and used at 1:1000 for immunofluorescence or 1:5000 for immunoblotting; anti-emerin is a mouse

monoclonal antibody IgG1 (clone 4G5) (Novocastra, Newcastle, UK) used at a dilution of 1:30 for immunofluorescence or 1:100 for immunoblotting.

The following antibodies were used against nuclear matrix proteins: anti-lamins A/C is an affinity purified goat polyclonal antibody raised against a peptide mapping at the amino terminus of lamin A from human origin (clone N-18) (Santa Cruz Biotechnology, Inc., California, USA) and used at 1:100 for immunofluorescence and immunoblotting; a second anti-lamins A/C is an affinity purified rabbit polyclonal antibody (kindly provided by Dr. Howard J. Worman, Departments of Medicine and of Anatomy and Cell Biology, Columbia University, NY, USA) and used at 1:200 for immunofluorescence or 1:500 for immunoblotting; anti-mouse/rat lamin B is a rabbit polyclonal antibody IgG (provided by Dr. Peter Traub, Max-Planck Institute, Germany) and used 1:1000 for immunofluorescence or 1:2000 for immunoblotting; anti-human lamin B is a mouse monoclonal antibody IgG1 (clone 101-B7) (Matritech Inc., Cambridge, UK) and used at 1:200 for immunofluorescence or 1:200 for immunoblotting; anti-2A7 is a mouse monoclonal antibody IgG1, hybridoma supernatant (Paulin-Levasseur and Julien, 1999) and used at 1:50 for immunofluorescence or 1:20 for immunoblotting; anti-2H12 is a mouse monoclonal antibody IgG1, hybridoma supernatant (Paulin-Levasseur *et al.*, 1995) and used at 1:20 for immunofluorescence or pure for immunoblotting; anti-fibrillarin is a mouse monoclonal antibody (provided by Dr. Krohne, Biocenter of the University of Wurzburg, Wurzburg, Germany) and used at a 1:25 for immunofluorescence or 1:100 for immunoblotting; anti-1B4 is a mouse monoclonal antibody IgE, hybridoma supernatant (Luus and Paulin-Levasseur, 1997) and used pure for immunofluorescence; anti-P160 is a mouse monoclonal antibody

(clone AM88) (kindly provided by Dr. De Graaf, University of Utrecht, Netherlands; De Graaf *et al.* 1992) and used at 1:300 for immunofluorescence; anti-PCNA is a mouse monoclonal IgG_{2a} (Santa Cruz Biotechnologies Inc.) and used at 1:200 for immunoblots.

The following antibody was used as a marker for hyperthermia: anti-Hsp70 is a rabbit polyclonal antibody (StressGen Biotechnologies Corp., Victoria, BC, Canada) and used at 1:2000 for immunofluorescence or 1:20000 for immunoblots.

The following probes were used for differentiation: anti-myosin is a mouse monoclonal antibody (clone MF20) (kindly provided by Dr. M. McBurney, Ottawa Health Research Institute, Cancer Therapeutics, Ottawa, Ontario, Canada) and used at 1:10 for immunofluorescence or 1:100 for immunoblotting; and anti-myogenin is a mouse monoclonal antibody IgG_1 (provided by Dr. M. McBurney) used at 1:10 for immunofluorescence. The following antibody was used for detection of apoptotic cells: anti-poly (ADP-ribose) polymerase (PARP) (Trevigen, Gaithersburg, MD, USA) is a mouse monoclonal antibody used at 1:200 for immunoblotting.

10.2. <u>SECONDARY ANTIBODIES</u>

The following secondary antibodies were used for immunofluorescence: CY3-conjugated polyclonal donkey anti-mouse IgG (Jackson) used 1:400; CY3-conjugated polyclonal donkey anti-rabbit IgG (Jackson) used 1:400; CY3-conjugated polyclonal donkey anti-rat IgG (Jackson) used 1:400; FITC-conjugated polyclonal donkey anti-goat/sheep IgG (Jackson) used at 1:50.

The following secondary antibodies were used for immunoblotting: biotinylated polyclonal donkey anti-goat/sheep Ig (Amersham) used at 1:8000; biotinylated polyclonal sheep anti-mouse Ig (Amersham) used at 1:5000; biotinylated polyclonal

donkey anti-rabbit Ig (Amersham) used at 1:5000.

III. RESULTS

1. RESPONSE OF HELA S3 CELLS TO HEAT-SHOCK

To evaluate the effects of heat-shock on HeLa S3 cell survival and to validate the system, two sets experiments were done: first, cell viability and growth were monitored; and second, the cellular distribution and expression of the inducible heat shock protein 70 (Hsp70) were studied.

1.1. Viability, growth and cell cycle distribution of HeLa S3 cells

Cell populations examined included: a) untreated (control) HeLa S3 cells; b) HeLa S3 cells heat-shocked at 42°C (mild) or 45°C (severe) for 90 minutes; c) heat-shocked cells recovering at 37°C for 1 hour, 5, 12, 20, and 25 hours. To assess the consequences of heat-shock on my experimental system, the viability and growth rate of HeLa S3 cells were first established under normal conditions. HeLa S3 cells were collected at different time intervals post forty-eight hours of culture (time 0), and subjected to counting using Trypan blue as a colorant for dead cells. Figure 2 shows a significant increase in cell numbers following 13.5 hours (this time equals the 90 minutes heat-shock period added to 12 hours recovery at 37°C); the increase is by a factor of 1.74. After 26.5 hours, the increase is by a factor of 1.84. It seems that the growth of the cell population starts reaching a plateau after 13.5 hours of culture, possibly coincident with cell confluence. Throughout the whole of experimentation period, the amount of dead cells did not increase significantly and remained low.

To monitor cell viability and growth after the different treatments, HeLa S3 cells were collected at the appropriate time and subjected to counting using

Figure 2: Histogram showing the normal growth of HeLa S3 cells. Control cells were treated with trypsin-EDTA, collected and counted using Trypan blue exclusion. The data for each time point is the mean of 3 separate experiments, 6 counts each. Error bars show the standard error from the mean.

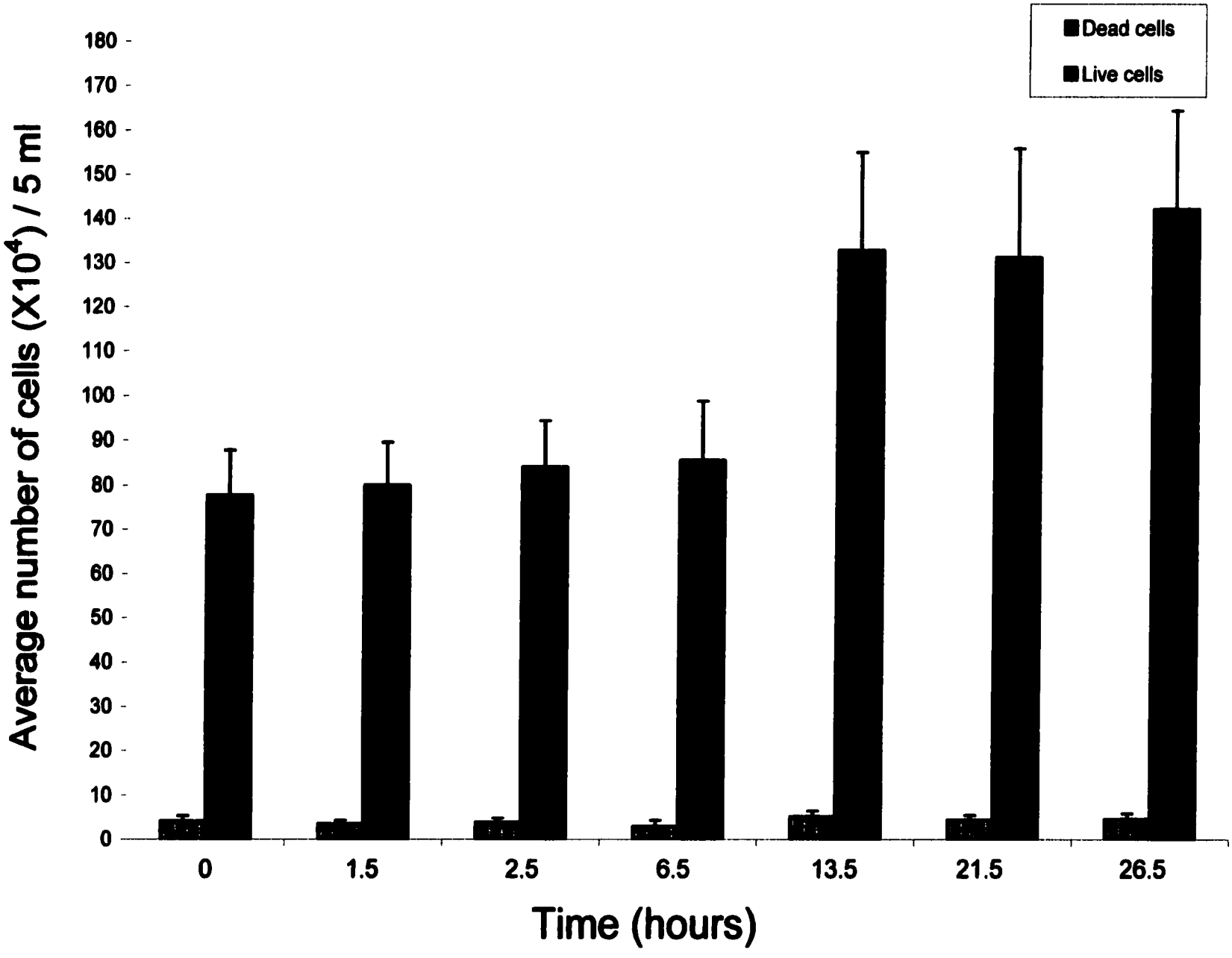
Dead cells
Live cells
Average number of cells (X10^4) / 5 ml
180
170
160
150
140
130
120
110
100
90
80
70
60
50
40
30
20
10
0
0
1.5
2.5
6.5
13.5
21.5
26.5
Time (hours)

Trypan blue as indicated above. Figures 3A (mild stress) and 3B (severe stress) demonstrate that the number of dead cells remains below 10% in both treatments. This permitted me to conclude that hyperthermia treatments - whether mild or severe- do not compromise significantly HeLa S3 cell survival. This observation stands throughout the 25 hour recovery period at 37°C. Figure 3A indicates also that the number of live cells did not increase significantly, only slightly after a mild treatment. A severe heat-shock (figure 3B) resulted in a small decrease in the number of live cells after 12-25 hours post-heat shock. These data indicated that, although HeLa S3 cells are surviving throughout the 25 hour recovery period, there appears to be no growth in the treated populations. Statistical analysis on both mild and severe stresses did not show any significant difference between dead or live cells. A comparison between figure 2 and 3 leads to the observation that a decrease in cell proliferation must occur prior to 12 hours of post-heat shock recovery.

Considering these results, it appeared important to determine whether the cell cycle distribution of HeLa S3 cells was affected by heat-shock. A flow cytometric analysis of cellular content in DNA was performed on the different populations of HeLa S3. Figure 4 shows the profile of PI fluorescence intensity amongst a control cell population. Figure 5A and 5B illustrate the results obtained after a mild and severe treatments. In control and heat-shocked samples without or with recovery at 37°C, most cells were shown to be in the G0/G1 phase of the cell cycle. The lowest number of cells was found in the S phase, except after 20 and 25 hours of recovery from a mild treatment, where the

Figure 3: Histogram showing the viability of HeLa S3 cells. Control HeLa S3 cells, HeLa S3 cells heat shocked at 42°C for 90 minutes (A) or 45°C for 90 minutes (B), and allowed to recover at 37°C for 1-25 hours were treated with trypsin-EDTA, collected and counted using Trypan blue exclusion. The data for each treatment is the mean of 5 separate experiments, 6 counts each. Error bars show the standard error from the mean.

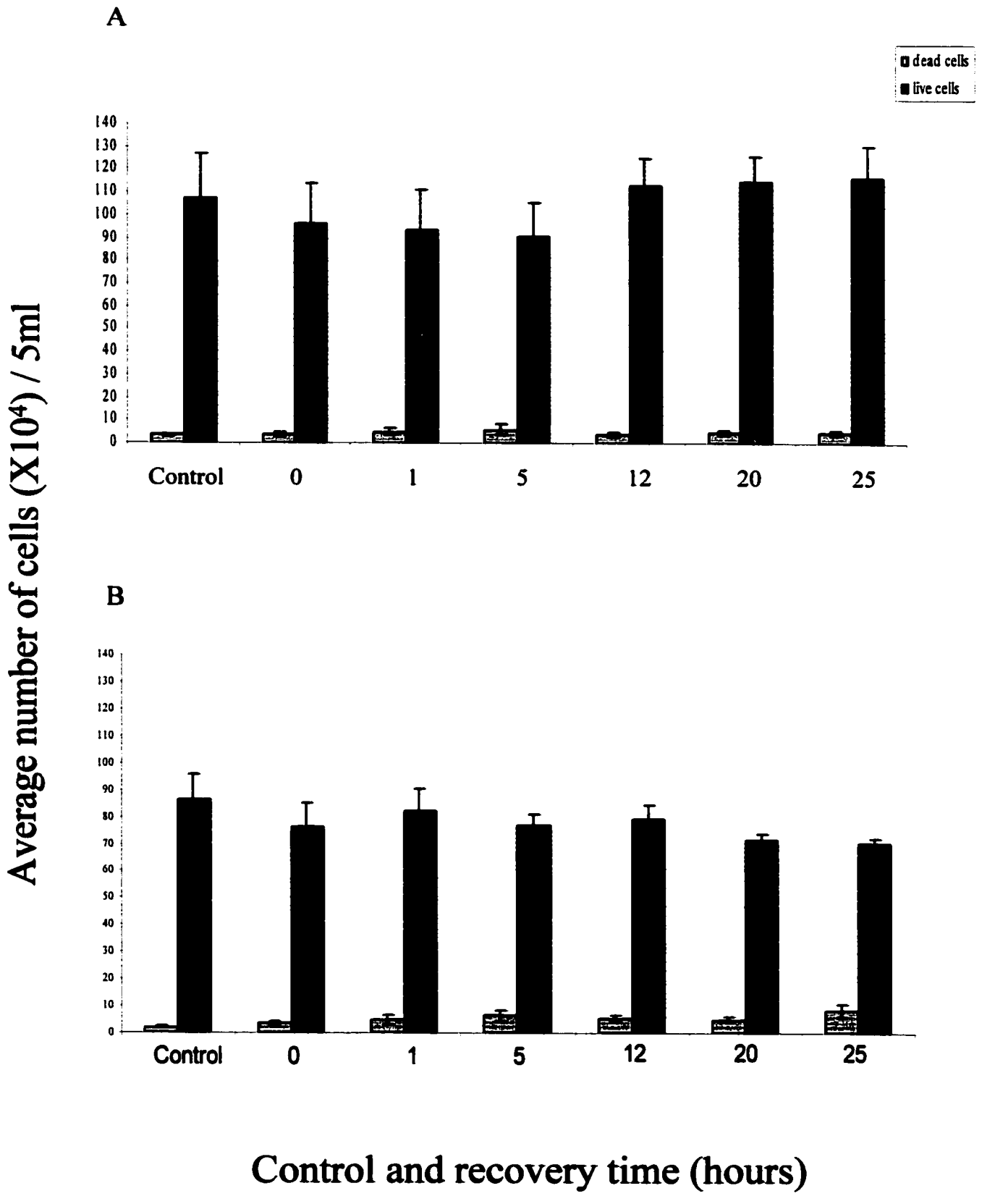
A
dead cells
live cells
140
130
120
110
100
90
80
70
60
50
40
30
20
10
0
Control
0
1
5
12
20
25
B
140
130
120
110
100
90
80
70
60
50
40
30
20
10
0
Control
0
1
5
12
20
25
Average number of cells (X10⁴) / 5ml
Control and recovery time (hours)

Figure 4: Histogram of PI fluorescence intensity amongst a typical population of control HeLa S3 cells. Cells were fixed in 100% ethanol, stained with PI and analyzed by flow cytometry. All other samples of HeLa S3 (see text) showed a similar profile.

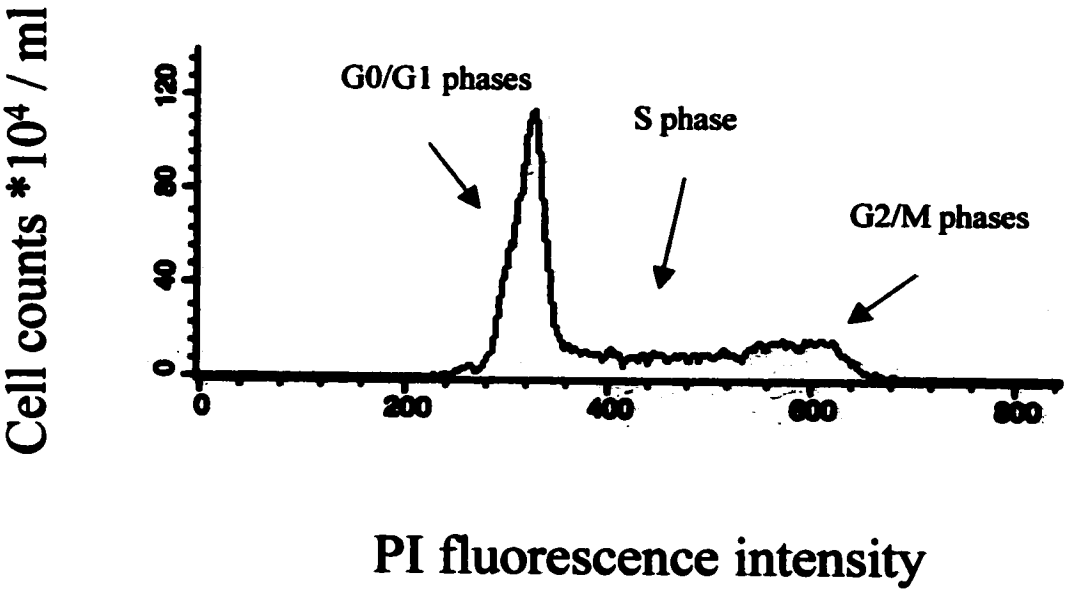
Cell counts *10⁴ / ml
G0/G1 phases
S phase
G2/M phases
0
40
80
120
0
200
400
600
800
PI fluorescence intensity

average number of cells undergoing G2/mitosis was lower than for the G0/G1 or S phases. The difference observed for the G2/mitosis phase is statistically significant ($p = 0.031$). This is relevant in samples between 5 and 20 hours of recovery ($p = 0.036$).

After a severe treatment, pattern of PI fluorescence remained similar to control for all samples examined (heat-shock and recovered populations).

Once it was determined that the cell cycle distribution of HeLa S3 cells did not change throughout the different treatments, I decided to determine whether DNA replication could be affected by monitoring the incorporation of BrdU in HeLa S3 cells. Table 2 shows the results obtained during this experiment. Following a mild heat-shock, the incorporation of BrdU into HeLa S3 cells decreased considerably throughout the treatment and recovery period with one exception: after 5 hours of recovery at 37°C, BrdU incorporation increases relative to the rest of the samples but remains lower than the control value. Following a severe treatment (table 2), it can be deduced that BrdU incorporation was reduced due to a severe heat-shock. This decrease in DNA replication is maintained at 37°C. Thus, mild and severe stresses have an evident negative effect on DNA replication; there is only an increase after a 5 hours recovery period at 37°C following a mild stress.

In order to confirm that HeLa S3 cells do not become apoptotic following mild or severe heat-shock, a specific antibody to the Poly (ADP-Ribose) Polymerase (PARP) was used to monitor the proteolytic cleavage of this protein. The proteolytic cleavage of PARP, a 116 KDa protein, into two fragments of 85

Figure 5: Histogram showing the cell cycle distribution of HeLa S3 cells. Control HeLa S3 cells, HeLa S3 cells heat shocked at 42°C for 90 minutes (A) or 45°C for 90 minutes (B), and allowed to recover at 37°C for different lengths of time in hours (1h-25h) were treated with trypsin-EDTA, collected and counted using Trypan blue exclusion. Cells were then fixed with pure ethanol and kept at 4°C. For flow cytometry analysis, see "materials and methods". The data for each treatment is the mean of 3 separate experiments. Error bars show the standard error from the mean.

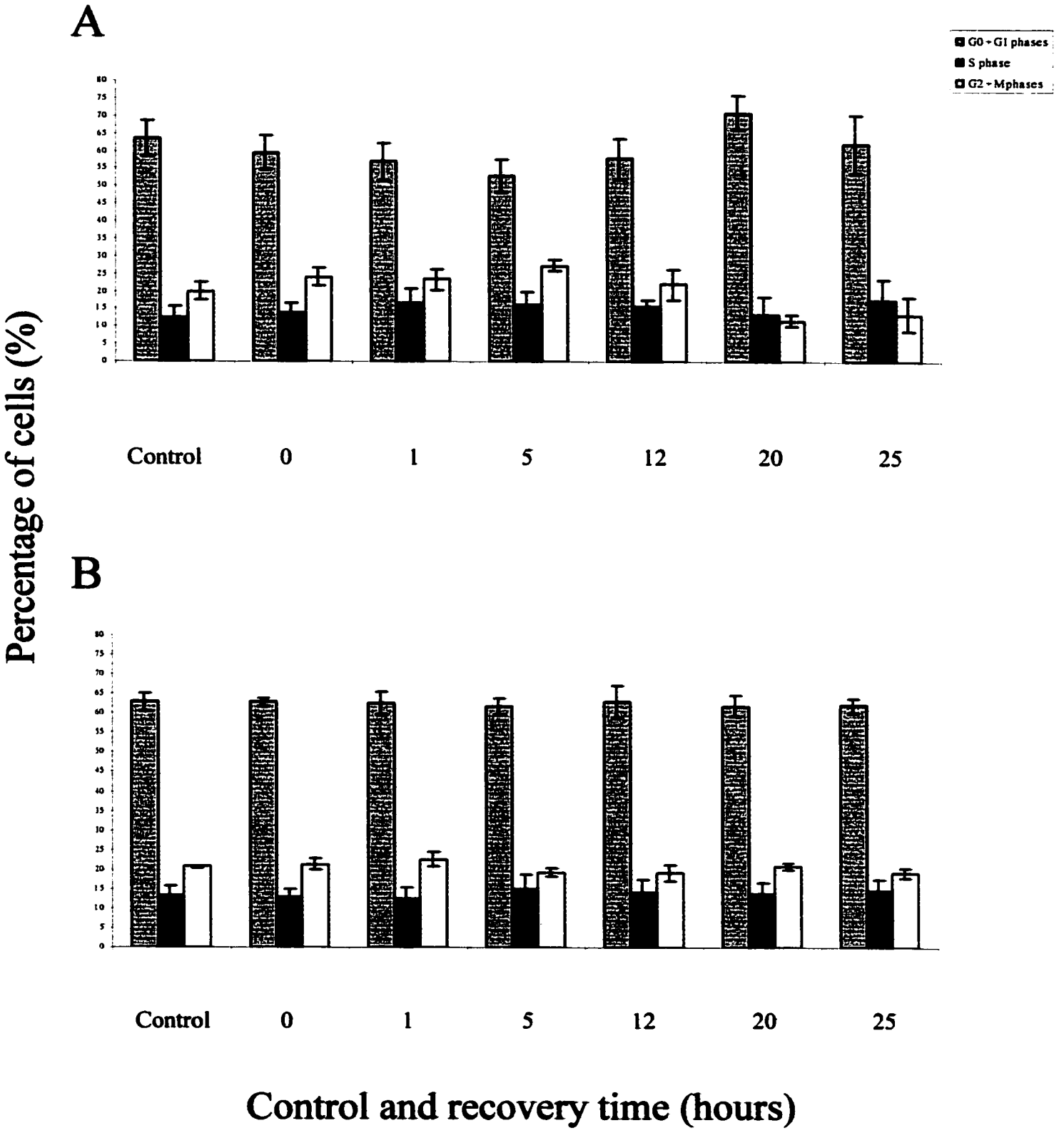
A
G0 - G1 phases
S phase
G2 - M phases
Percentage of cells (%)
Control
0
1
5
12
20
25
B
Control
0
1
5
12
20
25
Control and recovery time (hours)

Table 2: Percentages (%) of cells that incorporated BrdU amongst HeLa S3 populations subjected to mild or severe heat shock treatments. Cells allowed to recover at 37°C for different time lengths were also studied. The data of one experiment are summarized.

Hours at 37°C after heat-shock	Mild heat-shock	Severe heat-shock
Control	11.49	9.35
0 hour	1.09	0.16
1 hour	1.01	0.3
5 hours	7.79	1.17
12 hours	1.47	0.72
20 hours	1.25	1.02
25 hours	1.29	1

KDa and 26 KDa has been recognized as an indicator of apoptosis (Lamarre *et al.* 1988). I therefore used a mouse monoclonal antibody that recognizes the full length protein (116 KDa) and the 85 KDa fragment to assess the occurrence of apoptosis within my control and treated cell populations by immunoblotting. It can be seen in figure 6 that, after a mild (A) or severe (B) treatment, a single specific band of 116 KDa is seen; this corresponds to the intact PARP protein.

1.2. Immunofluorescence and immunoblotting analysis of Hsp70 expression

To evaluate the effects of mild and severe hyperthermia on the cellular localization and content of the inducible Hsp70 in HeLa S3 cells, immunofluorescence microscopy and quantitative immunoblotting analysis were performed. The cell populations examined included: a) control untreated HeLa S3 cells; b) HeLa S3 cells subjected to mild or severe heat-shocks; c) HeLa S3 cells heat-shocked at either temperatures for 90 minutes and then recovered at 37°C for 1, 5, 12, 20 and 25 hours.

The distribution of Hsp70 in HeLa S3 cells after a mild heat shock treatment is illustrated in figure 7. In control cells (fig. 7 a-a"), Hsp70 is localized diffusely in the nucleus (including the nucleoli) and found at basal levels throughout the cytoplasm. It is interesting to note that the shape of HeLa S3 cells is not altered in mildly treated cells as shown in figure 7 b-b"; Hoechst staining demonstrates that the shape of the nucleus and the chromatin organization remain similar as in control cells (compare figure 7 a-a" to figure 7 b-b"). According to the literature, I had predicted that Hsp70 expression would

Figure 6: Immunodetection of PARP following mild (A-B) or severe (C-D) heat-shock treatments of HeLa S3 cells. Mouse secondary antibody controls are shown in (B) and (D). HeLa S3 cells were untreated (c), or they were heat shocked for 90 minutes (0) and subsequently left to recover at 37°C for different lengths of time in hours (1h – 25h). Whole cell homogenates were solubilized in 2X SB and separated by SDS-PAGE on 8% resolving gels, then transferred onto nitrocellulose and blotted with the appropriate antibodies. Chemiluminescence detection of PARP on radiograms is shown.

A

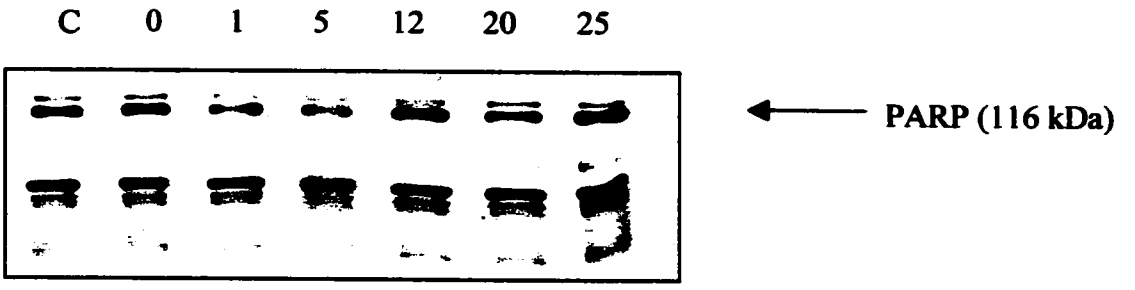

B

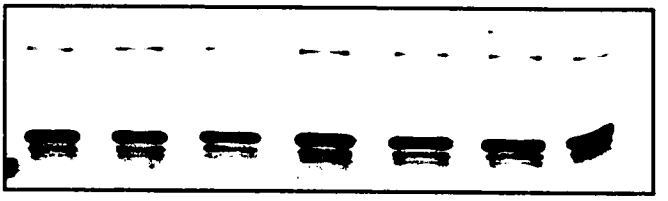

C

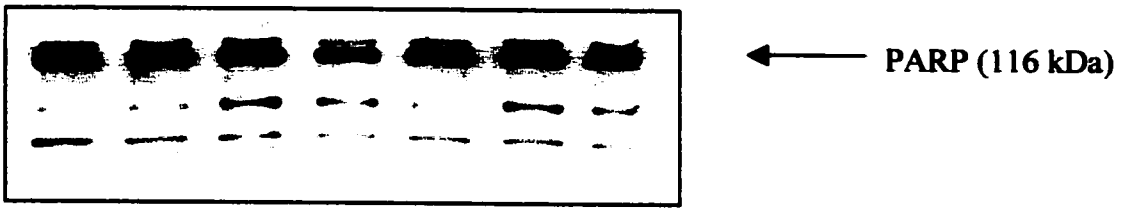

D

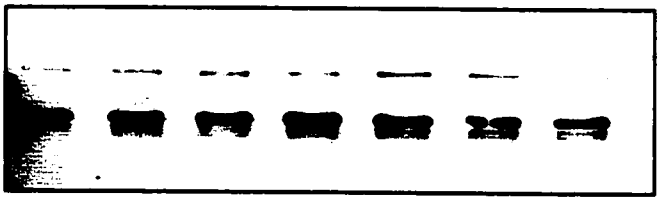

increase and its distribution would be more noticeable in the nucleus, becoming more prominent in nucleoli, due to mild and severe stress. Following a 42°C heat-shock for 90 minutes as shown in figure 7 b-b", Hsp70 is localized in the nucleus and staining of the nucleoli is more prominent (arrow). Following recovery at 37°C for 1 hour (figure 7 c-c") and 5 hours (figure 7 d-d"), Hsp70 remains nuclear although its prominence in the nucleoli diminishes. Figures 7 e-e", f-f" and g-g" represent 12, 20 and 25 hour recovery at 37°C respectively. It can be seen that Hsp70 is regaining its localization in the cytoplasm.

Following a severe (45°C) heat shock treatment (figure 8), HeLa S3 cells change their shape (compare control cells in figure 8 a and treated cells in figure 8 b): the overall shape is rounder and the volume ratio nucleus/cytoplasm is increased after heat shock. It is difficult to assess the nuclear-cytoplasmic boundary in such cells, because their cytoplasm seems to be more compact and has become less evident. The shape of the nuclei as shown by Hoechst staining can be changed into structures (figure 8 g-g", arrow) not observed in control cells (figure 8 a-a"). The results obtained indicate, that in control cells (figure 8 a-a") as mentioned above, Hsp70 was found in the nuclei (including the nucleoli) and cytoplasm (as in figure 7 a-a"). Upon a 45°C treatment for 90 minutes (figure 8 b-b"), Hsp70 was still found in both compartments. The same distribution was maintained following 1 and 5 hours recovery (figure 8 c-c" and d-d") respectively. The distribution of this antigen remains in both the nucleus and the cytoplasm throughout the 12, 20 and 25 hour recovery period (figure 8 e-e", f-f" and g-g"). The fluorescence intensity appeared to increase after 12 h recovery, and was

Figure 7: Immunolocalization of Hsp70 following mild heat-shock treatment of HeLa S3 cells. HeLa S3 cells were grown on coverslips and treated for the appropriate time; they were then fixed with 3% paraformaldehyde, permeabilized with Triton X-100 and stained. Cells were observed by phase contrast microscopy (a, b, c and d). Cells were single-labeled for immunofluorescence with anti-Hsp70 (a", b", c" and d"). Preparations were counterstained with Hoechst 33258 (a', b', c' and d'). The pictures show untreated cells (a-a"), heat shocked cells at 42°C for 90 minutes (b-b") and cells that subsequently recovered at 37°C for 1 hour (c-c") or 5 hours (d-d"). Bar represents 10 μm.

a
a'
a''
b
b'
b''
c
c'
c''
d
d'
d''

Figure 7 (continued): Immunolocalization of Hsp70 following mild heat-shock treatment of HeLa S3 cells. HeLa S3 cells were grown on coverslips and treated for the appropriate time; they were then fixed with 3% paraformaldehyde, permeabilized with Triton X-100 and stained. Cells were observed by phase contrast microscopy (e, f and g). Cells were single-labeled for immunofluorescence with anti-Hsp70 (e", f" and g"). Preparations were counterstained with Hoechst 33258 (e', f' and g'). The pictures show HeLa S3 cells that recovered at 37°C for 12 hours (e-e"), 20 hours (f-f") and 25 hours (g-g") after a mild treatment. Bar represents 10 μm.

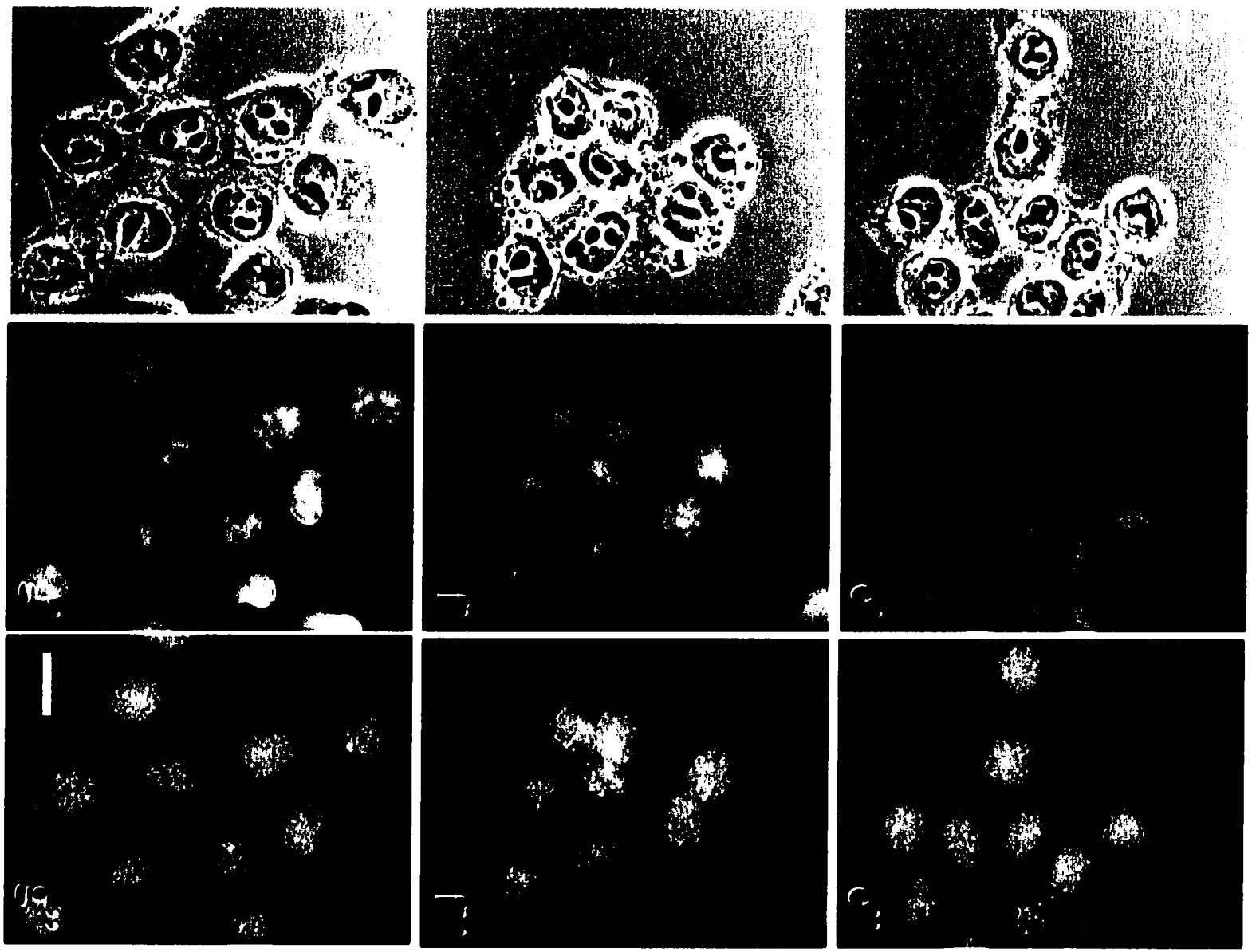

Figure 8: Immunolocalization of Hsp70 following severe heat-shock treatment of HeLa S3 cells. HeLa S3 cells were grown on coverslips and treated for the appropriate time; they were then fixed with 3% paraformaldehyde, permeabilized with Triton X-100 and stained. Cells were observed by phase contrast microscopy (a, b, c and d). Cells were single-labeled for immunofluorescence with anti-Hsp70 (a", b", c" and d"). Preparations were counterstained with Hoechst 33258 (a', b', c' and d'). The pictures show untreated cells (a-a"), heat shocked cells at 45°C for 90 minutes (b-b") and cells that subsequently recovered at 37°C for 1 hour (c-c") or 5 hours (d-d"). Bar represents 10 μm.

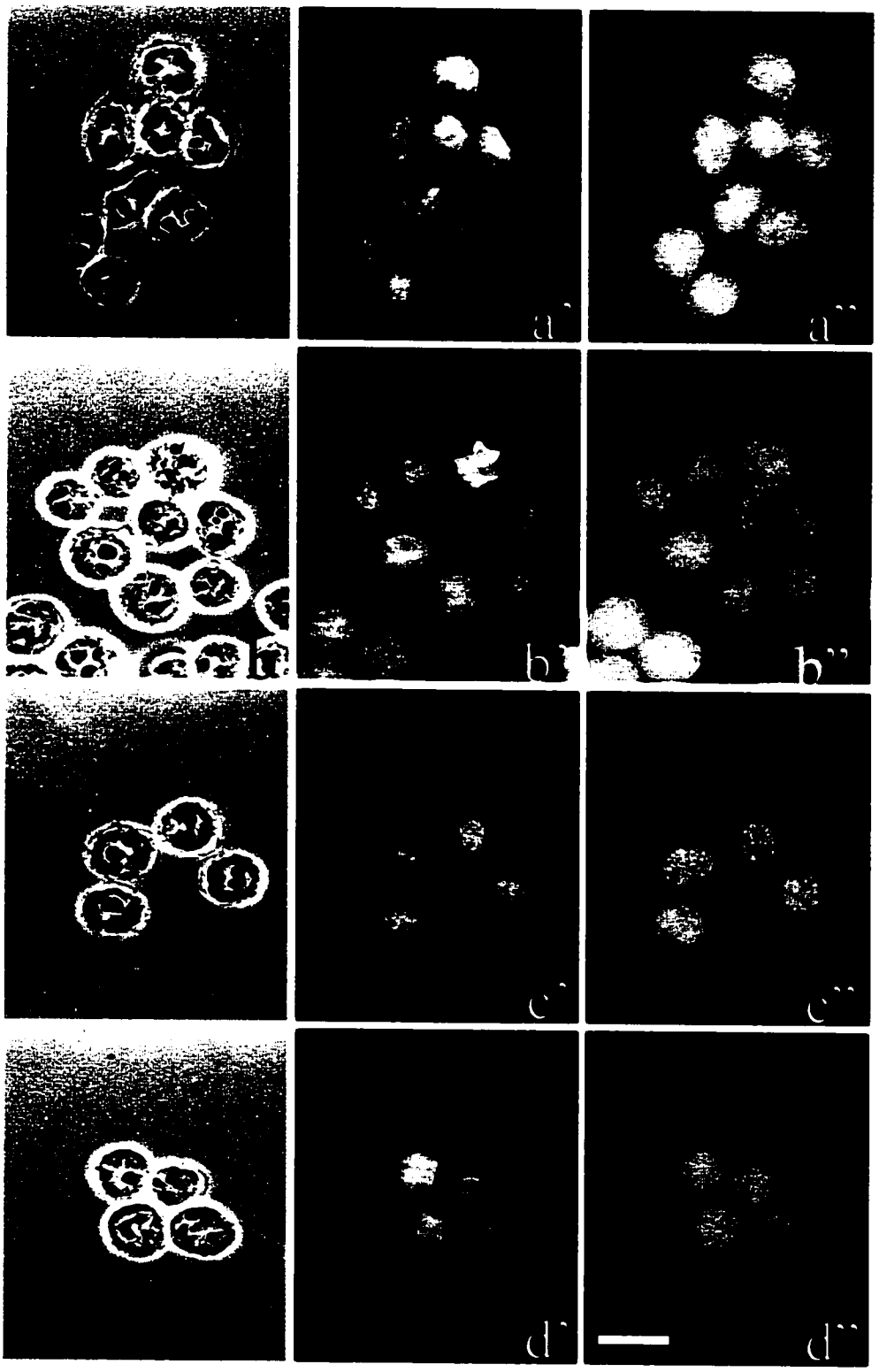
a'
a''
b'
b''
c'
c''
d'
d''

more prominent after 20h and 25h recovery at 37°C. Quantitative densitometric analysis of whole cell extracts by immunoblotting was then performed, demonstrating an overall increase in Hsp70 expression following heat-shock treatments.

Figure 9 shows Coomassie blue stained SDS-PAGE gels representing HeLa S3 samples from mild (A) and severe (B) treatments. These gels provided confirmation that equivalent numbers of cells were loaded in each lane.

Typical radiograms obtained by chemiluminescence detection of Hsp70 by Western Blot are depicted in figure 10. Quantitative results obtained by densitometric analysis are presented in figure 11. It is important to keep in mind that chemiluminescence detection on radiograms is not linear and can only provide only an indication about the changes occurring in the expression of antigens, but no quantitave information.

In figure 10, Western blot analysis was performed with specific antibodies to the heat-shock protein Hsp70. The analysis was done following mild (fig. 10 A) or severe (fig. 10 B) treatments and the reactivity of antibodies was visualized by chemiluminescence. In figure 10 A, HeLa S3 cells show an increase in the expression level of Hsp70 following a mild stress treatment and the recovery period at 37°C, in comparison to control cells. This result was confirmed by densitometry analysis as seen further below.

Figure 10 B shows that HeLa S3 cells maintain a relatively constant expression level of Hsp70 following a severe treatment and early during

Figure 8 (continued): Immunolocalization of Hsp70 following severe heat-shock treatment of HeLa S3 cells. HeLa S3 cells were grown on coverslips and treated for the appropriate time; they were then fixed with 3% paraformaldehyde, permeabilized with Triton X-100 and stained. Cells were observed by phase contrast microscopy (e, f and g). Cells were single-labeled for immunofluorescence with anti-Hsp70 (e", f" and g"). Preparations were counterstained with Hoechst 33258 (e', f' and g'). The pictures show HeLa S3 cells that recovered at 37°C for 12 hours (e-e"), 20 hours (f-f") and 25 hours (g-g") after a severe treatment. Bar represents 10 μm.

c
c'
c''
f
f'
f''
g
g'
g''

Figure 9: SDS-PAGE gel profiles from extracts of HeLa S3 cells following mild (A) or severe (B) heat-shock treatments. HeLa S3 cells were untreated (c), or they were heat shocked for 90 minutes (0) and subsequently left to recover at 37°C for different lengths of time in hours (1h-25h). Whole cell homogenates were prepared, analyzed by SDS-PAGE on 12% resolving gels and visualized by Coomassie blue-staining. *Black dots* at the left correspond to the position of prestained molecular weight markers: phosphorylase B, 106 KDa; bovine serum albumin, 81 KDa; ovalbumin 47.5 KDa; carbonic anhydrase, 35.3 KDa; soybean trypsin inhibitor, 28.2 KDa; lysozyme, 20.5 KDa.

A

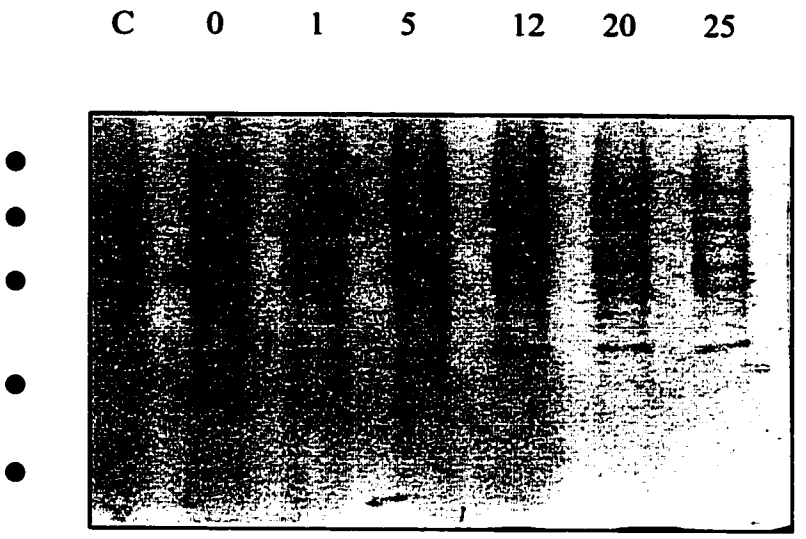

B

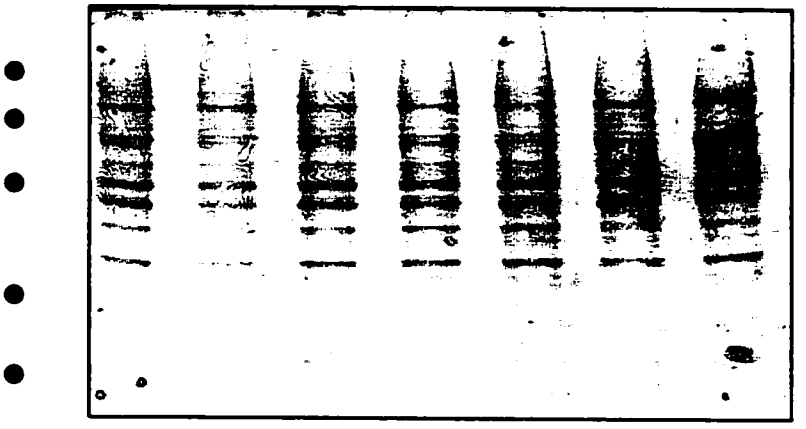

recovery. However, there appears to be an increase in the expression of this protein at 20 and 25 hours post heat-shock.

Figure 11 summarizes the quantitative changes that happened in the expression of Hsp70 following a mild (Fig. 11 A) or a severe (Fig. 11 B) treatments. There is an overall highly significant increase in the levels of Hsp70 ($p = 0.000$) when cells are mildly stressed. This increase is continuous throughout the 1 and 5 hour recovery period. The trend of the graph indicates that Hsp70 expression reaches its highest level at 5 hours post-heat shock; its expression starts to decrease slowly after this recovery period. A significant difference is observed between control cells and cells that recovered at 37°C for: 1 hour ($p = 0.013$), 5 hours ($p = 0.000$), 12 hours ($p = 0.000$), 20 hours ($p = 0.000$) and 25 hours ($p = 0.043$). There is a significant difference in the level of expression of Hsp70 between treated cells without recovery and cells that recovered for 5, 12 and 20 hours ($p = 0.006$; 0.007, 0.023 respectively).

Figure 11 B indicates an overall significant increase in the level of expression of Hsp70 following a 45°C heat shock treatment ($p = 0.000$). Hsp70 expression seems to decrease slightly after the shock, but this result is not statistically relevant. The cellular content of this protein has increased significantly at 25 hours post-heat shock when compared to treated cells ($p = 0.033$).

Figure 10: Immunodetection of Hsp70 following mild (A) or severe (B) heat-shock treatments of HeLa S3 cells. HeLa S3 cells were untreated (C), or they were heat shocked for 90 minutes (0) and subsequently left to recover at 37°C for different lengths of time in hours (1h – 25h). Whole cell homogenates were solubilized in 2X SB and separated by SDS-PAGE on 12% resolving gels, then transferred onto nitrocellulose and blotted with the appropriate antibodies. Chemiluminescence detection of Hsp70 on radiograms is shown.

A

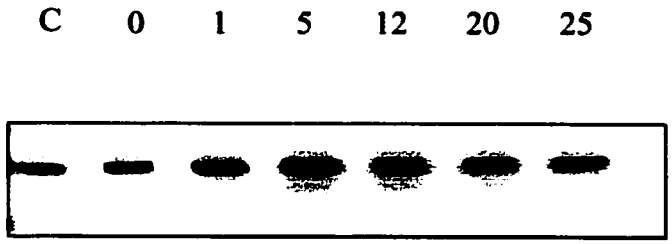

Hsp70 (70KDa)

B

Hsp70 (70KDa)

Figure 11: Histogram showing heat-induced quantitative changes in the expression of Hsp70 in HeLa S3 cells. Control HeLa S3 cells, cells heat shocked at 42°C for 90 minutes (A) or at 45°C for 90 minutes (B), and allowed to recover at 37°C for 1-25 hours were processed for SDS-PAGE and Western blotting as described in "Materials and Methods". Antibody reactivity was quantified by densitometry scans of individual bands. The data for each treatment is the mean of Residuals (n=4). Error bars show the standard error from the mean. * $p < 0.05$, Tukey.

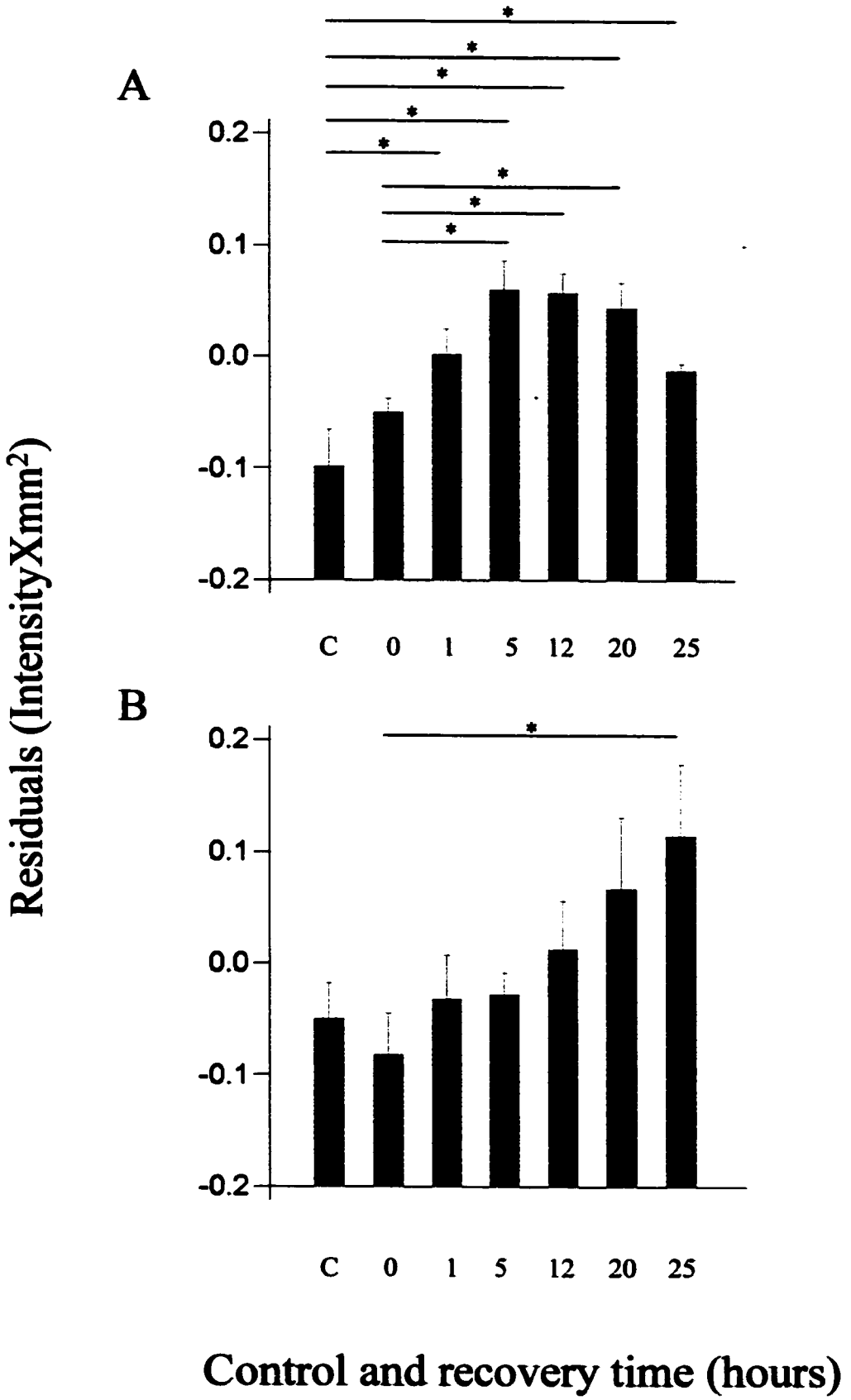
A
B
0.2
0.1
0.0
-0.1
-0.2
C
0
1
5
12
20
25
Residuals (IntensityXmm²)
Control and recovery time (hours)

2. THE EFFECTS OF HEAT-SHOCK ON NUCLEAR PROTEINS

2.1. Immunofluorescence monitoring and quantitative immunoblotting analysis of different proteins located at the nuclear periphery in HeLa S3 cells.

To gain insights into the nuclear organization of HeLa S3 cells after the heat stress, the nuclear envelope proteins LAP2β, emerin and lamins were used as markers. The experiments described below were carried on the following populations of HeLa S3 cells: a) control untreated cells; b) HeLa S3 cells heat-shocked at 42°C or 45°C for 90 minutes; c) HeLa S3 cells recovered at 37°C for 1-25 hours after heat-shock.

The localization of all antigens used in this study was assessed using immunofluorescence microscopy. The results obtained were confirmed at least twice for each antigen. Western blotting was repeated four times for each antigen and the quantitative data presented for densitometric analysis were the average of four different experiments.

Figure 12 shows the immunofluorescence data obtained for the inner nuclear membrane protein (INMP) LAP2β. In control HeLa S3 cells (fig. 12 a-a"), this type II integral protein is localized at the nuclear periphery (fig. 12 a"). HeLa S3 cells which were subjected to a mild shock (fig. 12 b-b") and then left to recover at 37°C for 20 hours after heat-shock (fig. 12 c-c") show a distribution of LAP2β that resembles that of control cells (fig. 12 a"). Likewise, LAP2β remained localized to the nuclear periphery in HeLa S3 cells exposed to a severe shock

(fig. 12 d-d"), and in cells recovered for 20 hours at 37°C following severe treatment (fig. 12 e-e").

Emerin is also a type II integral protein of the inner nuclear membrane that is located at the nuclear periphery in control HeLa S3 cells (fig. 13 a-a"). The distribution of this protein in control HeLa S3 cells and following heat-shock resembles that of LAP2β. Figures 13 b-b" and c-c" show the staining of HeLa S3 cells following a mild stress treatment and recovery for 20 hours at 37°C, respectively. It was observed that emerin maintains its distribution at the nuclear periphery. The same results were obtained following a severe treatment (fig. 13 d-d"). In cells recovered at 37°C for 20 hours after a severe heat-shock (fig. 13 e-e"), emerin localized at the nuclear periphery and a portion of this protein remained sequestered within the endoplasmic reticulum (fig. 13 e"). In a small portion of the cell population, emerin labeled the nuclear periphery in an uneven manner: it seemed to be enriched in some areas relative to the rest of the periphery. This "enrichment" resulted into the formation of dot-like brilliant structures (arrow, fig. 13 e").

Figures 14 and 15 summarize the immunofluorescence results obtained for lamins A/C and lamin B respectively. Both types of lamins are peripheral nuclear matrix proteins; they are located at the nuclear periphery in control HeLa S3 cells (fig. 14 a-a" and fig. 15 a-a" respectively). Lamins A/C do not change their distribution in mildly stressed cells (fig. 14 b-b"), neither in cells recovered at 37°C for 20 hours after a mild heat-shock (fig. 14 c-c"). The same results were obtained for lamin B after a mild stress (fig. 15 b-b" and c-c" respectively).

Figure 12: Immunolocalization of LAP2β following heat-shock treatments of HeLa S3 cells. HeLa S3 cells were grown on coverslips and treated for the appropriate time; they were then fixed with 3% paraformaldehyde, permeabilized with Triton X-100 and stained. Cells were observed by phase contrast microscopy (a, b, d, c and e). Cells were single-labeled for immunofluorescence with anti-LAP2β (a", b", c", d" and e"). Preparations were counterstained with Hoechst 33258 (a', b', c', d' and e'). The pictures show untreated cells (a-a"), heat-shocked cells at 42°C for 90 minutes (b-b"), cells that recovered at 37°C for 20 hours after a mild treatment (c-c"), cells heat-shocked at 45°C for 90 minutes (d-d"), cells that recovered at 37°C for 20 hours after a severe treatment (e-e"). Bar represents 10 μm.

a'
a''
b'
b''
c'
c''
d'
d''
e'
e''

Figure 13: Immunolocalization of emerin following heat-shock treatments of HeLa S3 cells. HeLa S3 cells were grown on coverslips and treated for the appropriate time; they were then fixed with 3% paraformaldehyde, permeabilized with Triton X-100 and stained. Cells were observed by phase contrast microscopy (a, b, d, c and e). Cells were single-labeled for immunofluorescence with anti-emerin (a", b", c", d" and e"). Preparations were counterstained with Hoechst 33258 (a', b', c', d' and e'). The pictures show untreated cells (a-a''), heat-shocked cells at 42°C for 90 minutes (b-b''), cells that recovered at 37°C for 20 hours after a mild treatment (c-c"), cells heat-shocked at 45°C for 90 minutes (d-d"), cells that recovered at 37°C for 20 hours after a severe treatment (e-e"). Bar represents 10 µm.

a'
a''
b'
b''
c'
c''
d'
d''
e'
e''

Figure 14: Immunolocalization of lamins A/C following heat-shock treatments of HeLa S3 cells. HeLa S3 cells were grown on coverslips and treated for the appropriate time; they were then fixed with 3% paraformaldehyde, permeabilized with Triton X-100 and stained. Cells were observed by phase contrast microscopy (a, b, d, c and e). Cells were single-labeled for immunofluorescence with anti-lamin A/C (a", b", c", d" and e"). Preparations were counterstained with Hoechst 33258 (a', b', c', d' and e'). The pictures show untreated cells (a-a"), heat-shocked cells at 42°C for 90 minutes (b-b"), cells that recovered at 37°C for 20 hours after a mild treatment (c-c"), cells heat-shocked at 45°C for 90 minutes (d-d"), cells that recovered at 37°C for 20 hours after a severe treatment (e-e"). Bar represents 10 µm.

a'
a''
b'
b''
c'
c''
d'
d''
e'
e''

Figure 15: Immunolocalization of lamin B during heat-shock of HeLa S3 cells. HeLa S3 cells were grown on coverslips, treated for the appropriate time; they were then fixed with 3% paraformaldehyde, permeabilized with Triton X-100 and stained. Cells were observed by phase contrast microscopy (a, b, d, c and e). Cells were single-labeled for immunofluorescence with anti-lamin B (a", b", c", d" and e"). Preparations were counterstained with Hoechst 33258 (a', b', c', d' and e'). The pictures show untreated cells (a-a"), heat-shocked cells at 42°C for 90 minutes (b-b"), cells recovered at 37°C for 20 hours after a mild treatment (c-c"), cells heat-shocked at 45°C for 90 minutes (d-d"), cells recovered at 37°C for 20 hours after a severe treatment (e-e"). Bar represents 10 μm.

a
a'
a''
b
b'
b''
c
c'
c''
d
d'
d''
e
e'
e''

Following a mild stress and 20 hour recovery, lamin B was seen to aggregate into intranuclear foci in some cells, while remaining at the nuclear periphery. HeLa S3 cells maintain also this nuclear periphery distribution of lamins A/C and lamin B after a severe stress (fig. 14 d-d" and fig. 15 d-d"). No change was observed at 20 hours recovery at 37°C after severe stress for lamins A/C (fig. 14 e-e"). However, in some cells, lamin B was seen to form intranuclear foci within the nucleus, while maintaining a rim-like distribution (Fig. 15 e-e").

Figure 16 depicts typical radiograms obtained during the Western blot analysis of nuclear envelope proteins LAP2β, emerin, and lamins A/C and lamin B using specific antibodies. The analysis included samples subjected to mild (fig. 16 A) and severe (fig. 16 B) heat-shock treatments as well as control samples. LAP2β was detected as a single band with a relative mobility of 55 KDa; the upper band seen in the corresponding panel was found to be due to non-specific binding of the detection system (data not shown). Emerin migrated as a 34-38 KDa doublet, most likely corresponding to the two phosphorylated states of this protein. Lamins A/C were visualized as individual protein species with a relative mobility of 70 and 60 KDa, respectively; the upper band seen in the corresponding panel was due to the detection system (data not shown). Lamin B was detected as a single protein species of 68 KDa; the upper two bands seen in the corresponding panels were due to the detection system (data not shown). In all cases, although to different extents, there appear to be changes in the expression levels of these proteins following the stress treatment (0) and during recovery at 37°C (1-25 hours), in comparison to control samples (c).

The immunoblotting analysis was further documented by quantitative densitometry. Figure 17 summarizes the quantitative changes in LAP2β expression as detected by densitometric analysis following heat shock at 42°C (fig. 17 A) or at 45°C (fig. 17 B). During both mild and severe treatments, there is an increase in the expression of this antigen after the 90 minute exposure to heat and during recovery. Lower control-like expression levels are resumed after 12 hour recovery from the mild treatment, but not after the severe treatment. The analysis indicates that the changes for this antigen lead to a significant difference between samples of a mild treatment ($p = 0.049$). There is a tendency to significance in severely treated samples ($p = 0.052$): statistical analysis showed a tendency to significance between control samples and cells recovered at 37°C for 1, 5 and 12 hours ($p = 0.061$; 0.062 and 0.051 respectively).

Figures 18 A and 18 B depict the densitometric analysis of emerin expression following a mild and severe heat-shock treatments respectively. There is a highly significant change in the expression level of this antigen from mild shock as observed in panel 19 A ($p = 0.028$). The level of expression of emerin seems to increase noticeably following 12 hours of recovery at 37°C. A highly significant change was observed at 25 hour post-heat shock period ($p = 0.007$) where emerin levels decrease drastically. It is observed that the levels of emerin following a severe heat shock fluctuate but remain within a range comparable to the control sample: the changes are not significant statistically (fig. 18 B).

Figure 16: Immunodetection of different proteins marking the nuclear periphery following mild (A) or severe (B) heat-shock treatments of HeLa S3 cells. HeLa S3 cells were untreated (C), or they were heat shocked for 90 minutes (0) and subsequently left to recover at 37°C for different lengths of time in hours (1h – 25h). Whole cell homogenates were solubilized in 2X SB and separated by SDS-PAGE on 12% resolving gels, then transferred onto nitrocellulose and blotted with the appropriate antibodies. Chemiluminescence detection of LAP2β, emerin, lamins A/C and lamin B on radiograms is shown.

A

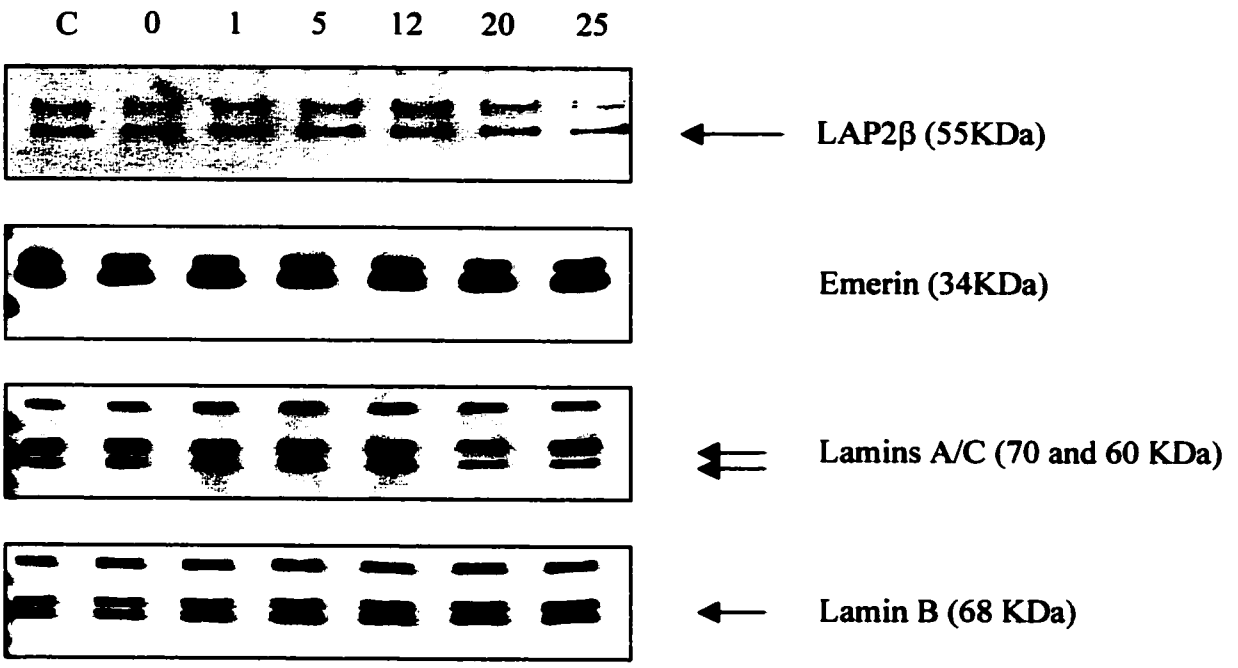
C 0 1 5 12 20 25
LAP2β (55KDa)
Emerin (34KDa)
Lamins A/C (70 and 60 KDa)
Lamin B (68 KDa)

B

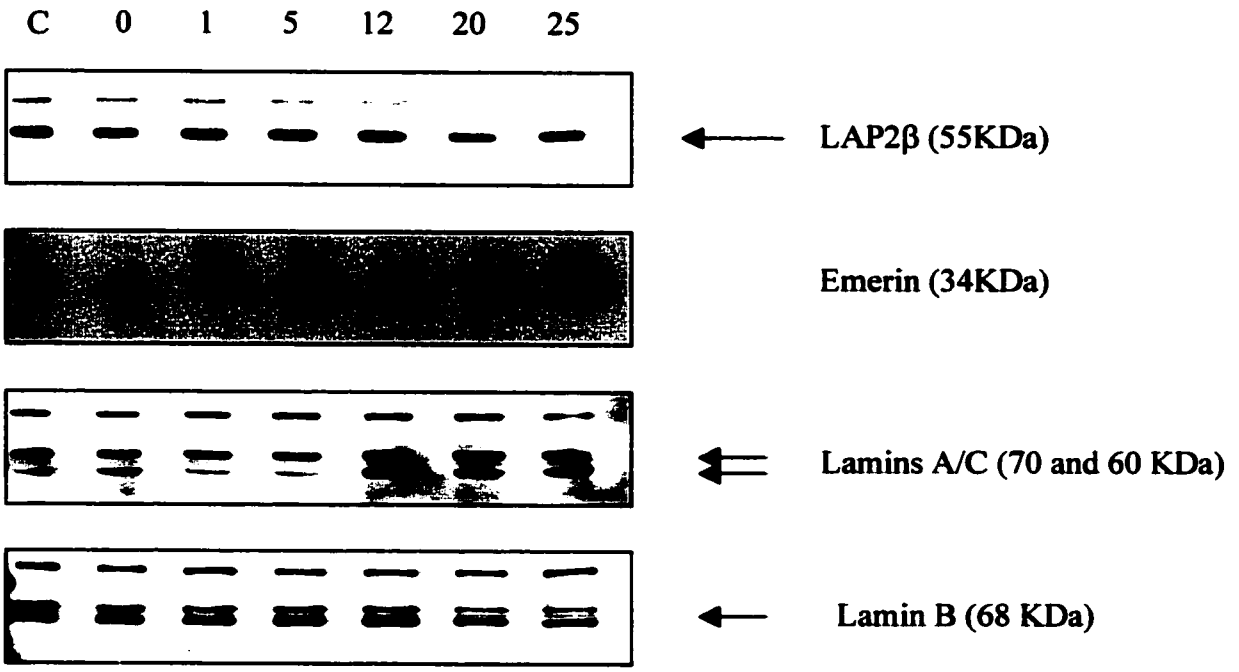
C 0 1 5 12 20 25
LAP2β (55KDa)
Emerin (34KDa)
Lamins A/C (70 and 60 KDa)
Lamin B (68 KDa)

Figure 17: Histogram showing heat-induced quantitative changes in the expression of LAP2β in HeLa S3 cells. Control HeLa S3 cells, cells heat shocked at 42°C for 90 minutes (A) or at 45°C for 90 minutes (B), and allowed to recover at 37°C for 1-25 hours were processed for SDS-PAGE and Western blotting as described in "Materials and Methods". Antibody reactivity was quantified by densitometry scans of individual bands. The data for each treatment is the mean of Residuals (n=4). Error bars show the standard error from the mean.

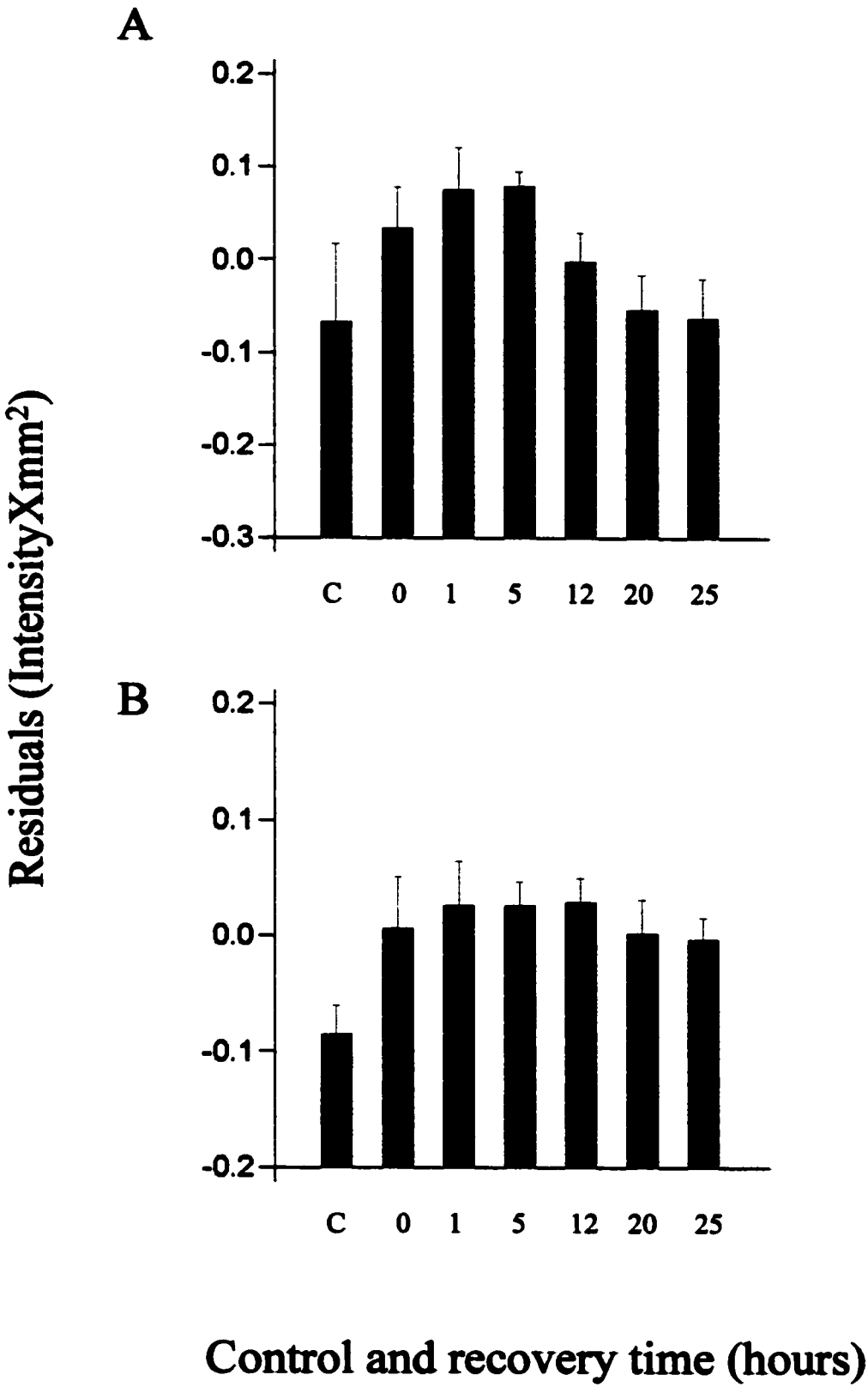
A
B
0.2
0.1
0.0
-0.1
-0.2
-0.3
C
0
1
5
12
20
25
Residuals (IntensityXmm²)
Control and recovery time (hours)

Figure 18: Histogram showing heat-induced quantitative changes in the expression of Emerin in HeLa S3 cells. Control HeLa S3 cells, cells heat shocked at 42°C for 90 minutes (A) or at 45°C for 90 minutes (B), and allowed to recover at 37°C for 1-25 hours were processed for SDS-PAGE and Western bloting as described in "Materials and Methods". Antibody reactivity was quantified by densitometry scans of individual bands. The data for each treatment is the mean of Residuals (n=4). Error bars show the standard error from the mean. * $p < 0.05$, Tukey.

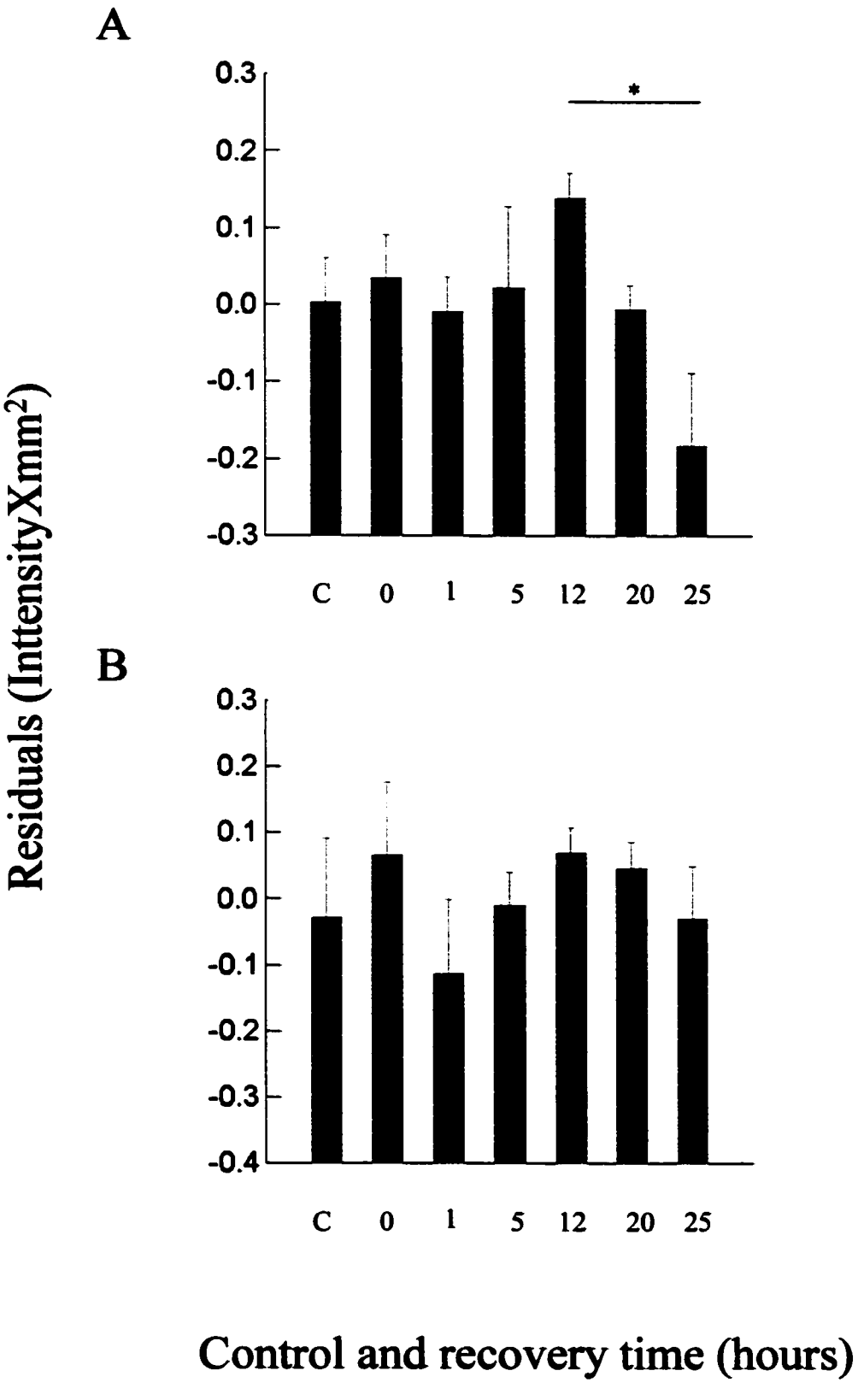
A
B
0.3
0.2
0.1
0.0
-0.1
-0.2
-0.3
-0.4
*
C 0 1 5 12 20 25
Residuals (IntensityXmm²)
Control and recovery time (hours)

Figure 19 and 20 show the changes in the expression of lamins A and C respectively by densitometric analysis. Figures 19 A (lamin A) and 20 A (lamin C) demonstrate that the expression of these lamins becomes greater following a mild treatment; they reach their highest levels after a 12 hour recovery period. However, this result is not statistically significant.

Figure 19 B (lamin A) and 20 B (lamin C) also indicates that the level of these lamins varies little upon a severe treatment and during recovery, except during the 20-25 hours recovery period where it reaches its lowest level. However, this result is not statistically significant.

Figure 21 shows the densitometric analysis of the changes in the expression of lamin B due to a mild (fig. 21 A) or severe (fig. 21 B) treatment. In panel A, the trend followed during a mild treatment is that of a gradual increase of lamin B following the treatment and the first post-treatment hours, an increase that reaches its height at 5 hours of recovery at 37°C. Then a gradual decrease is observed and the expression of this protein at 20 and 25 hours of recovery is comparable to control cells. As shown in panel B, the analysis reveals highly significant changes in the levels of expression of lamin B following a severe treatment ($p = 0.003$). Lamin B expression decreases following heat shock for 90 minutes, and then it increases after a 1-hour recovery period to restore control levels. This trend continues gradually throughout the 5 and 12 hour recovery period. The level of expression of lamin B drops considerably after 20 hour recovery time, and this reduction in protein levels is highly significant when

Figure 19: Histogram showing heat-induced quantitative changes in the expression of lamin A in HeLa S3 cells. Control HeLa S3 cells, cells heat shocked at 42°C for 90 minutes (A) or at 45°C for 90 minutes (B), and allowed to recover at 37°C for 1-25 hours were processed for SDS-PAGE and Western bloting as described in "Materials and Methods". Antibody reactivity was quantified by densitometry scans of individual bands. The data for each treatment is the mean of Residuals (n=4). Error bars show the standard error from the mean.

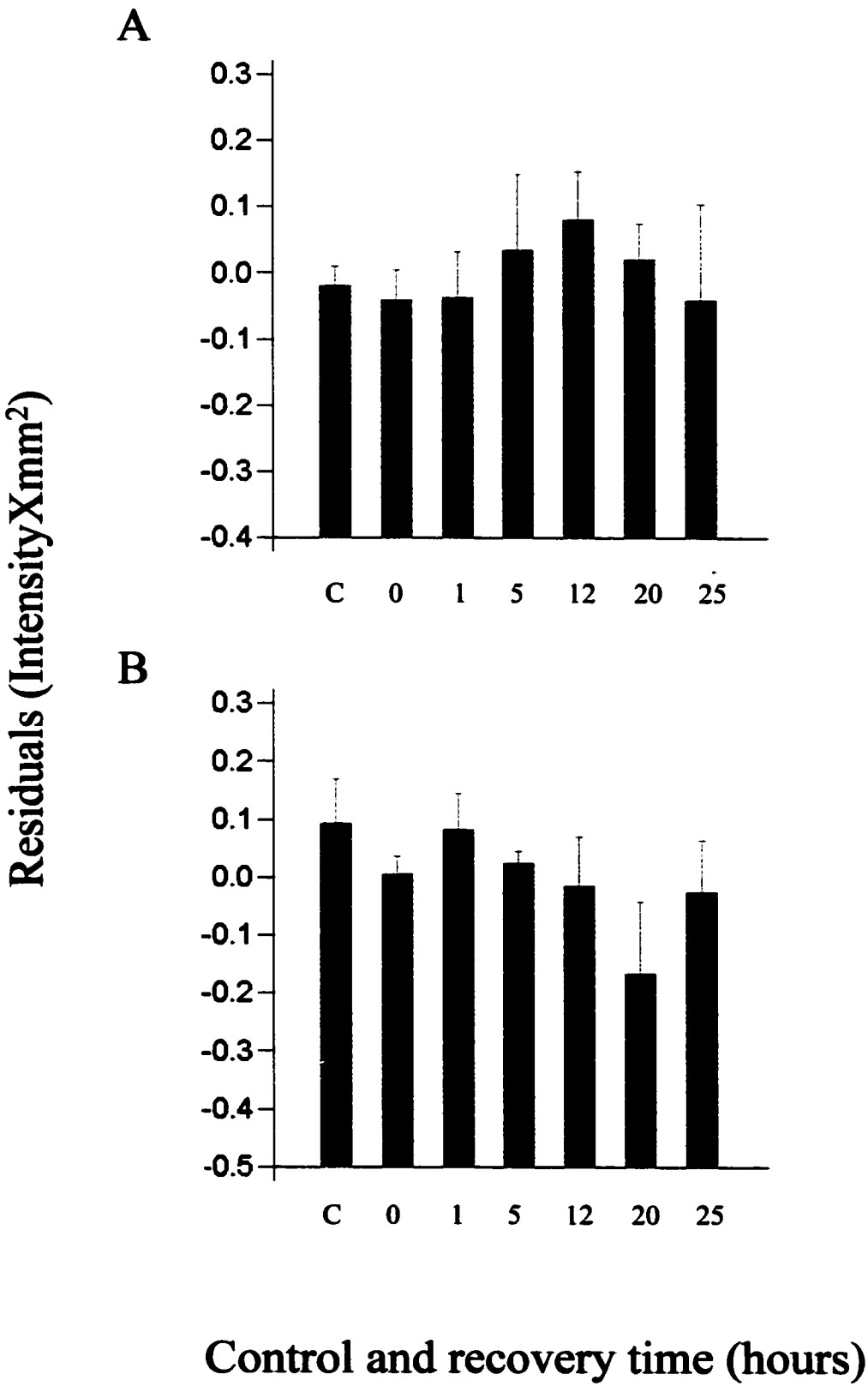
A
B
0.3
0.2
0.1
0.0
-0.1
-0.2
-0.3
-0.4
-0.5
C
0
1
5
12
20
25
Residuals (IntensityXmm²)
Control and recovery time (hours)

Figure 20: Histogram showing heat-induced quantitative changes in the expression of lamin C in HeLa S3 cells. Control HeLa S3 cells, cells heat shocked at 42°C for 90 minutes (A) or at 45°C for 90 minutes (B), and allowed to recover at 37°C for 1-25 hours were processed for SDS-PAGE and Western blotting as described in "Materials and Methods". Antibody reactivity was quantified by densitometry scans of individual bands. The data for each treatment is the mean of Residuals (n=4). Error bars show the standard error from the mean.

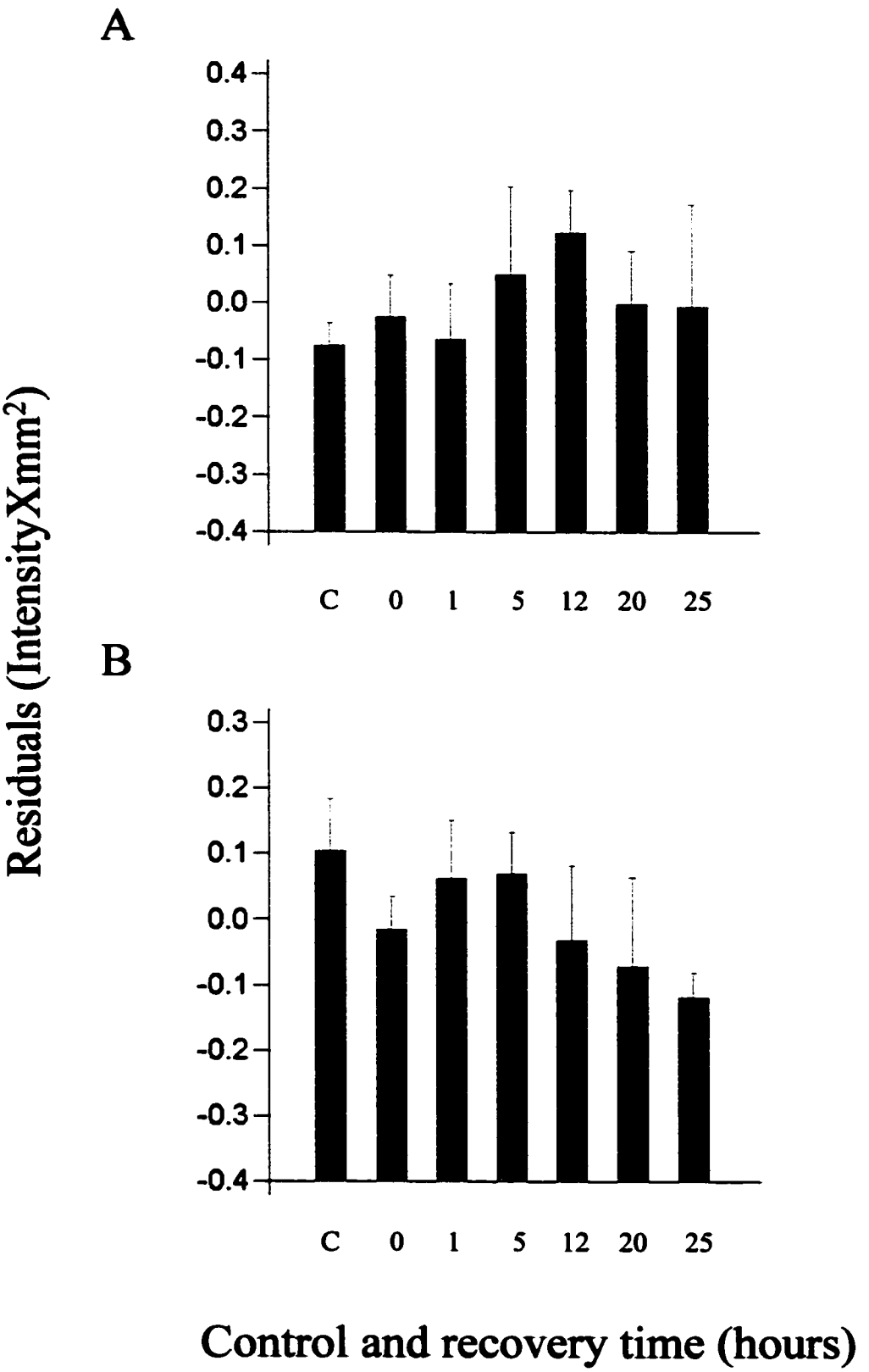
A
0.4
0.3
0.2
0.1
0.0
-0.1
-0.2
-0.3
-0.4
C 0 1 5 12 20 25
B
0.3
0.2
0.1
0.0
-0.1
-0.2
-0.3
-0.4
C 0 1 5 12 20 25
Residuals (IntensityXmm²)
Control and recovery time (hours)

compared to control samples ($p = 0.002$), and is still significant when compared to treated cells ($p = 0.05$). The reduction in the level of lamin B expression at 25 hours post-heat shock relative to 1 hour, 5 hours and 12 hours of recovery at 37°C is also highly significant ($p = 0.017$, 0.005 and 0.002 respectively).

Figure 21: Histogram showing heat-induced quantitative changes in the expression of lamin B in HeLa S3 cells. Control HeLa S3 cells, cells heat shocked at 42°C for 90 minutes (A) or at 45°C for 90 minutes (B), and allowed to recover at 37°C for 1-25 hours were processed for SDS-PAGE and Western blotting as described in "Materials and Methods". Antibody reactivity was quantified by densitometry scans of individual bands. The data for each treatment is the mean of Residuals (n=4). Error bars show the standard error from the mean. * $p < 0.05$, Tukey.

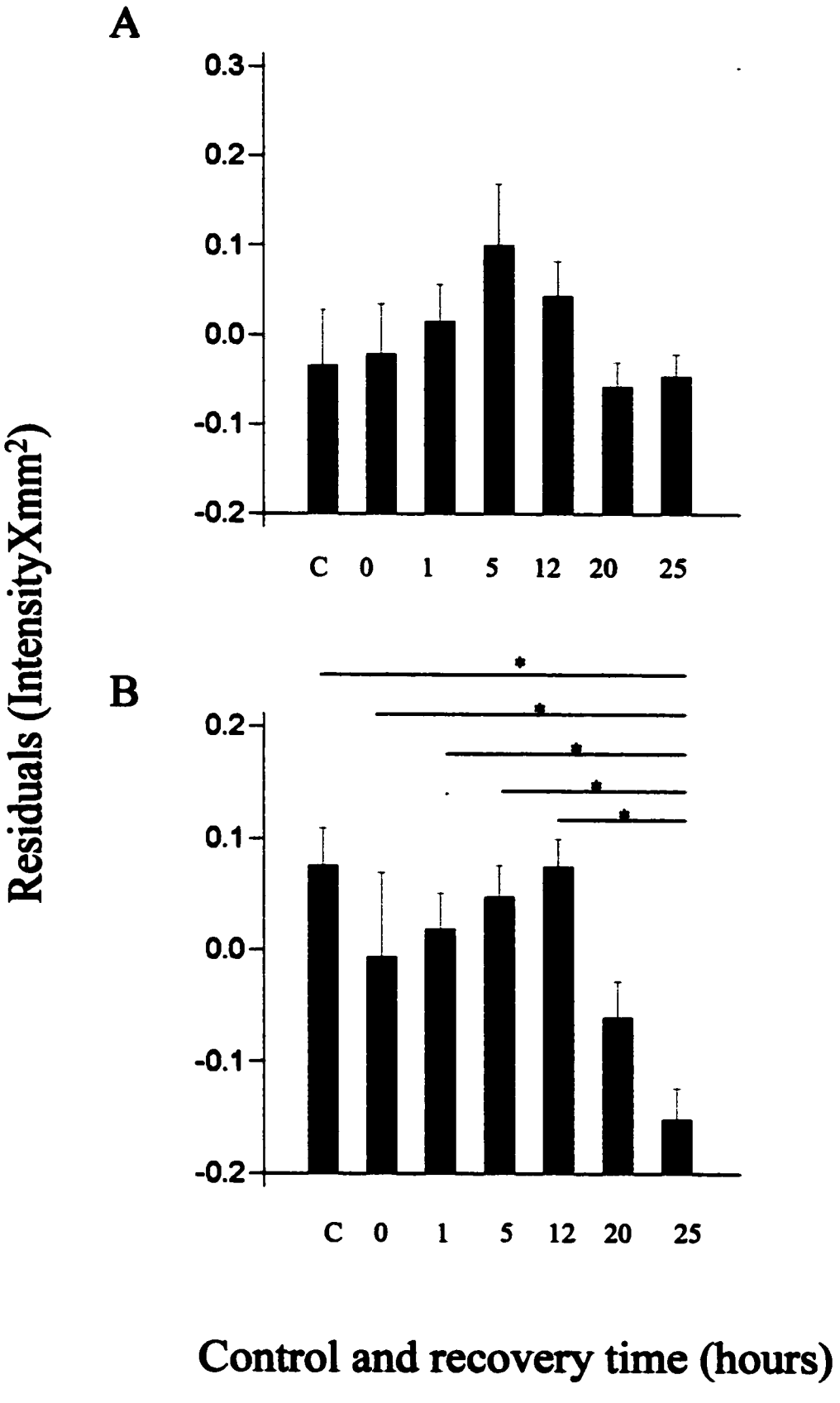
A
0.3
0.2
0.1
0.0
-0.1
-0.2
C 0 1 5 12 20 25
B
0.2
0.1
0.0
-0.1
-0.2
C 0 1 5 12 20 25
Residuals (IntensityXmm²)
Control and recovery time (hours)

2.2. Immunofluorescence monitoring and quantitative immunoblotting analysis of different proteins located in the nuclear interior of HeLa S3 cells.

Using specific antibodies, I further evaluated the effects of heat-shock stress on the structure and composition of the nuclear interior. Experiments were carried in parallel onto the following populations of HeLa S3 cells, as previously described in section 2.1 of this thesis: a) control untreated cells; b) cells heat-shocked at 42°C or 45°C for 90 minutes; and c) cells recovered at 37°C for a 25 hour period after heat-shock.

P160 is a protein first characterized by De Graaf *et al.* (1992). It is diffusely found throughout the fibrillogranular network of the nucleus, excluding the nucleoli. Studies on different cell lines, including HeLa cells, showed that upon mild treatment (42°C) for 3 hours, this protein changes its diffuse distribution within the nuclear interior to become clustered into 2-10 large bright foci.

Figure 22 summarizes the immunofluorescence results obtained using an anti-P160 antibody. In control HeLa S3 cells (figure 22 a-a") P160 is located diffusely in the nucleoplasm (excluding the nucleoli). A mild heat-shock for 90 minutes resulted in the cells showing a reorganization of this antigen into bright clusters: figure 22 b" shows a mildly stressed cell that has a few bright clusters in addition to its nucleoplasmic distribution. A mild stress for 3 hours (figure 22 c"), as previously described by De Graaf *et al.* (1992), promoted the formation of P160 clusters of varying size and brightness. However, this protein was still

located in the nucleoplasm to a lesser extent. Figure 22 d-d" shows cells mildly treated and recovered at 37°C for 20 hours. This protein has regained its diffused organization within the nucleoplasm, excluding the nucleoli (fig. 22 d"). Figure 22 e-e" and f-f" show HeLa S3 cells severely treated, and cells recovered at 37°C for 20 hours after a severe stress respectively. As seen in figure 22 e", the P160 protein is located throughout the nucleoplasm excluding the nucleoli, as in control cells (fig. 22 a"). Major reorganization of P160 occurred in HeLa S3 cells recovered for 20 hours after a severe stress (figure 22 f"). Over 90% of cells showed a change in the distribution of P160, although this protein remained nucleoplasmic, round clusters of varying sizes formed. The reorganization of P160 antigen in HeLa S3 cells supported the validation of the heat-shock system used in this study.

The 1B4 antigen localizes in nuclear "speckles", which are sites of mRNA splicing. The speckles usually vary in size and have irregular shapes. Figure 23 shows the distribution of the 1B4 protein in control HeLa S3 cells (fig. 23 a-a"). The anti-1B4 labels foci of irregular shape and size within the nucleoplasm (excluding the nucleoli). A mild heat-shock treatment (42°C) for 90 minutes (fig. 23 b-b") shows that HeLa S3 cells maintain the same spot-like distribution of 1B4 (fig. 23 b"), when compared to control cells (fig. 23 a"). A mild stress followed by 20 hours recovery at 37°C (fig. 23 c-c") does not affect the organization of this protein (fig. 23 c"). The speckled distribution of 1B4 in severely heat-shocked cells (fig. 23 d-d") usually resembles that of control cells. In some cases however, the intensity of 1B4 detection appeared to be diminished

Figure 22: Immunolocalization of P160 following heat-shock treatments of HeLa S3 cells. HeLa S3 cells were grown on coverslips and treated for the appropriate time; they were then fixed with 3% paraformaldehyde, permeabilized with Triton X-100 and stained. Cells were observed by phase contrast microscopy (a, b, d, c, e and f). Cells were single-labeled for immunofluorescence with anti-P160 (a", b", c", d", e" and f"). Preparations were counterstained with Hoechst 33258 (a', b', c', d', e' and f'). The pictures show untreated cells (a-a''), heat-shocked cells at 42°C for 90 minutes (b-b'') and for 3 hours (c-c"), cells that recovered at 37°C for 20 hours after a mild treatment (d-d"), cells heat-shocked at 45°C for 90 minutes (e-e"), cells that recovered at 37°C for 20 hours after a severe treatment (f-f"). Bar represents 10 μm.

a
a'
a''
b
b'
b''
c
c'
c''
d
d'
d''
e
e'
e''
f
f'

Figure 23: Immunolocalization of 1B4 following heat-shock treatments of HeLa S3 cells. HeLa S3 cells were grown on coverslips and treated for the appropriate time; they were then fixed with 3% paraformaldehyde, permeabilized with Triton X-100 and stained. Cells were observed by phase contrast microscopy (a, b, d, c and e). Cells were single-labeled for immunofluorescence with anti-1B4 (a", b", c", d" and e"). Preparations were counterstained with Hoechst 33258 (a', b', c', d' and e'). The pictures show untreated cells (a-a''), heat-shocked cells at 42°C for 90 minutes (b-b''), cells that recovered at 37°C for 20 hours after a mild treatment (c-c"), cells heat-shocked at 45°C for 90 minutes (d-d"), cells that recovered at 37°C for 20 hours after a severe treatment (e-e"). Bar represents 10 μm.

a
a'
a''
b
b'
b''
c
c'
c''
d
d'
d''
e
e'
e''

considerably. In cells recovered at 37°C for 20 hours after a severe stress (fig. 23 e-e"), the intensity of the 1B4 antibody signal has lessened and few cells maintain their control distribution.

2A7 is a nucleocytoplasmic shuttling protein localized in the nucleoplasm, sometimes including the nucleoli (fig. 24 a-a") of control HeLa S3 cells. In HeLa S3 cells subjected to mild stress (fig. 24 b-b"), 2A7 remained nucleoplasmic. However, this antigen seemed to gain a more granular appearance. This result is more evident in figure 24 c-c" where four cells that recovered for 20 hours at 37°C following mild treatment are shown. In figures 24 b" and c", anti-2A7 labels the nuclear contour in an uneven manner or "flower-shape". Figure 24 d-d" and e-e" represent severely treated cells and cells recovered at 37°C for 20 hours after a severe shock respectively. It can be seen in both panels that 2A7 is reorganized in HeLa S3 cells. This antigen shows a lesser nucleolar distribution and it seems that, at least partially, it migrated from the nucleoli to the nucleoplasm (arrows in fig. 24 d" and e"), for the nucleolar space is well defined in these cells as compared to control cells (fig. 24 a"). The nucleolus seems devoid of 2A7. In all mild and severely treated cells, 2A7 seems to gain an inward compaction towards the nuclear interior.

The next microscopic observations concentrated on nucleolar proteins 2H12 (figure 25) and fibrillarin (figure 26). 2H12 is a structural protein found in the nucleolus of HeLa S3 cells, as depicted in figure 25 a". The nucleolar distribution of this protein remains unchanged after a mild heat-shock treatment (fig. 25 b-b"), and after cells recover at 37°C for 20 hours (fig. 25 c-c"). A severe

Figure 24: Immunolocalization of 2A7 following heat-shock treatments of HeLa S3 cells. HeLa S3 cells were grown on coverslips and treated for the appropriate time; they were then fixed with 3% paraformaldehyde, permeabilized with Triton X-100 and stained. Cells were observed by phase contrast microscopy (a, b, d, c and e). Cells were single-labeled for immunofluorescence with anti-2A7 (a", b", c", d" and e"). Preparations were counterstained with Hoechst 33258 (a', b', c', d' and e'). The pictures show untreated cells (a-a''), heat-shocked cells at 42°C for 90 minutes (b-b''), cells that recovered at 37°C for 20 hours after a mild treatment (c-c"), cells heat-shocked at 45°C for 90 minutes (d-d"), cells that recovered at 37°C for 20 hours after a severe treatment (e-e"). Bar represents 10 μm.

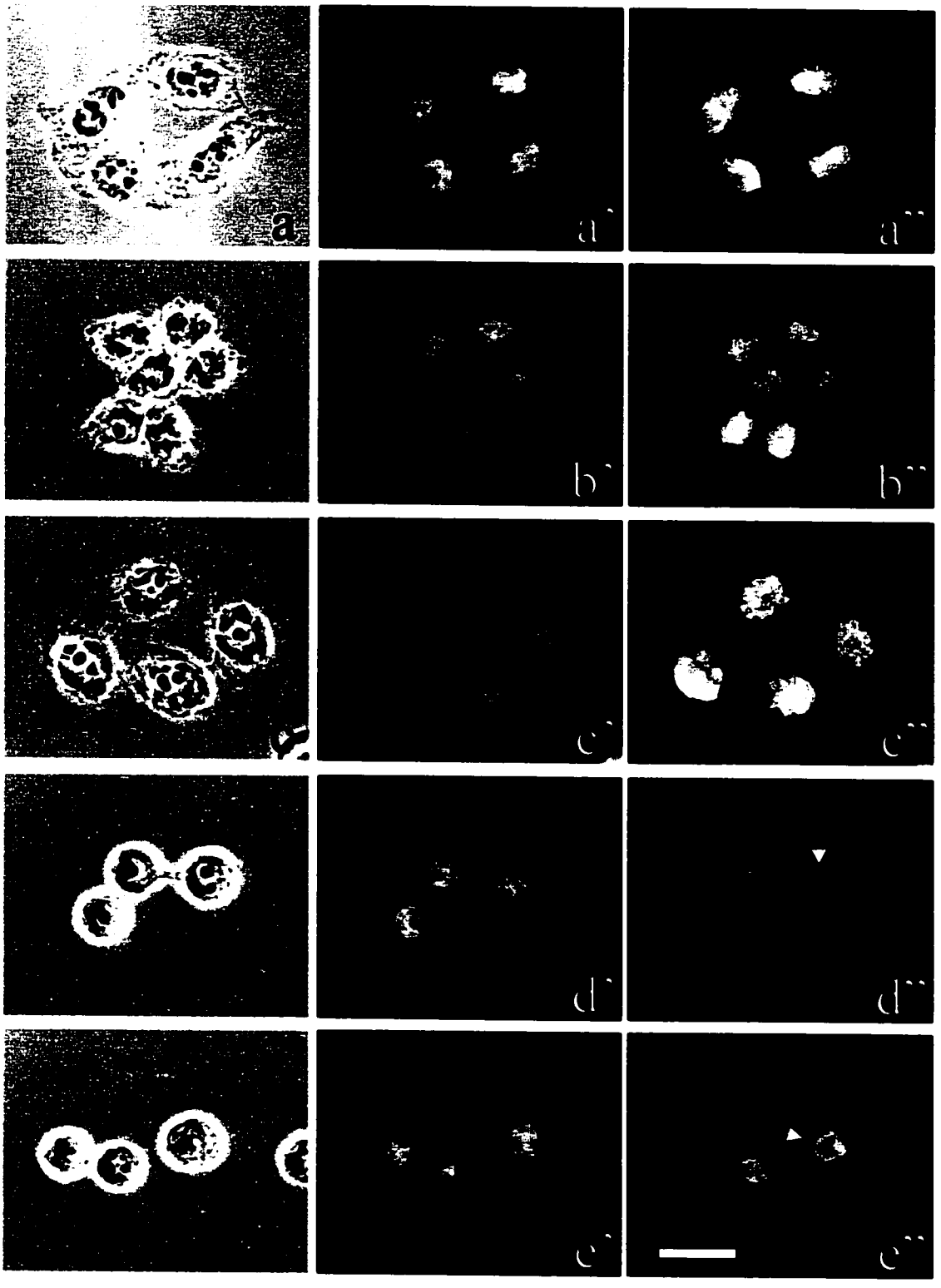
a
a'
a''
b'
b''
c'
c''
d'
d''
e'
e''

Figure 25: Immunolocalization of 2H12 following heat-shock treatments of HeLa S3 cells. HeLa S3 cells were grown on coverslips and treated for the appropriate time; they were then fixed with 3% paraformaldehyde, permeabilized with Triton X-100 and stained. Cells were observed by phase contrast microscopy (a, b, d, c and e). Cells were single-labeled for immunofluorescence with anti-2H12 (a", b", c", d" and e"). Preparations were counterstained with Hoechst 33258 (a', b', c', d' and e'). The pictures show untreated cells (a-a''), heat-shocked cells at 42°C for 90 minutes (b-b''), cells that recovered at 37°C for 20 hours after a mild treatment (c-c"), cells heat-shocked at 45°C for 90 minutes (d-d"), cells that recovered at 37°C for 20 hours after a severe treatment (e-e"). Bar represents 10 μm.

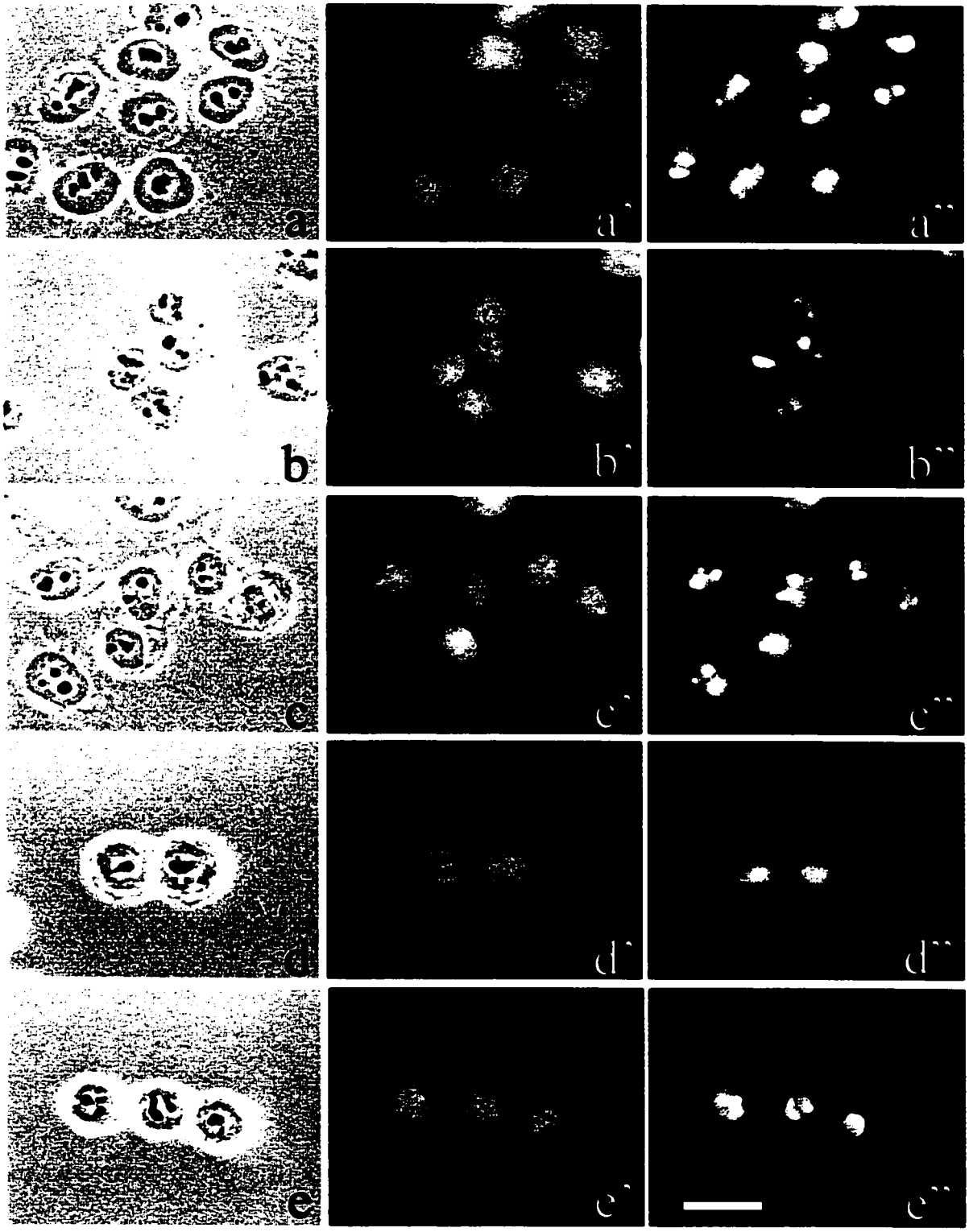
a
a'
a''
b
b'
b''
c
c'
c''
d
d'
d''
e
e'
e''

treatment (fig. 25 d-d") did not induce any detectable change in the form of the nucleoli (fig. 25 d). However, 2H12 seems "hidden", as if a veil covered it (fig. 25 d"). In cells recovered at 37°C for 20 hours (fig. 25 e-e"), the masking effect over 2H12 is still present, although 40-50% of cells resemble control HeLa S3.

Fibrillarin, a protein involved in ribosomal RNA (rRNA) processing is found in nucleoli and in Cajal bodies (or coiled bodies) of HeLa S3 cells (figure 26 a-a"). A mild heat-shock treatment (fig. 26 b-b") shows that HeLa S3 cells maintain a similar distribution of fibrillarin as in control cells. A 20 hour recovery at 37°C after a mild stress (fig. 26 c-c") results in the same localization of fibrillarin in HeLa S3 cells. However, the presence of this protein in coiled bodies seems more prominent than in nucleoli (fig. 26 c"). Figure 27 d-d" shows four severely heat-shocked cells. It is evident that the localization of fibrillarin within the nucleoli of these cells (arrows in fig. 26 d") is altered. Fibrillarin is found in smaller dot-like structures close to one another, indicative of possible alterations in the distribution of this protein. Figure 26 e-e" shows the distribution of fibrillarin in HeLa S3 cells after a severe heat-shock and 20 hours of recovery. It is clear that there is a reorganization of fibrillarin, as this protein is now found into the nucleoplasm and the number of the dot-like structures has increased (arrow in fig. 26 e").

In figure 27, Western blot analysis was done with specific antibodies to the nuclear interior proteins PCNA, 2A7, 2H12 and fibrillarin, and typical radiograms are depicted. P160 was not analyzed by Western blotting due to antibody

Figure 26: Immunolocalization of fibrillarin following heat-shock treatments of HeLa S3 cells. HeLa S3 cells were grown on coverslips and treated for the appropriate time; they were then fixed with 3% paraformaldehyde, permeabilized with Triton X-100 and stained. Cells were observed by phase contrast microscopy (a, b, d, c and e). Cells were single-labeled for immunofluorescence with anti-fibrillarin (a", b", c", d" and e"). Preparations were counterstained with Hoechst 33258 (a', b', c', d' and e'). The pictures show untreated cells (a-a''), heat-shocked cells at 42°C for 90 minutes (b-b''), cells that recovered at 37°C for 20 hours after a mild treatment (c-c"), cells heat-shocked at 45°C for 90 minutes (d-d"), cells that recovered at 37°C for 20 hours after a severe treatment (e-e"). Bar represents 10 μm.

a'
a''
b'
b''
c'
c''
d'
d''
e'
e''

Figure 27: Immunodetection of different proteins marking the nuclear interior following mild (A) or severe (B) heat-shock treatments of HeLa S3 cells. HeLa S3 cells were untreated (C), or they were heat shocked for 90 minutes (0) and subsequently left to recovered at 37°C for different lengths of time in hours (1h - 25h). Whole cell homogenates were solubilized in 2X SB and separated by SDS-PAGE on 12% resolving gels, then transferred onto nitrocellulose and blotted with the appropriate antibodies. Chemiluminescence detection of PCNA, 2A7, 2H12 and fibrillarin on radiograms is shown.

A

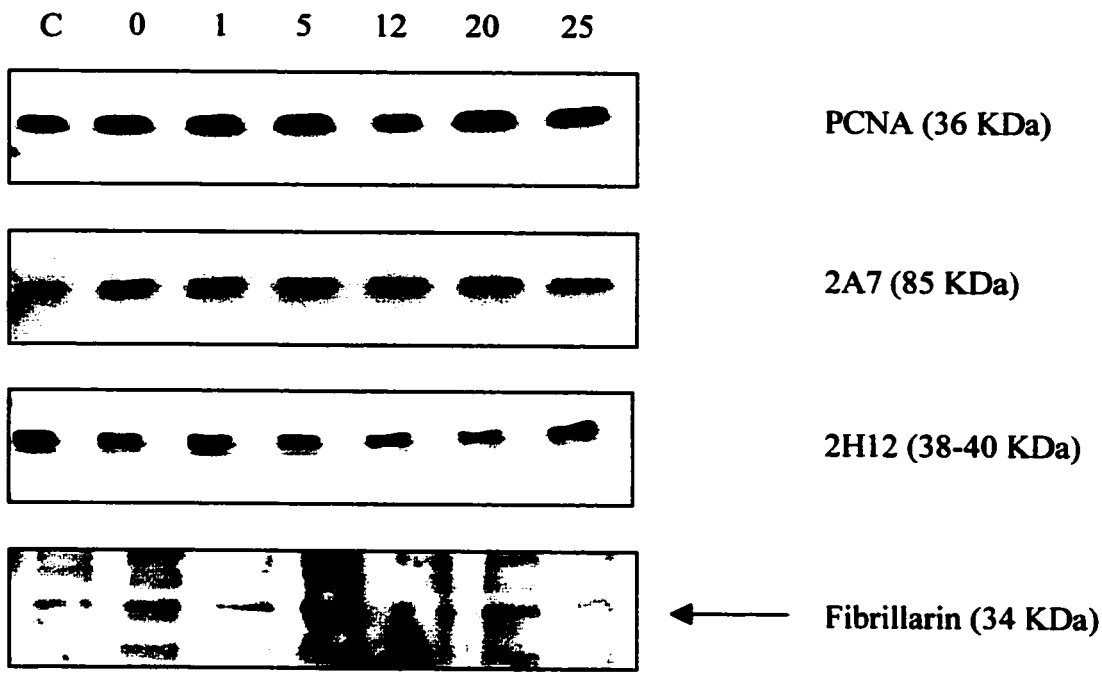
C 0 1 5 12 20 25
PCNA (36 KDa)
2A7 (85 KDa)
2H12 (38-40 KDa)
Fibrillarin (34 KDa)

B

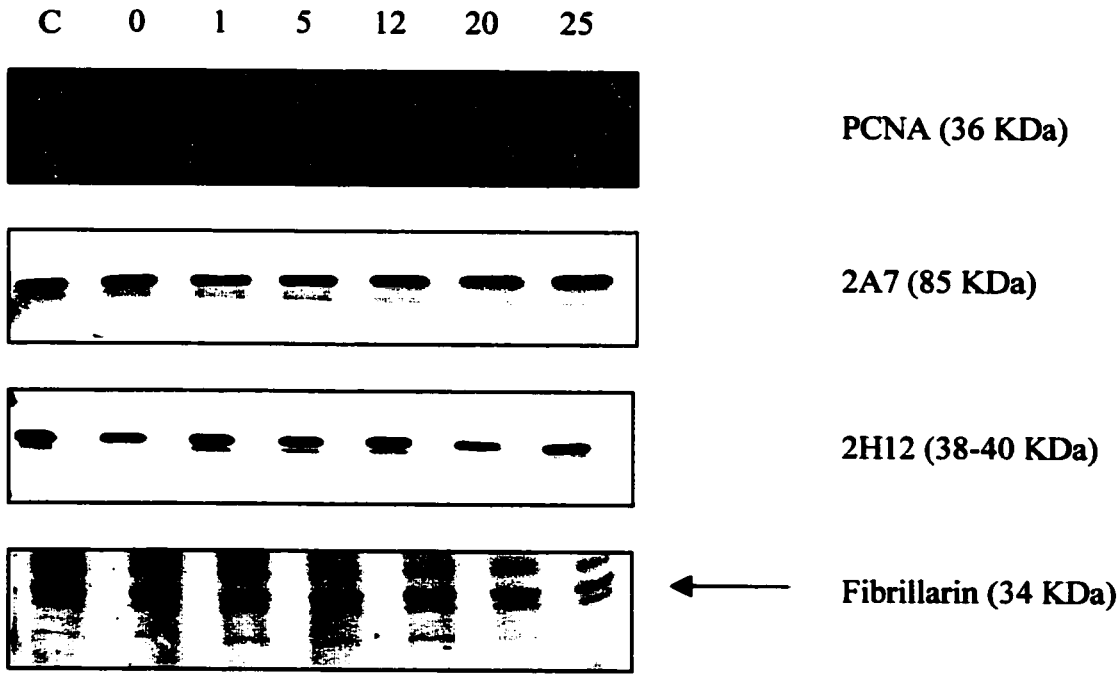
C 0 1 5 12 20 25
PCNA (36 KDa)
2A7 (85 KDa)
2H12 (38-40 KDa)
Fibrillarin (34 KDa)

availability. The 1B4 antigen was not analyzed by Western blot because the denatured form of this protein is not recognized by the antibody. As seen in this figure, PCNA and 2A7 were detected as single bands with a relative mobility of 36 KDa and 85 KDa respectively. 2H12 migrated as a 38-40 KDa doublet. Fibrillarin was visualized as an individual protein species with a relative mobility of 34 KDa. The upper and lower bands seen in the corresponding panel were found to be due to non-specific binding of the detection system (data not shown). Figure 27A indicates that the expression of this protein increases at 5 hours post-mild treatment. This increase is not sustained afterwards throughout the rest of the 25 hour recovery period. Whereas figure 27B indicates that the concentration of this protein appears to decrease due to a severe heat shock and to be further reduced throughout the recovery period. Unfortunately, quantitative analysis for this antigen was assayed and could not be obtained due to a weak signal.

The quantitative changes in the level of expression of PCNA as analyzed by densitometric analysis are shown in figure 28 A for a mild heat-shock and figure 28B for a severe one. The general incline of graph 28 A indicates that PCNA levels increased when compared to control, this change was maintained throughout the recovery period at 37°C. This increase of expression was found to be statistically not significant. In figure 28B, a change in the level of expression of PCNA between treatments was highly significant ($p = 0.031$). The tendency of the graph indicates that PCNA levels diminish gradually following the treatment and 1 hour recovery at 37°C. At 5 and 12 hour recovery, PCNA levels

become greater and are similar to those in control cells following 20 hours recovery. PCNA levels reach their highest levels following 25 hours recovery post-heat shock; this increase is highly significant when compared to the 1-hour recovery period ($p = 0.039$).

Figure 29 indicates the quantitative changes observed in the level of expression of the nucleocytoplasmic shuttling protein 2A7. Figure 29 A shows the resulting analysis of a mild heat shock. It seems generally that 2A7 has a tendency to augment following heat shock, although its expression after 5 and 20 hours recovery resembles that of control cells.

Figure 29 B demonstrates a highly significant reduction in the expression of 2A7 ($p = 0.000$). The trend of this graph indicates that 2A7 levels within cells decrease gradually following severe heat shock. This gradual decrease is highly significant as observed between control cells and cells that recovered at 37°C for: 5 hours ($p = 0.014$), 12 hours ($p = 0.009$), 20 hours ($p = 0.000$) and 25 hours ($p = 0.001$). A significant difference is observed between treated cells and the 20 hour recovery period ($p = 0.007$). Also, a tendency to significance was observed between treated cell samples, and samples recovered at 37°C for 25 hours ($p = 0.064$). 2A7 reaches its lowest level of expression following the 20 hours recovery period, and it is significantly lower when compared to 1 hour post-treatment ($p = 0.028$).

Figure 30 shows densitometric analysis of mild (fig. 30 A) and severe (fig. 30 B) heat-shock treatments on the nucleolar protein 2H12. A mild heat shock treatment results in a significant reduction in the expression of this protein ($p =$

Figure 28: Histogram showing heat-induced quantitative changes in the expression of PCNA in HeLa S3 cells. Control HeLa S3 cells, cells heat shocked at 42°C for 90 minutes (A) or at 45°C for 90 minutes (B), and allowed to recover at 37°C for 1-25 hours were processed for SDS-PAGE and Western bloting as described in "Materials and Methods". Antibody reactivity was quantified by densitometry scans of individual bands. The data for each treatment is the mean of Residuals (n=4). Error bars show the standard error from the mean. * $p < 0.05$, Tukey.

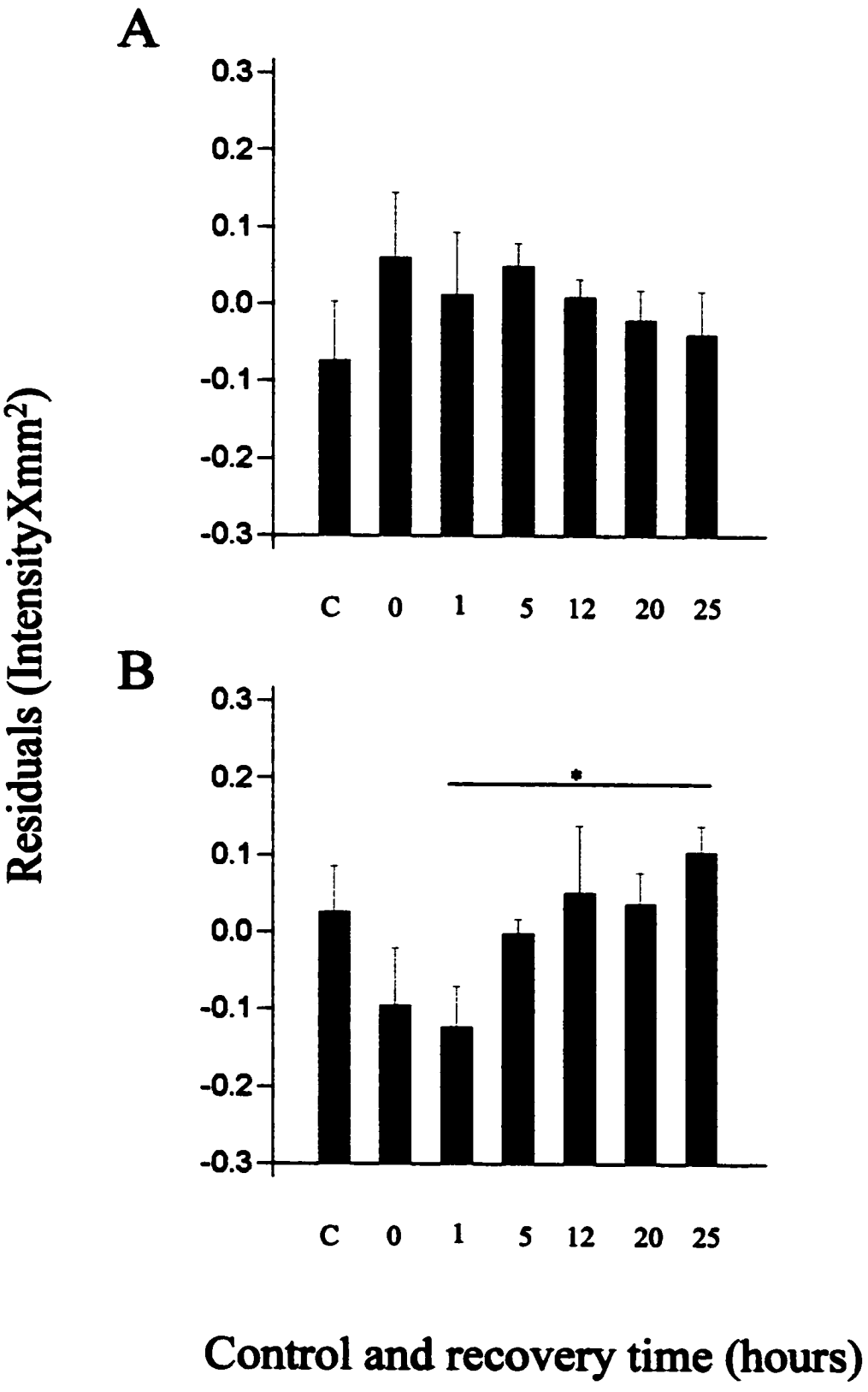
A
B
0.3
0.2
0.1
0.0
-0.1
-0.2
-0.3
C
0
1
5
12
20
25
*
Residuals (IntensityXmm²)
Control and recovery time (hours)

Figure 29: Histogram showing heat-induced quantitative changes in the expression of 2A7 in HeLa S3 cells. Control HeLa S3 cells, cells heat shocked at 42°C for 90 minutes (A) or at 45°C for 90 minutes (B), and allowed to recover at 37°C for 1-25 hours were processed for SDS-PAGE and Western bloting as described in "Materials and Methods". Antibody reactivity was quantified by densitometry scans of individual bands. The data for each treatment is the mean of Residuals (n=4). Error bars show the standard error from the mean. * $p < 0.05$, Tukey.

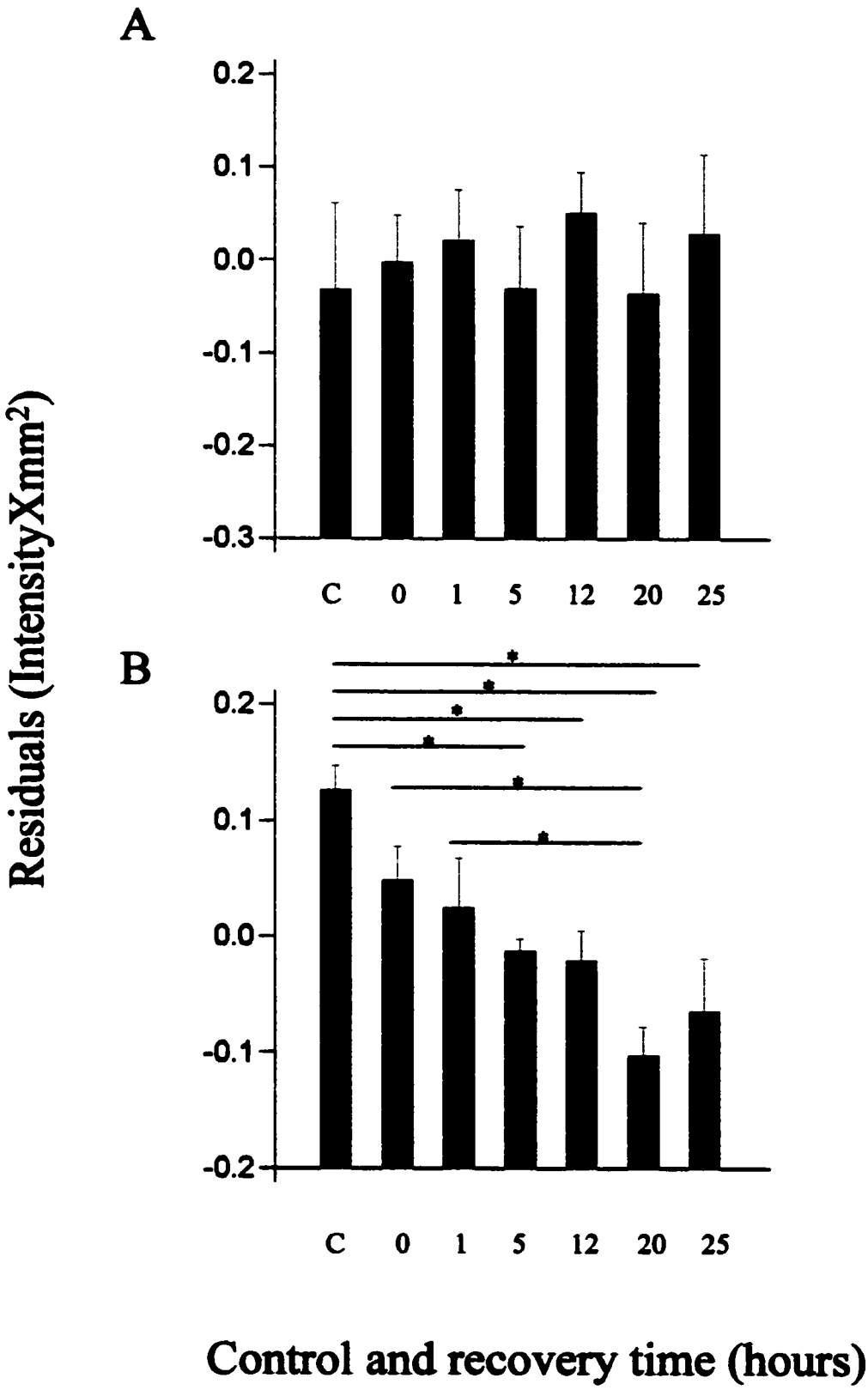
A
B
0.2
0.1
0.0
-0.1
-0.2
-0.3
C 0 1 5 12 20 25
Residuals (IntensityXmm²)
Control and recovery time (hours)

Figure 30: Histogram showing heat-induced quantitative changes in the expression of 2H12 in HeLa S3 cells. Control HeLa S3 cells, cells heat shocked at 42°C for 90 minutes (A) or at 45°C for 90 minutes (B), and allowed to recover at 37°C for 1-25 hours were processed for SDS-PAGE and Western blotting as described in "Materials and Methods". Antibody reactivity was quantified by densitometry scans of individual bands. The data for each treatment is the mean of Residuals (n=4). Error bars show the standard error from the mean. * $p < 0.05$, Tukey.

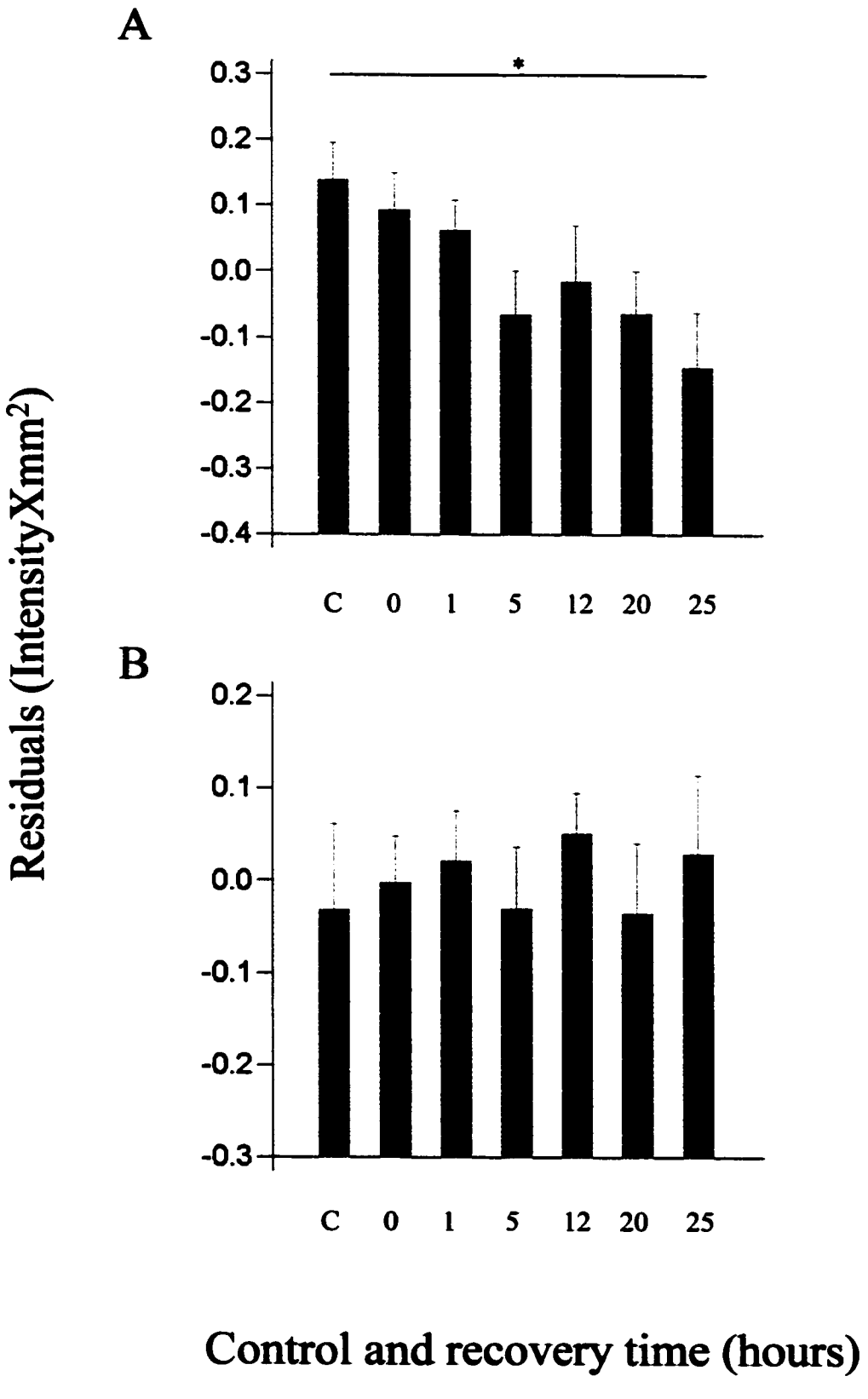
A
*
0.3
0.2
0.1
0.0
-0.1
-0.2
-0.3
-0.4
C 0 1 5 12 20 25
B
0.2
0.1
0.0
-0.1
-0.2
-0.3
C 0 1 5 12 20 25
Residuals (IntensityXmm²)
Control and recovery time (hours)

0.019). The trend of the graph indicates that 2H12 expression decreases gradually following heat shock and recovery at 37°C for 1 and 5 hours when compared to control levels. This decrease in expression is accentuated after 5 hours recovery; then it starts augmenting again at 12 hours post-heat shock. A significant difference is obtained between control samples and samples collected at 25 hours post-heat shock ($p = 0.024$), where this protein reaches its lowest levels of expression. A tendency to significance is observed between mildly treated cells and the 25 hour recovery time at 37°C ($p = 0.08$).

Figure 30 B indicates that the expression of 2H12 fluctuates following a severe treatment but to levels comparable to control samples. Statistical analysis did not indicate any significant change in the level of expression of 2H12 in this case.

2.3. Immunofluorescence monitoring of Hsp70, fibrillarin and 2A7 in nuclear matrices of HeLa S3 cells

The changes observed in the localization of the Hsp70, fibrillarin, and 2A7 antigens following heat-shock prompted us to investigate their relationship to the nuclear matrix under stress conditions. This was done by monitoring the behavior of these three proteins following *in situ* isolation of nuclear matrices from HeLa S3 cells using immunofluorescence microscopy.

HeLa S3 cells processed for *in situ* nuclear matrices (NM) preparations (Chaly *et al.* 1985) included the following cell populations: a) control untreated HeLa S3 cells; b) HeLa S3 cells heat-shocked at 42°C or 45°C for 90 minutes; c) HeLa S3 cell heat-shocked at either temperatures for 90 minutes and recovered at 37°C for 20 hours. Nuclear matrices preparations were subsequently fixed and stained for the detection of Hsp70, fibrillarin and 2A7. Each preparation was compared to control intact HeLa S3 cells.

Figure 31 summarizes the results obtained for *in situ* nuclear matrices stained with Hsp70. In control intact cells (fig. 31 a-a"), Hsp70 localizes in the nucleus (including the nucleoli) and the cytoplasm (fig. 31a"). When cells are processed for *in situ* NM preparations, they are subjected to harsh salt extractions and permeabilization with 0.5% Triton X-100, so there is little cytoplasmic fraction left. In NM preparations of control cells digested with DNase I (fig. 31 b-b") or with DNase I and RNase A (fig. 31 c-c"), Hsp70 maintains its nuclear localization (including the nucleoli) as in intact cells. However, its brightness diminished, as some of this antigen may have been lost during the extraction.

After a mild heat-shock and DNase I digestion, Hsp70 became prominent in the nucleoli (fig. 31 d-d"), although anti-Hsp70 did stain the nucleoplasm to a lesser extent. This may be due to a translocation of this antigen to the nucleoli following heat-shock (fig. 8 b-b"). A mild stress and sequential digestions with DNase I and RNase A resulted in Hsp70 maintaining its nucleoplasmic localization, excluding the nucleoli (fig. 31 e-e"). Rarely was Hsp70 more prominent in the nucleoli. It is possible that some Hsp70 was lost during the extraction, its brightness seemed to have diminished when compared to control cells (fig. 31a"). Figure 31 e" also demonstrates that Hsp70 is less found in the areas apposed the nuclear periphery.

In situ NM preparations of HeLa S3 cells recovered for 20 hours at 37°C and digested with DNase I showed that Hsp70 redistributed itself within the rest of the nucleoplasm, while remaining in the nucleoli (fig. 31 cont. f-f"). The same observations occurred for recovered cells digested with DNase I and RNase A (fig. 31. g-g") meaning that Hsp70 regained its nucleolar distribution as well. This relocalization of Hsp70 resembles that of control cells (fig. 31a-a").

A severe heat stress and digestions with DNase I only (fig. 31 h-h") or with DNase I and RNase A (fig. 31 i-i") showed that Hsp70 had a distribution similar to control cells (fig. 31 b" and c" respectively). It remained associated with the NM, although some of this antigen may have been lost during the extraction. In cells recovered at 37°C for 20 hours following a severe shock and digested with DNase I (fig. 31 j-j"), Hsp70 distribution is nucleoplasmic, including the

Figure 31: Immunolocalization of Hsp70 during *in situ* nuclear matrices (NM) preparations of heat-shocked HeLa S3 cells. Cells were observed by phase contrast microscopy (a, b, c, d and e). Cells were single-labeled for immunofluorescence with anti-Hsp70 (a", b", c", d" and e"). Preparations were counterstained with Hoechst 33258 (a', b', c', d' and e'). The pictures show untreated intact cells (a-a"); control NM preparations digested with DNase I (b-b"), or with DNase I and RNase A (c-c"); mildly stressed NM preparations digested with DNase I (d-d"), or with DNase I and RNase A (e-e"). Bar represents 10 μm.

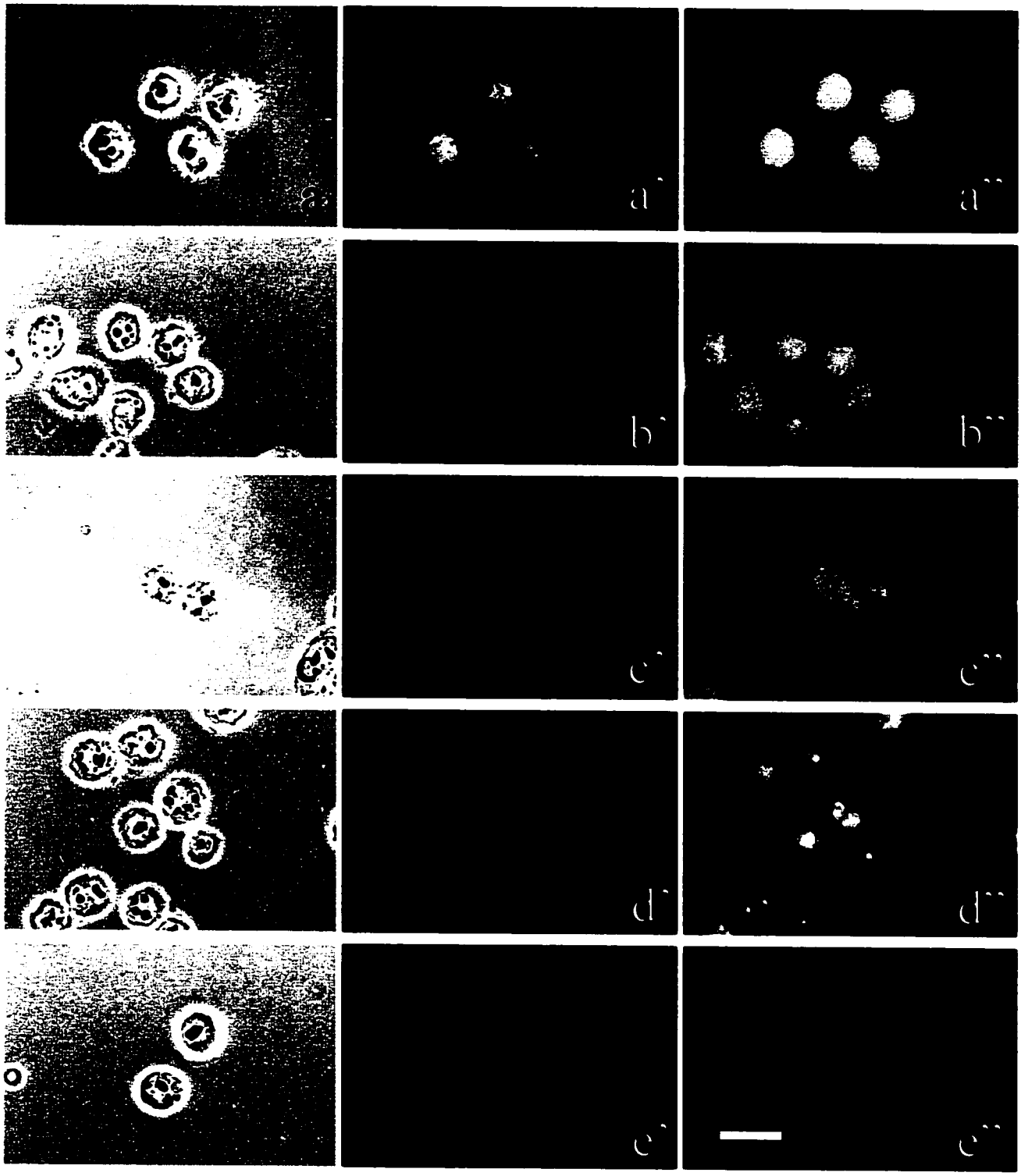
a
a'
a''
b
b'
b''
c
c'
c''
d
d'
d''
e
e'
e''

Figure 31 (continued): Immunolocalization of Hsp70 during *in situ* nuclear matrices (NM) preparations of heat-shocked HeLa S3 cells. Cells were observed by phase contrast microscopy (f, g, h, i, j and k). Cells were single-labeled for immunofluorescence with anti-Hsp70 (f", g", h", i", j" and k"). Preparations were counterstained with Hoechst 33258 (f', g', h', i', j' and k'). The pictures show NM preparations of mildly stressed HeLa S3 cells recovered at 37°C for 20 hours and digested with DNase I (f-f") or with DNase I and RNase A (g-g"); severely stressed NM preparations digested with DNase I (h-h") or with DNase I and RNase A (i-i"); NM preparations of severely stressed HeLa S3 cells recovered at 37°C for 20 hours and digested with DNase I (j-j") or with DNase I and RNase A (k-k"). Bar represents 10 μm.

f
f'
f''
g
g'
g''
h
h'
h''
i
i'
i''
j
j'
j''
k
k'
k''

nucleoli. After a double digestion with DNase I and RNase A, (fig. 31 k-k"), Hsp70 maintains this distribution. In both figures 31 j" and k", Hsp70 seems also to form nuclear circular structures which do not always coincide with nucleolar staining.

Figure 32 shows the results obtained for *in situ* NM matrices stained with anti-fibrillarin. In control untreated cells, fibrillarin localizes in nucleoli and coiled bodies of HeLa S3 cells (fig. 32a-a"). In NM preparations of control cells digested with DNase I (fig. 32 b-b"), this antigen is localized in nucleoli and coiled bodies of HeLa S3 NM, as in intact cells (fig. 32 a"). A double digestion with DNase I and RNase A results in some antigen redistributing within the nucleoplasm, while mainly fibrillarin remained nucleolar (fig. 32 c-c"). Following digestion with nucleases, fibrillarin may have been lost during the extraction.

A mild stress and DNase I digestion does not change the distribution of fibrillarin; this antigen was detected in the nucleoli and coiled bodies (fig. 32 d-d") of HeLa S3 NM, this result is similar to control NM digested with DNase I only (fig.32 b") and to intact cells (fig. 32 a"). A sequential digestion with DNase I and RNase A showed that some of this antigen remains associated with the NM and is more prominent in the nucleoli (fig. 32 e-e"). This result is similar to fig. 33 c" that represents untreated cells digested with DNase I and RNase A.

The results for a mild stress and 20 hours recovery at 37°C are shown in figures 32 f-f" and g-g" for digestion with DNase I or digestion with DNase I and

Figure 32: Immunolocalization of fibrillarin during *in situ* nuclear matrices (NM) preparations of heat-shocked HeLa S3 cells. Cells were observed by phase contrast microscopy (a, b, c, d and e). Cells were single-labeled for immunofluorescence with anti-fibrillarin (a", b", c", d" and e"). Preparations were counterstained with Hoechst 33258 (a', b', c', d' and e'). The pictures show untreated intact cells (a-a"); control NM preparations digested with DNase I (b-b"), or with DNase I and RNase A (c-c"); mildly stressed NM preparations digested with DNase I (d-d"), or with DNase I and RNase A (e-e"). Bar represents 10 µm.

a
a'
a''
b
b'
b''
c
c'
c''
d
d'
d''
e
e'
e''

Figure 32 (continued): Immunolocalization of fibrillarin during *in situ* nuclear matrices (NM) preparations of heat-shocked HeLa S3 cells. Cells were observed by phase contrast microscopy (f, g, h, i, j and k). Cells were single-labeled for immunofluorescence with anti-fibrillarin (f", g", h", i", j" and k"). Preparations were counterstained with Hoechst 33258 (f', g', h', i', j' and k'). The pictures show NM preparations of mildly stressed HeLa S3 cells recovered at 37°C for 20 hours and digested with DNase I (f-f") or with DNase I and RNase A (g-g"); severely stressed NM preparations digested with DNase I (h-h") or with DNase I and RNase A (i-i"); NM preparations of severely stressed HeLa S3 cells recovered at 37°C for 20 hours and digested with DNase I (j-j") or with DNase I and RNase A (k-k"). Bar represents 10 μm.

f
f'
f''
g'
g''
h
h'
h''
i'
i''
j'
j''
k'
k''

RNase A respectively. Figure 32 f" indicates that fibrillarin remains associated with the nuclear matrix as it localizes in the nucleoli and the coiled bodies of HeLa S3 NM. Figure 33 g" shows that fibrillarin is dispersed in the nucleoplasm, but it also labels the nucleoli. A severe shock is represented in figure 32 h-h" (DNase I digestion) and i-i" (DNase I and RNase A sequential digestions). Both show an association of fibrillarin with the NM of HeLa S3 cells, however there is a reorganization of the nucleolus as fibrillarin is dispersed in the nucleoli remnants and the nucleoplasm in dot-like structures of varying in size upon a severe treatment (as in fig. 26 d" and e"). After a 20 hours recovery at 37°C following a severe treatment, NM of HeLa S3 cells maintain the nucleolar reorganization and the dot-like distribution of fibrillarin digested with DNase I (fig. 32 j-j") or with DNase I and RNase A (fig. 32 k-k").

Figure 33 depicts the results obtained for the nucleocytoplasmic shuttling protein 2A7. The 2A7 antigen is found in the nucleoplasm of control cells, in most cases it is found in the nucleoli as well (fig. 33 a-a"). Control NM preparations with DNase I digestion showed 2A7 staining the nucleoplasm but is more prominent in the nucleolus of HeLa S3 cells (fig. 33 b-b"). Control NM digested with DNase I and RNase A indicated that 2A7 is associated with the nuclear matrix of HeLa S3 cells (fig. 33 c- c"): anti-2A7 labels the nucleolar remnants and to a lesser extent the nucleoplasm where some of this antigen seems to have been lost during the extraction.

A mild heat-shock and DNase digestion indicates that 2A7 has mainly a nucleolar distribution (fig. 33 d-d"). A digestion with DNase I and RNase A

indicates that very little 2A7 is associated with the nucleolar remnants of mildly treated cells (fig. 33 e-e").

HeLa S3 cells subjected to a mild stress and 20 hours recovery at 37°C, processed for NM preparations and digested with DNase I, maintained the nucleolar distribution of 2A7 (fig. 33 f-f"). A digestion with DNase I and RNase A indicated that the 2A7 antigen is not associated with the NM of HeLa S3 cells in most of the cell population. However, in certain cases, 2A7 associates with the nucleolar remnants of HeLa S3 cells (fig. 33 g-g").

A severe heat-shock and DNase I digestion (fig. 33 h-h") shows that 2A7 is localized in the nucleoplasm and the nucleolar remnants. The same result is obtained when NM are prepared with double digestion with DNase I and RNase A (fig. 33 i-i").

Following a 20 hours recovery at 37°C and DNase I digestion, the 2A7 antigen seems to gain a more prominent nucleolar staining and is not associated with the internal nuclear interior (fig. 33 j-j"). A digestion with DNase I and RNase A shows that 2A7 remains associated to the NM, its distribution is nucleoplasmic and nucleolar (fig. 33 k-k").

Figure 33: Immunolocalization of 2A7 during *in situ* nuclear matrices (NM) preparations of heat-shocked HeLa S3 cells. Cells were observed by phase contrast microscopy (a, b, c, d and e). Cells were single-labeled for immunofluorescence with anti-2A7 (a", b", c", d" and e"). Preparations were counterstained with Hoechst 33258 (a', b', c', d' and e'). The pictures show untreated intact cells (a-a"); control NM preparations digested with DNase I (b-b"), or with DNase I and RNase A (c-c"); mildly stressed NM preparations digested with DNase I (d-d"), or with DNase I and RNase A (e-e"). Bar represents 10 µm.

a
a'
a''
b
b'
b''
c
c'
c''
d
d'
d''
e
e'
e''

Figure 33 (continued): Immunolocalization of 2A7 during *in situ* nuclear matrices (NM) preparations of heat-shocked HeLa S3 cells. Cells were observed by phase contrast microscopy (f, g, h, i, j and k). Cells were single-labeled for immunofluorescence with anti-2A7 (f", g", h", i", j" and k"). Preparations were counterstained with Hoechst 33258 (f', g', h', i', j' and k'). The pictures show NM preparations of mildly stressed HeLa S3 cells recovered at 37°C for 20 hours and digested with DNase I (f-f") or with DNase I and RNase A (g-g"); severely stressed NM preparations digested with DNase I (h-h") or with DNase I and RNase A (i-i"); NM preparations of severely stressed HeLa S3 cells recovered at 37°C for 20 hours and digested with DNase I (j-j") or with DNase I and RNase A (k-k"). Bar represents 10 μm.

f'
f''
g'
g''
h'
h''
i
i'
i''
j'
j''
k'
k''

3. NUCLEAR ORGANIZATION OF RAT L6E9 CELLS

To evaluate the effects of functional changes that accompany skeletal muscle differentiation on the organization and the composition of the nuclear interior, localization and quantitative biochemical analyses of LAP2β, LAP1C, emerin, lamins A/C, lamin B, PCNA and 1B4 were carried on L6E9 cells. Rat myoblasts were plated at a density of $4X10^5$ cells per 10 ml of complete medium containing 10% FCS. After 24 hours, cells formed a semi-confluent monolayer of mononucleated myoblasts, and were induced to differentiate into multinucleated myotubes by nourishing them with 10% HS for 9 days.

Prior to assessing the structural modifications that accompany differentiation, the first step was to validate the *in vitro* differentiation system. The expression of muscle-specific markers was studied. The level of expression of the myosin heavy chain and the transcription factor myogenin was analyzed in L6E9 myoblasts and myotubes. Figure 34 shows the Western blot analysis of control L6E9 cells (c) and L6E9 myotubes (D9) probed with the anti-myosin MF20. This skeletal muscle marker is not expressed in control cells (C). However it is expressed in differentiated cells (D9). The myogenin antigen was not detected by western blot analysis. Figure 35 depicts the immunofluorescence microscopy of control L6E9 cells and 9 day differentiated myotubes. As seen by phase contrast microscopy (fig. 35 a and b), undifferentiated myoblasts are characterized by an irregular shape. When induced to differentiate for 9 days, their morphology changes and cells fuse into elongated multinucleated muscle fibers or myotubes. The nuclear shape of

Figure 34: Expression levels of myosin in L6E9 myoblasts (C) and L6E9 multinucleated myotubes induced to differentiate with 10% HS for 9 days (D9). Proteins were precipitated with TCA and solublilized in 1X SB and separated by SDS-PAGE on 7% resolving gels, then transferred onto nitrocellulose and blotted with anti-myosin. A typical radiogram for myosin (200 KDa) is shown. The arrow indicates the protein of interest.

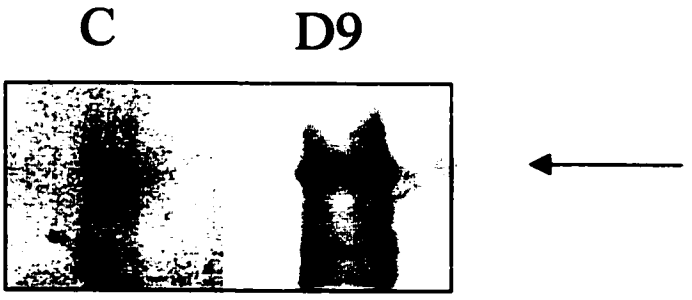
C
D9

Figure 35. Immunofluorescence detection of muscle-specific markers in L6E9 cells. Cells were single-labeled for immunofluorescence with anti-myosin (a" and b") or with anti-myogenin (c" and d"). Preparations were counterstained with Hoechst 33258 (a', b', c' and d'). Cells were also observed by phase contrast microscopy (a, b, c and d). The pictures show undifferentiated L6E9 myoblasts (a-a" and c-c"), 9 day L6E9 differentiated myotubes (b-b" and d-d"). Bar represents 11.7 μm.

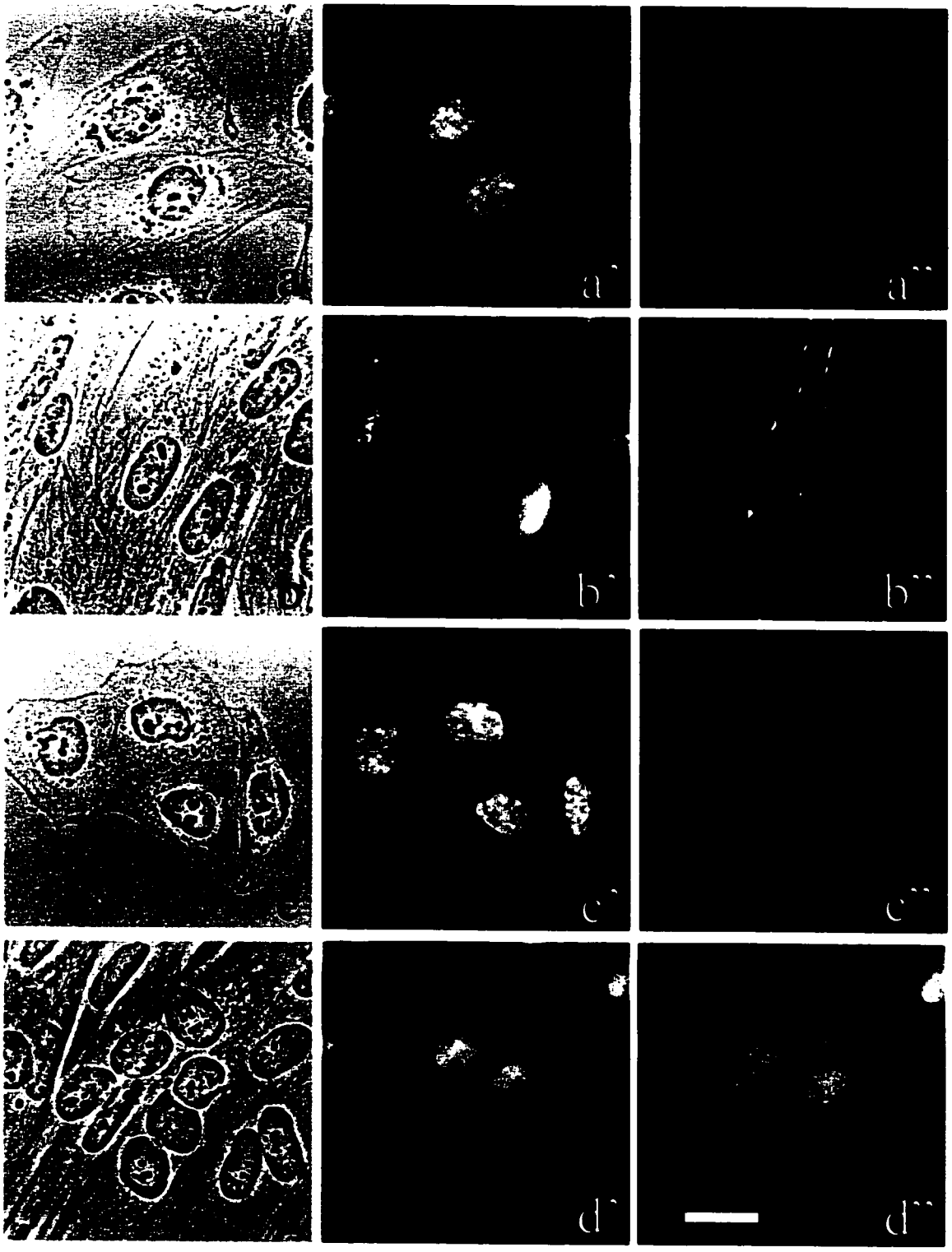
a
a'
a''
b
b'
b''
c
c'
c''
d
d'
d''

undifferentiated myoblasts is ovoid but it became elongated after cell fusion. The nuclei of differentiated myotubes also became closer to one another as the differentiation process was happening. The first two panels compare the expression of cytoplasmic myosin in control cells (fig. 35 a-a") and in differentiated cells (fig. 35 b-b"). As seen in figure 35 a" and b", myosin is exclusively expressed in differentiated myotubes. Panels c-c" and d-d" represent the immunofluorescence localization of the nuclear protein myogenin. This protein is also exclusively expressed in nuclei of muscle cells (fig. 35 d"). The *in vitro* differentiation system of L6E9 myoblasts was validated. The next step was to analyze the changes in localization and levels of expression of different nuclear markers by immunofluorescence microscopy and biochemical quantitative analysis.

Type II integral membrane protein LAP2β localizes at the nuclear-rim of undifferentiated cells (fig. 36 a-a"). This protein may assist in maintaining nuclear organization and it may play a role in nuclear reorganization following mitosis (see introduction). Immunofluorescence microscopy indicated that LAP2β expression is still restricted to the nuclear periphery in L6E9 myotubes (fig. 36 b-b"). Western blot analysis (fig. 37 A) clearly demonstrated that control cells (C) express this protein at a higher levels than differentiated L6E9 myotubes (D9); quantitative analysis (Table 3) of two separate experiments indicated that the decrease of this protein in differentiated cells when compared to control is above 6 folds.

LAP1C is another type II integral membrane protein which is derived by alternative splicing from a gene coding also for two other isoforms, LAP1A and 1B, with a similar structure. Immunofluorescence microscopy showed the nuclear periphery localization of this protein in myoblasts (fig. 36 c-c"). A similar localization is maintained in rat myotubes differentiated for 9 days (fig. 36 d-d"). Western blotting (fig. 37 B) indicated that the level of expression of LAP1C in L6E9 myotubes (D9) is reduced when compared to control myoblasts (C). This result is similar to the one obtained for LAP2β. Quantitative analysis (Table 3) shows a decrease of approximately 4 folds.

The localization of emerin, the 34 KDa protein involved in EDMD, was examined by immunofluorescence microscopy. This protein, as LAP2β and LAP1C, is found at the nuclear periphery in undifferentiated myoblasts (fig. 38 a-a"). The localization of this protein remains unchanged in 9 day differentiated muscle fibers (fig. 38 b-b"). In undifferentiated cells, emerin labels the nuclear-rim in a uniform continuous manner (fig. 38 a"). However, its distribution is altered in muscle fibers (fig. 38 b"): anti-emerin stains the nuclear periphery with a discontinuous dot-like structure. The level of expression of emerin was analyzed by Western blotting analysis (fig. 37 C). It is seen that the level of this protein decreases noticeably in rat L6E9 myotubes (D9) compared to undifferentiated cells (C). Quantitative densitometric analysis indicates a reduction in the level of expression of this protein (Table 3) by 3.68 folds in L6E9 differentiated cells, as compared to control cells.

Figure 36. Immunofluorescence detection of nuclear antigens in L6E9 cells. Cells were single-labeled for immunofluorescence with anti- LAP2β (a" and b") or with anti- LAP1C (c" and d"). Preparations were counterstained with Hoechst 33258 (a', b', c' and d'). Cells were also observed by phase contrast microscopy (a, b, c and d). The pictures show undifferentiated L6E9 myoblasts (a-a" and c-c"), 9 day L6E9 differentiated myotubes (b-b" and d-d"). Bar represents 11.7 μm.

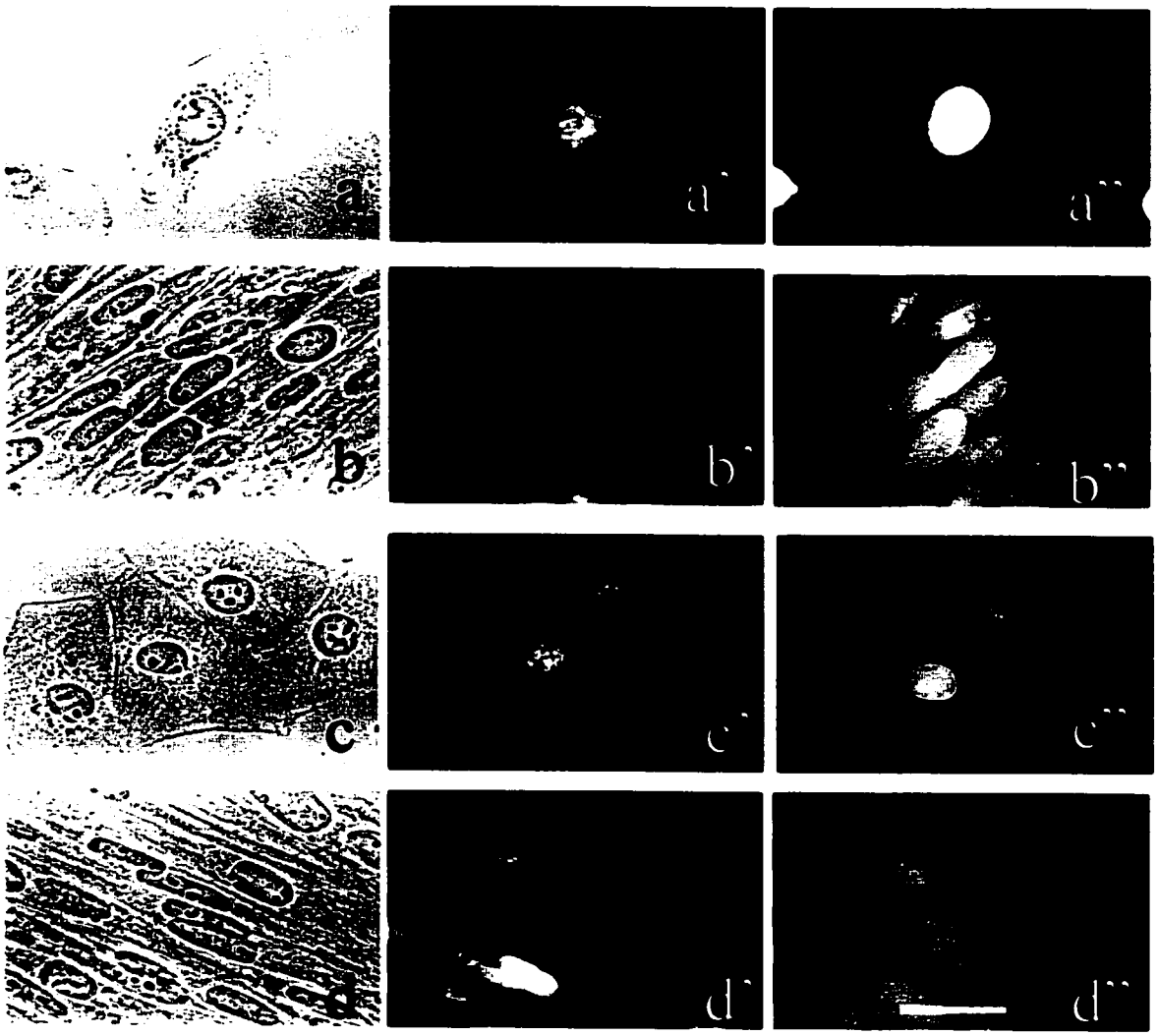
a
a'
a''
b
b'
b''
c
c'
c''
d
d'
d''

Figure 37: Expression levels of different nuclear proteins in L6E9 myoblasts (C) and L6E9 multinucleated myotubes induced to differentiate with 10% HS for 9 days (D9). Proteins were precipitated with TCA and solublilized in 1X SB and separated by SDS-PAGE on 12% resolving gels, then transferred onto nitrocellulose and blotted with the appropriate antibodies. Typical radiograms for LAP2β (A), LAP1C (B), emerin (C), lamins A/C (D) and lamin B (E) are shown. *Black lines* at the left of the lower and upper panels correspond to the position of low range molecular weight markers: phosphorylase B, 97.4 KDa; bovine serum albumin, 66.2 KDa; ovalbumin, 45.0 KDa; carbonic anhydrase, 31.0 KDa; and soybean trypsin inhibitor, 21.5 KDa. The arrows indicate the proteins of interest.

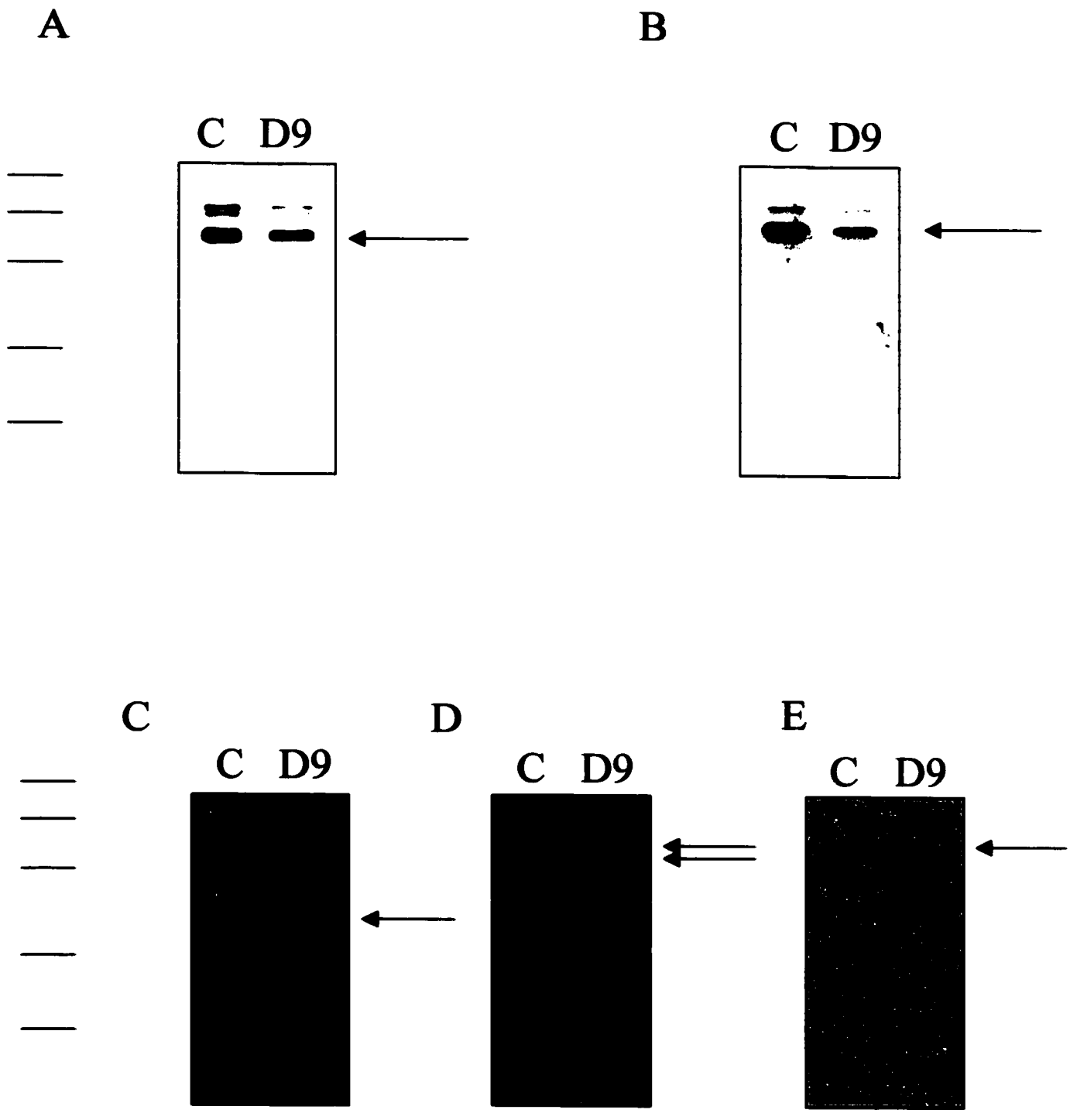
A
C D9
B
C D9
C
C D9
D
C D9
E
C D9

The distribution of lamins A/C and lamin B was also studied. Figure 38 summarizes the results obtained by immunofluorescence microscopy. Lamins A/C localize to the nuclear periphery in control myoblasts (fig. 38 c-c") and 9 day differentiated myotubes (fig. 38 d-d"). The same results were observed for lamin B: this protein localized to the nuclear periphery in undifferentiated L6E9 cells (fig. 38 e-e") and in myoblasts (fig. 38 f-f"). The changes in expression levels of lamins A/C and lamin B in L6E9 myotubes are shown in figure 37 D and 37 E respectively. Both lamins are peripheral proteins of the nuclear matrix. Lamins A/C and lamin B are found to diminish in L6E9 multinucleated myotubes (D9) as indicated by Western blot (fig. 37 D and 37 E respectively). Quantitative analysis led to the demonstration that lamins A/C diminish by 2 and 3 folds respectively in myotubes (Table 3). Lamin B antigen is reduced by 1.7 folds in skeletal muscle fibers when compared to control cells (Table 3).

The 1B4 antigen is found in "speckles" associated with splicing factors. This antigen may play a structural role essential for the splicing machinery but is not a splicing factor. 1B4 is found in small irregular dots within the nucleoplasm of L6E9 myoblasts, excluding the nucleoli (fig. 39 a-a"). Differentiation of L6E9 cells into myotubes seems to result in a reorganization of this protein (fig. 39 b-b"). 1B4 seems to have lost its speckled distribution and it seems that it spread within the nucleoplasm. Quantitative analysis could not be performed for this antigen, the monoclonal antibody failed to recognize the denatured form of this antigen (Luus and Paulin-Levasseur, 1997).

Figure 38. Immunofluorescence detection of nuclear antigens in L6E9 cells. Cells were single-labeled for immunofluorescence with anti-emerin (a" and b"), with anti-lamins A/C (c" and d") or with anti-lamin B (e" and f"). Preparations were counterstained with Hoechst 33258 (a', b', c', d', e' and f'). Cells were also observed by phase contrast microscopy (a, b, c, d, e and f). The pictures show undifferentiated L6E9 myoblasts (a-a", c-c", e-e"), 9 day L6E9 differentiated myotubes (b-b", d-d" and f-f"). Bar represents 11.7 μm.

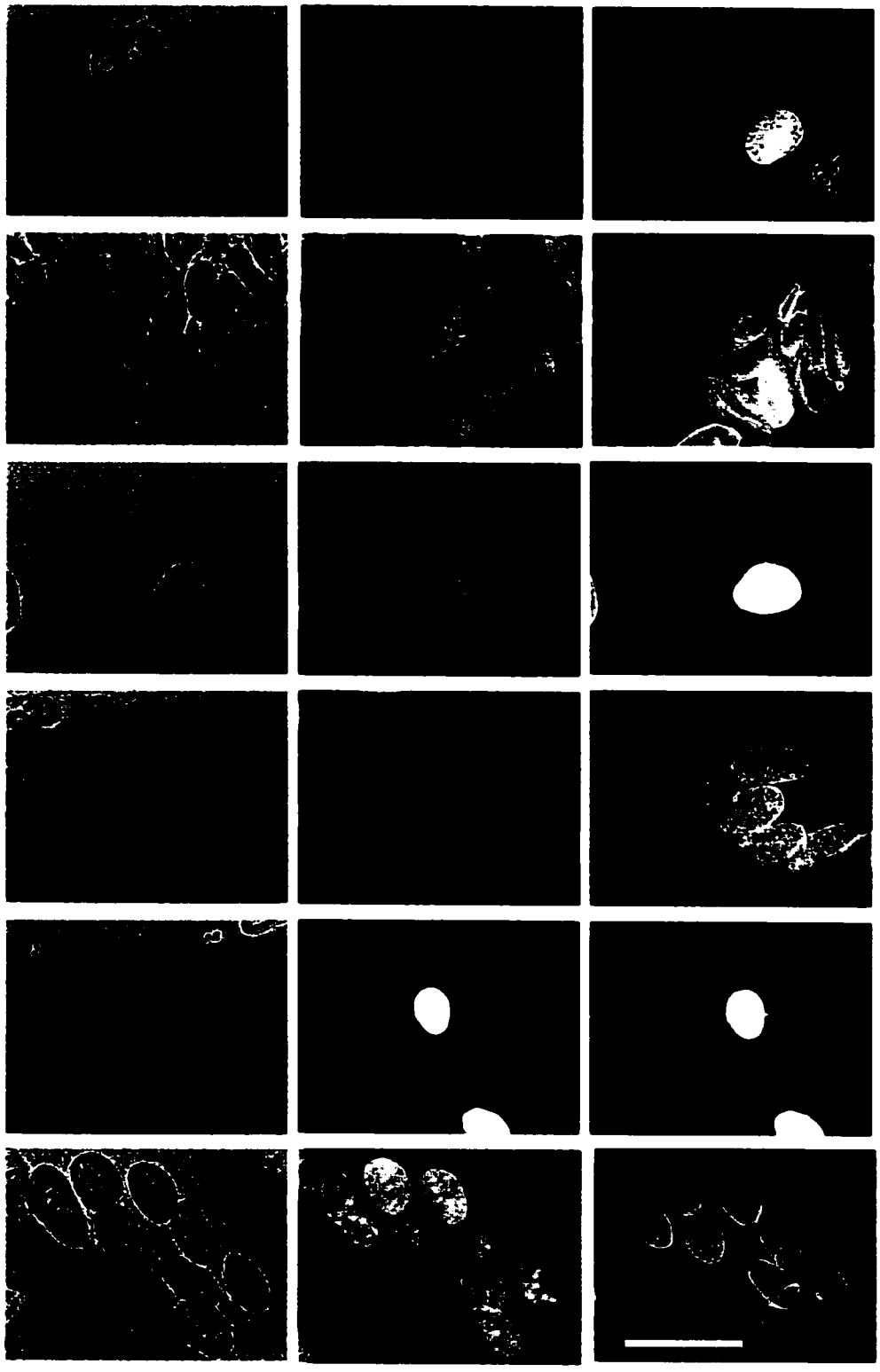

Figure 39. Immunofluorescence detection 1B4 in L6E9 cells. Cells were single-labeled for immunofluorescence with anti-1B4 (a" and b"). Preparations were counterstained with Hoechst 33258 (a' and b'). Cells were also observed by phase contrast microscopy (a and b). The pictures show undifferentiated L6E9 myoblasts (a-a") and 9 day L6E9 differentiated myotubes (b-b"). Bar represents 11.7 μm.

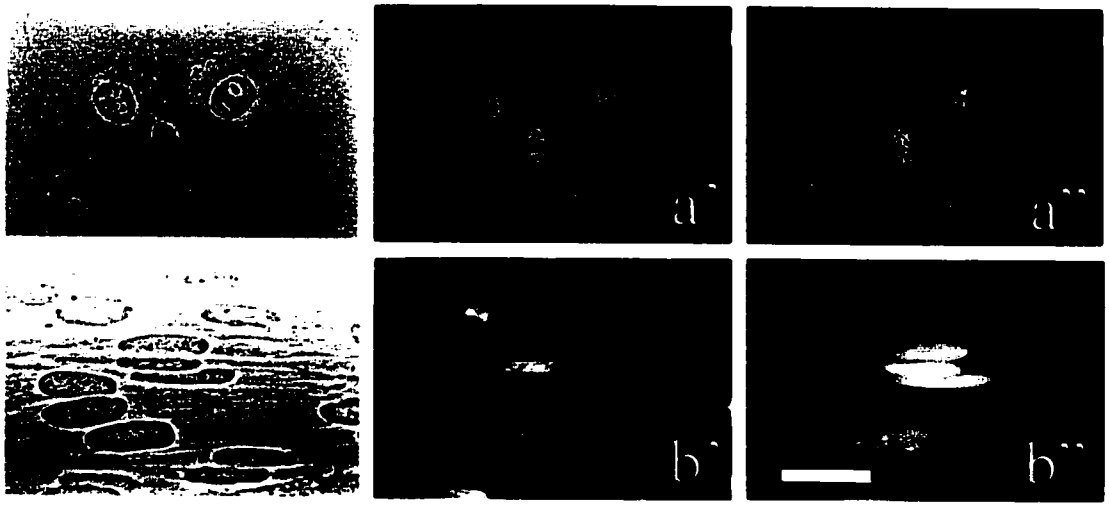
a'
a''
b'
b''

The expression of PCNA, a marker for cell proliferation was studied. The expression of this protein was expected to diminish following differentiation. L6E9 cells withdraw from the cell cycle and fuse into multinucleated myotubes. Figure 40 shows the biochemical analysis of control (C) and 9 day differentiated myotubes (D9). It is clear that a PCNA level of expression is reduced in the latter. A quantitative densitometric analysis showed that PCNA levels decrease by 3.76 folds (Table 3).

Figure 40: Expression of PCNA in L6E9 cells. L6E9 myoblasts (C) and L6E9 multinucleated myotubes induced to differentiate with 10% HS for 9 days (D9). Proteins were precipitated with TCA and solublilized in 1X SB and separated by SDS-PAGE on 12% resolving gels, then transferred onto nitrocellulose and blotted with anti-PCNA. A typical radiogram for PCNA is shown. *Black lines* at the left of the lower and upper panels correspond to the position of low range molecular weight markers: phosphorylase B, 97.4 KDa; bovine serum albumin, 66.2 KDa; ovalbumin, 45.0 KDa; carbonic anhydrase, 31.0 KDa; and soybean trypsin inhibitor, 21.5 KDa. The arrow indicates the protein of interest.

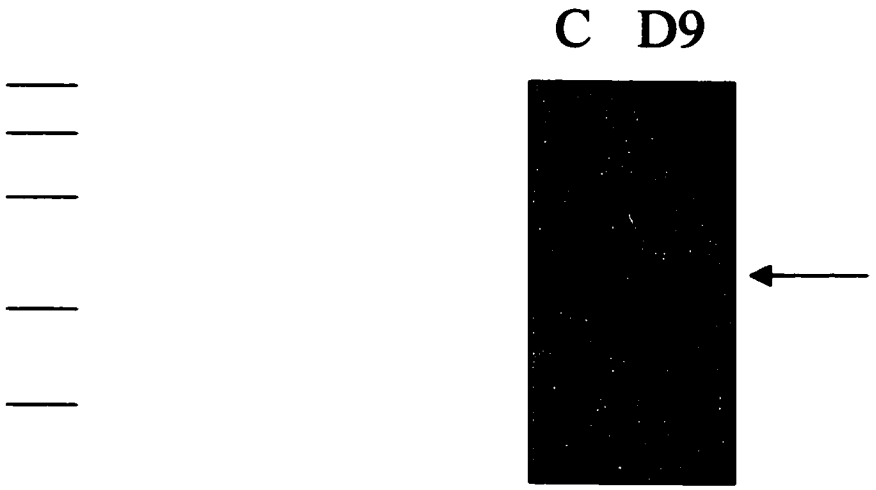
C
D9

Table 3: Quantitative values of the level of expression for different nuclear markers in L6E9 myoblasts (Control) or myotubes (D9). The results of two separate experiments are averaged. The last row presents the level of decrease in the expression of specific proteins in differentiated cells relative to normalized Control average.

Volume (Intensity X mm^2)

Antigens	Control	D9	Changes
LAP2β	2297.45	354.83	6.47
LAP1C	712.93	179	3.98
Emerin	882.6	239.6	3.68
Lamin A	229.29	106.44	2.15
Lamin C	574.90	192.92	2.985
Lamin B	195.65	115.18	1.7
PCNA	342.57	91.113	3.76

IV. DISCUSSION

4.1. HYPERTHERMIA

1. The response of HeLa S3 cells to heat-shock stress

1.1. The viability, growth and cell cycle distribution of HeLa S3 cells

The data presented in the first section of this thesis demonstrated that HeLa S3 cells survive the stress of mild or severe heat-shock and remain fully viable throughout a 25 hour recovery period at 37°C. The growth of treated populations was however inhibited. Many ideas have emerged in order to explain the mechanisms behind the cellular responses to heat-shock stimuli and the maintenance of cellular survival. It has been established that heat stress and equivalent conditions have the ability to induce protein denaturation and / or aggregation; cells respond to these threats by producing HSPs to repair damaged proteins and to ensure their survival (Pelham, 1986; Hightower, 1991; Edington *et al.*, 1989). Misfolded proteins bind to cytoplasmic / nuclear Hsp70 chaperones (Beckmann *et al.*, 1990); while free "unengaged" Hsp70 proteins activate the heat shock transcription factors, which in their turn activate heat-shock genes by binding heat-shock elements found upstream of many heat-inducible genes (Wu, 1993). Thus the expression of Hsp70 (explained further below) plays a protective role to ensure cellular survival. Several reports support these ideas. For example, Li *et al.* (1995) studied the effect of Hsp70 and its deletion derivatives on heat killing. They established stable rat fibroblasts transfected with intact or mutant Hsp70, and they determined the effect on cellular survival. Their data showed that exponentially growing stable

transfectants exposed to a temperature of 45°C for 0-75 minutes, and expressing intact human Hsp70 or fragments containing portions of its carboxyl half possessed higher thermal resistance than cells transfected with an empty vector.

The experiments using the anti-PARP antibody demonstrate that HeLa S3 cells survive heat stress without any indication of apoptosis following mild or severe heat-shocks and the recovery period at 37°C. Furthermore, it had been previously shown that lamins A/C, lamin B2 (Tinnemans *et al.* 1995) and LBR (Duband-Goulet *et al.* 1998) are degraded in apoptotic cells. In this study, immunofluorescence and biochemical analysis did not show any degradation of antigens specific to the nuclear periphery. Thus, I can conclude cell death due to apoptosis did not occur.

I have shown that HeLa S3 cells maintain a cell cycle distribution similar to that of normal cells when exposed to mild or severe heat-shock and following the recovery period at 37°C with the majority being in G0/G1 phases of the cell cycle. A different response has been observed in yeast. There is evidence that high temperature causes the cell to enter into a non-proliferating "heat-shocked" state in the budding yeast *Saccharomyces cerevisiaie* (Johnston and Singer, 1980; Rowley *et al.*, 1993). For instance, earlier studies on *S. cerevisiaie* have demonstrated that yeast cells subjected to heat-shock (23°C-36°C) become transiently arrested in the G1 phase of the cell cycle (Rowley *et al.*, 1993). Is this cell cycle arrest in G1 due to protein misfolding? Is it due to membrane damage? According to the study by Rowley *et al.* (1993), the G1 arrest is due to the loss of G1 cyclin function, where expression of cyclin 1 (CLN1) and cyclin 2 (CLN2) is

transiently repressed by temperature up-shift. In *S. cerevisiaie*, cell proliferation is regulated primarily at a central control step in G1 called START. This step requires the activation of the highly conserved protein kinase p34, encoded by the CDC28 gene (Lorincz and Reed, 1984). P34 kinase is active when it forms a complex with other G1 cyclin proteins CLN1, CLN2 and cyclin 3 (CLN3) (Hadwiger *et al.* 1989; Wittenberg *et al.* 1990). In absence of expression of the CLN gene family, there is arrest of yeast cell proliferation at START (Cross, 1990). Thermal shock of wild type cells to an elevated temperature induces the transient inhibition of START (Johnston and Singer, 1980; Shin *et al.*, 1987). This group showed that heat-shock blocks START temporarily without removing cells from the mitotic cell cycle (Drebot *et al.*, 1990).

Based on my data, it is highly unlikely that the non-proliferative state of populations of HeLa S3 cells exposed to mild or severe heat treatment may result of a single arrest point in G1 phase. If so, the number of cells in this phase of the cell cycle would be expected to increase after the heat-shock and less cells would be found in S and / or M phases. This was only observed after 20 hours of recovery at 37°C following a mild treatment as discussed below. My results are in accordance with those of Zhu *et al.* (1999). They measured the changes in the cell cycle distribution by flow cytometry and did not observe any cell cycle changes from HeLa cells or U-1 human melanoma cells heat-shocked at 45.5°C for 30 minutes and / or recovered at 37°C for different periods of time. However, in this research thesis, statistical analysis of my data showed a significant decrease in the percentage of cells undergoing mitosis at 20 hours

post-mild treatment when compared to cell samples at 5 hours of recovery. Also, at 20 hour of recovery, there is a higher percentage of cells in the G0/G1 phase of the cell cycle. It is possible that the cells were transiently arrested in this phase.

My data indicated that BrdU incorporation in treated cells decreases abruptly after mild or severe treatment, the latter being more dramatically affected. The incorporation of BrdU in cells has been widely accepted as a proliferation marker (Pellicciari *et al.* 1995). The group of Pellicciari *et al.* (1995) showed that human fibroblasts that are BrdU positive constituted 13% of cycling cells and 1% of quiescent cells. My data agrees with these results where 9-12% control HeLa S3 cells have incorporated BrdU. The fact that BrdU incorporation decreased significantly due to heat-shock indicates that DNA replication is inhibited in HeLa S3 cells. Thus, mild and severe heat-shocks have a dramatic effect on cellular proliferation and DNA replication.

At 5 hours recovery after a mild treatment, BrdU incorporation was higher than for the rest of the samples, but remained lower than in control samples.

1.2. <u>The heat-shock response and Hsp70 expression</u>

The microscopic localization and the levels of expression of Hsp70 have been examined closely in this study. I observed that Hsp70 localized in the nucleus (including the nucleoli) and at basal levels in the cytoplasm of control HeLa S3 cells. The result obtained in this research thesis is not entirely in accordance with previous reports. A study by Welch and Mizzen (1988) studied the distribution of Hsp70 in HeLa cells after methanol fixation for 2 minutes: in

control cells, Hsp70 was found to be present in the nucleus - excluding the nucleolus - and to a lesser extent, it was found in the cytoplasm. Ohtsuka *et al.* (1986) showed that Hsp70 has an exclusively cytoplasmic localization in methanol-fixed (for 10 minutes) control HeLa cells. Another study by Welch and Feramisco (1984) had shown that Hsp70 localized in the cytoplasm and the nucleus (excluding the nucleoli) in gerbil fibroma cells after fixation in 3% formaldehyde and extraction with acetone. It is important to keep in mind that different cell lines may not necessarily have the same distribution of Hsp70. Also, different fixation methods (formaldehydes versus alcohols) may provide different distributions of Hsp70 within cellular compartments.

My data showed that upon mild treatment for 90 minutes, Hsp70 is localized in the nucleus and is more prominent in the nucleoli. The group of Ohtsuka *et al.* (1986) showed that HeLa cells treated mildly for 2 hours resulted in Hsp70 localizing mainly in the nucleolus; my results agree with these data. The same group observed that at 1 hour of recovery at 37°C after a mild treatment, Hsp70 disappeared from the nucleoli rapidly. My results are in accordance to what this group has obtained: Hsp70 was not as prominent in the nucleoli at 1 hour of recovery at 37°C. Their study also showed that after a prolonged recovery period at 37°C (12-25 hours), Hsp70 regained its cytoplasmic distribution while remaining nuclear (including the nucleolus). My data indicated that Hsp70 starts regaining a cytoplasmic distribution 5 hours post-mild treatment.

Welch and Feramisco (1984) observed an increase in both cytoplasmic and nuclear staining of Hsp70 in gerbil fibroma cells, and reported that 4 and 5 hours after heat-shock, this protein was found in the nucleolus. It is important to keep in mind that different cellular systems may have divergent responses to heat-shock stimuli.

Upon severe treatment of HeLa S3 cells, my data demonstrated that Hsp70 remains in the cytoplasm and the nucleus; this distribution of Hsp70 did not change throughout the recovery time at 37°C. Welch and Mizzen (1988) studied the distribution of Hsp70 in severely heat-shocked HeLa cells (45°C for 45 minutes) after methanol fixation. In control HeLa cells, Hsp70 was nuclear (excluding the nucleoli) and it was found in the cytoplasm at low levels. A severe treatment without recovery showed an increase in the level of Hsp70 in the nucleus and in the nucleolus. After a severe treatment and 3 hours or 5 hours recovery at 37°C, Hsp70 expression increased more in the nucleus and the nucleolus. Following 5 hours recovery at 37°C, Hsp70 regained a cytoplasmic distribution. In this research thesis, anti-Hsp70 always labeled the cytoplasm as well throughout the treatment and the recovery period. The difference in the localization of Hsp70 could be due to a difference in the fixation methods used. It seems that Hsp70 is prominent in the nucleolus in mildly treated cells, at least temporally. After a severe heat-shock, Hsp70 is present constantly in the nucleolus. It is possible that this antigen provides a protective role to the nucleolar structure. A milder shock might indicate a short-term threat to the cells.

The expression of Hsp70 was expected to increase following heat stress. Western blotting and densitometry confirmed this result. Hsp70 expression reached its highest levels at 5 hours of recovery at 37°C following a mild treatment and its expression starts decreasing 20 hours post-heat shock. This may provide another indication that a mild stress does not cause a long-term threat to the cell. The expression level of Hsp70 following a severe heat-shock increase gradually and reach their highest expression levels at 20-25 hours of recovery at 37°C.

Ohtsuka *et al.* (1986) used densitometric analysis to demonstrate changes in the level of expression of Hsp70 in HeLa cells following mild stress. A 42°C heat-shock for 2 and 4 hours caused the expression of Hsp70 to increase as the time of exposure to heat-stress increases; they compared this to control cells. This group however did not analyze the level of expression of Hsp70 after different times of recovery at 37°C. To my knowledge, I provide here the first report of the changes occurring in the level of expression of Hsp70 during recovery at 37°C from heat stress.

The effects of heat-shock on Hsp70 in nuclear matrices (NM) from HeLa S3 demonstrated the following major changes: in control intact cells, Hsp70 is found in the nucleus and the cytoplasm including the nucleoli. This is in accordance with my previous results where I observed a similar localization of Hsp70. Treatment of control HeLa S3 cells with DNase I or with DNase I and RNase A does not alter this distribution. A mild treatment and DNase I digestion shows that Hsp70 has a nucleolar distribution. This supports my previous result

where Hsp70 migrated into the nucleoli of mildly treated intact cells. Previous reports have indicated that Hsp70 migrates from the cytoplasm to the nucleus where it associates with the granular region of the nucleoli that contains preribosomes. During the recovery period at normal temperature, this protein exists the nucleoli and migrates again to the cytoplasm where it associates with polyribosomes (Welch and Feramisco, 1984; Welch and Suhan, 1986; Welch and Mizzen, 1988).

In contrast, when mildly treated cells were digested with DNase I and RNase A, Hsp70 is only found in the nucleoplasm, excluding the nucleoli. This may be an indication that Hsp70 could associate with the karyoskeletal framework of the nucleoli through interactions with RNA moieties; and therefore, this antigen is released from the nucleolar remnants upon digestion with RNase A.

A mild treatment and recovery at 37°C for 20 hours results in Hsp70 localizing in both the nucleus and the nucleolus in DNase I digested cells and in cells digested with both DNase I and RNase A. This is in accordance with my previous results, where Hsp70 is found in the nucleus and the nucleolus of intact cells post-mild heat-shock.

A severe treatment shows that Hsp70 maintains its nuclear/nucleolar distribution after DNase I or DNase I and RNase A digestions. The same result is obtained after 20 hours of recovery period at 37°C and DNase I digestion. However, a sequential digestion with DNase I and RNase A results in Hsp70 prominently found in the nucleoli of HeLa S3 cells. Hsp70 may provide a

protective role within the nucleolar compartment. As shown in the Results section, my data reports indicate that a severe treatment affects the localization and the expression of nucleolar proteins such as 2H12 and fibrillarin. Another explanation may be that heat-shock causes a tight association between nuclear antigens and the nuclear matrix, and anti-Hsp70 labelled the nucleoli even after digestion with RNase A.

2. The effects of heat-shock on nuclear proteins

2.1. The effects of heat-shock on peripheral nuclear antigens

In order to evaluate the effects of heat-shock on nuclear architecture, a series of nuclear antigens were used as markers to monitor the changes that occur at the nuclear periphery due to heat-shock. My data indicated that LAP2β, emerin, lamins A/C and lamin B remained localized mostly at the nuclear periphery. However, quantitative biochemical analysis showed that the level of expression of some antigens is altered upon a mild or severe heat-shock. LAP2β increased significantly following a mild treatment, but regained levels similar to the control samples at 20 hours post heat-shock. A severe heat-shock resulted in an overall increase of the level of expression of this antigen that is maintained throughout the whole recovery period. The level of expression of emerin decreases significantly 25 hours post-mild heat-shock. The levels of expression of lamin B diminish considerably also after 20-25 hours of recovery from severe heat-shock. Previous evidence had indicated that morphological and functional changes happen in heat-shocked cells. For example, an earlier study by Blair *et al.* (1979) indicated that measurements made from their

photomicrographs show slightly larger nuclei from heat-shocked HeLa cells than in control nuclei (12.1 μm vs. 11.6 μm respectively). In my case, the nuclear diameter remained relatively similar in stressed and control cells. But, the cell diameter seemed to shrink: the volume ratio cytoplasm/nucleus decreased. The group of Blair *et al.* (1979) also isolated nuclei from HeLa S3 cells; they used FITC fluorescence to show an increase in protein content of nuclei isolated from treated HeLa cells compared to control cells. Protein content was higher in cells exposed longer to heat: nuclei exposed for 7.5, 15 or 30 minutes at 45°C showed an increasing protein content of 1.18, 1.30 and 1.39 respectively. These authors suggested that the increase in protein content may be due to: a) soluble nuclear proteins or loosely bound chromosomal proteins lost during nuclear isolation of normal cells which would be retained in heat-shocked cells; it is possible that heat-shock may tighten the binding of proteins to chromatin and favor their retention during nuclear isolation; and b) additional cytoplasmic proteins may enter the nucleus upon heat-induced physiological alterations in the cellular milieu.

Out of four peripheral nuclear proteins, only LAP2β was found to increase during the heat response. It is interesting to consider that LAP2β binds lamin B and chromosomes. Such an association could be involved in attaching the lamina and chromatin to the INM during interphase and may help in preserving nuclear architecture (Foisner and Gerace, 1993). Since the nucleus undergoes architectural (nuclear shape) and functional (chromatin, protein content) changes when the cells are exposed to stress, an augmentation in the level of expression

of LAP2β may be a response to a perceived threat on nuclear structure. The expression of this antigen diminishes gradually at 12 hours of recovery after a mild shock and regains control levels soon after. Following a severe shock, it remains higher than control levels for the entire recovery period. This may suggest that HeLa S3 cells perceive a severe shock as a longer-term threat.

A study by Yang *et al.* (1997) analyzed the effect of different LAP2β fragments on nuclear volume during the cell cycle and on the progression into S phase. Using HeLa cells, they showed that injection of the lamin B - binding fragment of LAP2β sequence (fragments 298-373) in early G1 phase blocked cell progression into S phase (G1 block) and inhibited nuclear volume increase that is required for G1cells to enter S phase (Yen and Pardee, 1979; Fidorra *et al.*, 1981; Yang *et al.*, 1997). The fragments used in their study did not include the transmembrane domain of LAP2β and were not integrated in NE. Their presence could have hindered the interactions between the endogenous LAP2β-nuclear lamina. However, there was no detectable disruption of the NE structure. Indeed, it was shown that lamins A/C and lamin B remain at the nuclear periphery. Alternatively the fragments could have perturbed the interaction LAP2β-chromatin. In my study, I did not observe any structural change at the nuclear periphery by conventional immunofluorescence microscopy during the response to mild or severe heat-shock. However, it may be suggested that overexpression of LAP2β due to heat-shock (both mild and severe) may alter the interactions NE-chromatin, and in consequence, DNA replication is impaired. On

the other hand, an increase in the expression of this protein may be because DNA replication is inhibited.

Other significant changes in the protein content at the nuclear periphery include the levels of emerin. This integral membrane protein contains a hydrophilic amino terminal domain oriented towards the nucleoplasm. This domain has 22 potential phosphorylation sites for a one or more undefined kinases (Bione *et al.*, 1994). Ellis *et al.* (1998) used lymphoblastoid cell lines from two EDMD patients. They observed that emerin is phosphorylated at interphase in a cell cycle-dependent manner into different isoforms. In both EDMD patients, they observed altered emerin expression. This group showed that phosphorylation is the only possible explanation for the appearance of emerin as 2 bands on SDS-PAGE: they used steady-state *in vivo* labeling of the lymphoblastoid cell lines with [^{33}P] orthophosphate to confirm that wild type emerin (34 KDa) and emerin from patients K3 and Y1 are endogenously phosphorylated and each migrated as a single band (34 KDa and 36 KDa). In my case, two bands for emerin are shown in control and throughout the mild treatment. It is difficult to prove whether phosphorylation of this protein underwent low or high turnover rates by addition of phosphate groups during the different treatment. But one can speculate that the phosporylation state of the 36 KDa protein remained unchanged during the mild treatment and the recovery time. If it does change, I would observe a change in distance between the 34 KDa and the 36 KDa emerin isoforms. On the Western blot representing a severe heat-shock, the distance between the 34 and 36 KDa proteins does

decrease starting at 5 hours post-heat shock. It is possible that there is a change in the phosphorylation patterns of emerin, where the 36 KDa protein becomes less phosphorylated.

As I mentioned above, cell proliferation in heat-shocked cells is arrested. Nigg (1992) suggested that nuclear membrane structural proteins, nuclear lamina and chromatin are essential in order to preserve the integrity of the NE-chromatin during interphase and for the disassembly of the NE during mitosis. It is known that protein phosphorylation has a role to play in the involvement of INM proteins in NE assembly/disassembly. For example LAP2β is phosphorylated in the early stage of mitosis, which precedes its dissociation from the lamina network and from chromatin (Foisner and Gerace, 1993). At late anaphase this protein reassociates with the chromatin and targets lamin B1 to its correct localization for initiation of nuclear envelope reassembly (Foisner and Gerace, 1993). Ellis *et al.* (1998) suggested that the cell cycle dependent phosphorylation of emerin may play a role in its binding to nuclear lamina components in a manner similar to that of LAP2β. Cartegni *et al.* (1997) suggested that emerin may have a phosphatase associated with it.

The levels of expression of emerin as shown by quantitative densitometry does decrease significantly at 25 hours post-mild treatment. The reasons behind this change are not clear. At this time, DNA replication is still inhibited and cell proliferation is arrested. Thus, I cannot conclude that this change is directly associated with these nuclear functions. If so, I would suspect that the

expression levels of emerin would have changed before the 25 hour recovery period.

Interestingly, lamin B is the only antigen of the nuclear periphery that undergoes noticeable changes following a severe heat-shock - its levels decrease 20-25 hours after recovery - but no significant change is obtained after a mild shock. Dynlacht *et al.* (1999) studied the expression of lamin B when U-1 cells were heated at 42°C for 7 hours and did not observe any change in the level of its expression when compared to control samples. My data supports the results obtained by this team. Previous reports by Dynlacht *et al.* (1999) and by Zhu *et al.* (1999) showed that lamin B expression following a severe shock (45.5°C) increases in U-1 cells. Lamin B increases within the first 5 minutes and continuous to do so at 10 minutes of exposure where it reached a plateau. In HeLa cells, the content of lamin B increased significantly as well. Quantitative analysis supported their results. Zhu *et al.* (1999) observed an increase in the expression of this antigen after 7 hours of recovery at 37°C following a treatment at 45.5°C for 30 minutes. In contrast, I observed a significant decrease of lamin B content 20 and 25 hours post-severe heat-shock. This difference in results is difficult to explain. It is known that lamin B forms a scaffold upon which replication factors can bind through LAPs in order to form replication centers (Berezney *et al.*, 1995; Newport *et al.*, 1990). However, this change in lamin B expression is not likely to result because DNA replication is inhibited. It is unknown whether lamin B undergoes structural or functional change and thus, it can affect DNA replication. Interestingly, lamin B expression is the highest at 5

hours post-mild heat shock. This is the period where BrdU incorporation is higher than the rest of the samples, but lower than in control cells.

2.2. The effect of heat-shock on internal nuclear antigens

The effects of mild and severe heat-shocks on internal nuclear organization was investigated using protein markers for different nuclear domains such as: 1B4, a protein associated with splicing sites; PCNA, a component of active replication foci; 2A7, a nucleocytoplasmic shuttling protein; and 2H12 and fibrillarin, two nucleolar proteins.

mRNA splicing is facilitated by nuclear proteins and snRNP particles (Staley and Guthrie, 1998). Earlier studies have indicated that mRNA splicing is inhibited by heat-shock and by chemical stress *in vivo* and *in vitro* (Behrens and Luhrmann, 1991; Bond and Schlesinger, 1986; Yost and Lindquist, 1986). Using anti-1B4, I analyzed the effects of heat-shock on 1B4 distribution by immunostaining. This antibody does not recognize 1B4 under its denatured form. I therefore could not examine the expression levels of this protein during the response to heat-shock. In control cells, 1B4 localized in varying sized splicing sites, called "speckles". Major changes in the distribution of this protein were observed after severe treatment: 1B4 staining seemed to diminish in intensity and less "speckles" were present. No change was detectable after a mild treatment.

Welsh and Mizzen (1988) examined the distribution of snRNPs which are also components of nuclear speckles, in control and heat-shocked cells They heat-shocked rat REF-52 fibroblasts for 30 minutes at 45°C, let them recover at

37°C for 2 hours and observed that the speckled staining characterizing control cells changed to a diminished or diffuse staining. The data obtained in this research thesis for the 1B4 antigen agrees with these previous data.

Previous reports have indicated that the reorganization of 1B4 and SC35 in HeLa cells upon exposure to drugs may inhibit transcription (Luus, M.Sc. thesis, 1997). Two drugs that inhibit transcription in nuclear and nucleolar structure are actinomycin-D and 5,6-dichloro-1-β-D-ribofuranosylbenzimidazole (DRB). The first one intercalates with double stranded DNA and inhibits transcription by RNA polymerases (Sobell 1985). DRB inhibits transcription by inhibiting protein kinases that phosphorylate the large subunit of RNA pol II (Stevens and Maupin, 1989). Huang *et al.*, (1994) and O'Keefe *et al.*, (1994) have observed the number of speckles to be reduced in cells when splicing and transcription are inhibited. This may suggest that a severe heat-shock affects these functions. Luus (M.Sc. thesis, 1997) observed that 1B4 maintained its colocalization with the splicing factor SC35 throughout all drug treatments in HeLa cells. She observed that a 2 hour treatment with actinomycin D or with DRB reorganized the distribution of 1B4 and SC35. This corresponded with a decrease in the level of transcription as assayed by uridine incorporation. It would have been informative to conduct double labeling studies to observe whether 1B4 and SC35 colocalize in HeLa S3 cells following heat-shock treatments. This may have provided a clearer indication about the effects of stress on mRNA splicing.

PCNA is a nuclear protein involved in regulating cell proliferation (Bravo *et al.*, 1982). The content proportion of this protein is high in proliferating cells, and its abundance is reduced almost 6 folds in slowly growing cells and in non-cycling cells (Bravo *et al.*, 1982). Whereas non-cycling cells synthesize very little PCNA, normal cycling cells synthesize it as needed and transformed immortal cells express it constitutively (Bravo and Celis, 1980; Bravo *et al.*, 1981). My results by quantitative densitometric analysis show that PCNA levels increase following a mild heat-shock and remain higher than control samples throughout the recovery period. In contrast, the expression levels of PCNA decrease significantly after a severe treatment and start increasing 5 hour post-heat shock to reach higher levels at 25 hours after recovery.

Bravo and Celis (1985) analyzed the amount of PCNA in different cell lines to determine if PCNA abundance correlates with changes in the rate of cell proliferation. They chose two situations in which the rate of cell proliferation is altered: a) they used HeLa cells and subjected them to stress by irradiation with lethal doses of X-rays. and b) they used low passage and senescent skin fibroblasts. In their first experiment, Giant HeLa cells were obtained with 1000 rads of X-rays (110 rad/min) and they pulsed the cells 5-6 days after irradiation with [^{3}H]-thymidine. Only 8% of the irradiated cell population was observed to be in "S" phase, while 31% of control cells were in this phase of the cycle. Two dimensional gel electrophoresis (2-D) showed that the amount of PCNA in HeLa Giant cells is reduced prominently compared to control cells. In their second experiment, skin fibroblasts were pulsed for 20 minutes with [^{3}H]-thymidine;

30% of low passage cells were shown to synthesize DNA while only 0.1% of senescent cells synthesized it. 2-D gel electrophoresis indicated that the amount of PCNA is 0.12% of the total protein in low passage cells, while it is only 0.03% in senescent cells. In conclusion, stressed, slowly dividing or non-dividing cells synthesized very little PCNA polypeptides in both cases.

My data indicated that PCNA levels in HeLa S3 cells do not necessarily correlate with cell proliferation. As mentioned in section 1 of the Discussion, cell proliferation is arrested following mild and severe treatments and during the recovery period at 37°C. How could these results be explained? It is possible that PCNA does not behave solely as a key factor in cell proliferation and that it has other functions.

Based on PI analysis and BrdU incorporation, the amount of cells in S phase is similar in mild or severe treatment and during the recovery period, while DNA replication is inhibited strongly in both cases. The fact that DNA replication is inhibited strongly and that PCNA levels decrease only briefly after a severe heat-shock and during the first hour of recovery at 37°C may indicate that only a portion of this antigen plays a role in DNA replication. The reasons why PCNA levels increase due to a mild shock are not evident. It may be that regulatory mechanisms within HeLa S3 cells are trying to promote cellular proliferation and PCNA overexpression is allowed to counteract threats that would hinder this process.

Another antigen of the nuclear interior affected by mild and severe heat-shock is the nucleocytoplasmic shuttling protein 2A7. Immunofluorescence

microscopy showed a change in the organization of 2A7 in mildly and severely heat-shocked cells. Densitometric analysis indicated a significant decrease in the level of expression of 2A7 after a severe treatment and during recovery at normal temperature. A study by Paulin-Levasseur and Julien (1999) showed that 2A7 is a nucleocytoplasmic shuttling protein (human-mouse heterokaryons). They also studied the effect of mild (42.5°C) and severe (45°C) heat-shocks on the distribution of 2A7 using HeLa cells. They heat-shocked cells at either temperature for 1 hour and observed the following: a mild treatment resulted in 2A7 accumulating prominently in the nucleoli while remaining in the rest of the nucleoplasm. Following a severe treatment, 2A7 reorganized into an irregular lattice with track-like structures that seemed to be in contact with the NE. These results are different from the ones obtained here. After a mild treatment, 2A7 maintained its nucleoplasmic and nucleoar distribution. I did observe an inward compaction of the 2A7 antigens towards the interior of the nucleus, with a distinct "flower" shape array at the nuclear periphery, but I did not observe an increased staining of the nucleoli. After a severe treatment, 2A7 seemed to have further compacted towards the interior of the nucleus, with no nucleolar staining evident.

There have been many studies related to the effect of heat shock on splicing and on nucleocytoplasmic transport (Yost and Lindquist, 1986; Bond 1988). The latter function is related to hnRNPs. These particles have been shown to shuttle between the nucleus and the cytoplasm (Borer *et al.*, 1989; Pinol-Roma and Dreyfuss, 1991, 1993, Dreyfuss *et al.*, 1993, Nakielny and Dreyfuss, 1997). Mahl *et al.* (1989) suspected that the substructure of hnRNPs

would be altered in heat-shocked cells. Using HeLa S3 cells and heat-stress, they analyzed the behavior of two hnRNPs. They observed that treatment at 45°C for 10 minutes resulted in reorganization of both proteins. However, densitometric analysis of treated cells and recovered cells for different time periods did not indicate any change in the level of expression of these proteins. They did not observe any change after a mild treatment, which supports the data that I obtained by densitometric analysis obtained in this study.

The reorganization of 2A7 may reflect a reorganization of intranuclear domains. The exclusion of 2A7 from the nucleolus following a severe treatment is interesting. I also observed changes in the distribution of two nucleolar proteins during a severe treatment as seen below. This may support a change in nucleolar structure, and possibly its functions.

Heat-shock has been shown to change the structure and the function of the nucleolus, leading to a reduction in its size and its granularity in animal cells (Lewis and Pelham, 1985; Warner, 1990; Welsh, 1992; Jordan and Shaw, 1995; Schneiter *et al.*, 1995). I used the nucleolar proteins 2H12 and fibrillarin as markers of the effects of heat-shock on the nucleolus. 2H12 is found in the granular component of the nucleolus and plays a role in the organization of this non-membranous compartment (Paulin-Levasseur *et al.*, 1995). Fibrillarin, a protein of the DFC (Ochs *et al.*, 1985; Lischew *et al.*, 1985a and b) is involved in the first cleavage steps of rRNA processing. Immunofluorescence analysis demonstrated that 2H12 remained sequestered in the nucleolus in both mild and severe treatments. However, it seemed masked by a "veil" following a severe

one. Quantitative analysis indicated that the expression levels of this protein decrease significantly following a mild treatment. Fibrillarin was studied by immunofluorescence microscopy and was shown to reorganize within the nucleolus in severely treated cells into circular structures, and to relocate to the nucleoplasm at 20 hours after recovery from a severe heat-shock. Liu *et al.* (1997) studied the effect of heat-shock on the nucleolar structure in *S. cerevisiaie*. They observed that many yeast nucleolar proteins including fibrillarin relocate to the cytoplasm after a severe shock (41-42.5°C) and suggested a disassembly of the nucleolar apparatus. In their article, they reported about unpublished data where fibrillarin relocates to the cytoplasm in HeLa cells upon heat-shock. However, they did not mention the temperature or the time of exposure used.

My data as seen by phase contrast microscopy and as demonstrated by anti-2H12 labeling does not suggest any disassembly of the nucleolus. It is possible however, that the nucleolus undergoes anatomical changes after a severe shock. Possibly the functions within the nucleolus are altered or inhibited: the organization and the distribution of fibrillarin due to severe shock undergo enormous change. Previous reports (Caizergues-Ferrer *et al.*, 1984) have shown that many nuclear matrix proteins induced due to heat-shock are nucleolar proteins, related to the 100 KDa major nucleolar protein component of preribosomes. They suggested that this increase in protein synthesis could result in the fixation of preribosomes on the nucleolar matrix.

There is also evidence that heat-shock inhibits transcription by RNA polymerase I in yeast cells: transiently at 37°C and more permanently at higher temperature. Paulin-Levasseur *et al.* (1999) studied the effects of actinomycin-D and DRB on the nucleolar structure in HeLa cells using double labelling experiments with anti-2H12 and anti-fibrillarin as markers. They observed a dot-like organizational change in DRB treated HeLa cultures. I also observed this redistribution with anti-fibrillarin after a severe treatment. They also observed that 2H12 and fibrillarin maintain a close spatial relationship. This indicates that nucleolar functions may be altered or inhibited. However, it is difficult to confirm that nucleolar fragmentation occurs.

Ochs and Smetana (1991) examined the distribution of fibrillarin in nucleolar remnants of *in situ* NM preparations from HeLa cells. They observed that fibrillarin remained associated with the NM after sequential digestion with DNase I and RNase A. My data supported this literature: fibrillarin remained associated with the NM of intact control HeLa S3. In mildly treated and in recovered cells fibrillarin maintained its control-like distribution after DNase I digestion. However, a sequential digestion with DNase I and RNase A resulted in some of this antigen relocalizing into the nucleoplasm. This is possibly due to the release of RNA. The reason why fibrillarin is maintained in the nucleolus upon RNase A digestion is not evident. However, two populations of fibrillarin may exist: one may play a role in the early processing of pre-mRNA - fibrillarin has been shown to be a member of U3 snRNP and functions in pre-rRNA processing (Lischwe *et al.*, 1985; Parker *et al.*, 1987; Kass *et al.*, 1990).

Another population of fibrillarin may possess a structural role. Fibrillarin may be used as a scaffold upon which rRNA processing and packaging occurs. This protein is highly charged (Lischwe *et al*, 1985). Thus it may accommodate interactions between itself, ribosomal DNA, rRNA and other proteins such as B23 and nucleolin, which are members of the DFC as well (reviewed by Bosman, 1999).

A severe heat-shock results in a major reorganization of fibrillarin in NM of HeLa S3 cells. Fibrillarin is found in dot-like structures of variable sizes. A severe shock followed by 20 hours of recovery at 37°C results in fibrillarin dispersing throughout the nucleoplasm in dot-like structures. This reorganization of fibrillarin is in accordance with my previous data where intact cells were studied.

Physiological stress due to heat-shock seems to affect extensively the distribution and the expression of internal nuclear antigens in HeLa S3. A mild heat-shock resulted in a reorganization of the 2A7 antigen and in a reduced expression of the nucleolar 2H12 protein. A severe stress resulted in the reorganization of 1B4, 2A7 and two nucleolar proteins, 2H12 and fibrillarin. A reduction in the level of expression of 2A7 was also observed following a severe treatment. These results are in contrast to the ones obtained when proteins to the nuclear periphery were studied. Peripheral antigens did not undergo organizational changes due to mild or severe heat-shock. Quantitative analysis indicated that LAP2β increased in its level of expression after mild and severe heat-shocks. The levels of expression of emerin and lamin B changed at the end

of the recovery period in mild and severe treatments respectively. These results were surprising. Why did these changes happen late during recovery? It is not likely that these changes are due to inhibition of DNA replication, arrest of cell proliferation or possible alterations to nucleocytoplasmic shuttling and mRNA splicing. If so, I would have observed changes in the level of expression of these proteins earlier.

The results obtained with 2H12 and fibrillarin further emphasize changes in nucleolar function and possible alterations but not fragmentation to the nucleolar structure.

The data presented in this thesis suggests that mild and severe heat-shock have similar effects on the cellular metabolism in HeLa S3 cells. The response of HeLa S3 cells to both types of stresses was similar in their survival , proliferation and in the inhibition of DNA replication. However, these two types of physiological stresses can have different effects on nuclear proteins. While a mild stress has an effect on the distribution and the expression of some antigens, a severe stress has a stronger effect and thus a more pronounced response. This may suggest that a severe stress may pause a longer-term threat to HeLa S3 cells. The purpose of this study was to provide a clearer picture of the structure/function relationships within the nuclear compartment. It supports the idea that nuclear organization and nuclear functions are interrelated. However, the "big picture" provided here suggests that the reorganization within the nuclear compartment may be happening to help HeLa S3 cells accommodate functional alterations due to stressful conditions, that threaten their survival. On the other

hand, these changes in structure may reflect the consequences of functional change.

4.2. DIFFERENTIATION

The effects of differentiation on nuclear organization in L6E9 myoblasts and in L6E9 myotubes

The data presented in section 3 of the Results chapter showed that L6E9 myoblasts differentiate into multinucleated myotubes using 10% horse serum for 9 days. I used the myosin heavy chain (MHC) and transcription factor myogenin as skeletal muscle markers to validate the differentiation system. Immunofluorescence microscopy showed that both markers are expressed in multinucleated myotubes but not in undifferentiated L6E9 cells. Biochemical analysis by Western blotting demonstrated the expression of myosin at high levels only from protein samples originating from myotubes. An early study by Bennoff and Nadal-Ginard (1979) showed that the level of MHC mRNA increase by 200 folds as L6E9 myoblasts differentiate into muscle. The levels of MHC mRNA have not been studied here but change in protein levels supports the evidence presented by Bennoff and Nadal-Ginard (1979).

Chaly *et al.* (1996) studied the same differentiation system using medium supplemented with 2% Hybrimax CPSR4 up to 7 days in culture. Their study was based on a time course analysis of control L6E9 myoblasts and cells in the process of myotubes formation: 1, 3, 5 and 7 days post-differentiation. They counted the number of nuclei per muscle fiber. Their results indicated that, 7 days post-differentiation, over 90 % of the cells exhibited 3-4 nuclei and were moderately or brightly stained by anti-myosin. My data showed that 9 days post-differentiation, at least 6 nuclei were present in each myotube. Also, over 90% of

the cells were differentiated and positive to cytoplasmic myosin and nuclear myogenin, while control cells were negative for these markers.

Lawson and Purslow (2000) studied the effect of the differentiation medium on different cell lines. They concluded that rat L6 cells form myotubes in medium containing 2% serum; while the C2C12 mouse cell line can be differentiated using serum-free medium. They showed that different cell lines respond in a divergent manner to the same medium. It is possible to suggest that differentiation occurs at variable rhythms in the same cell line if different medium components are used.

The data presented in this research thesis shows that LAP2β, LAP1C, emerin, lamins A/C and lamin B maintain their localization at the nuclear periphery. However, biochemical densitometric studies by Western blotting indicated that the levels of expression of these proteins decrease considerably in differentiated myotubes when compared to undifferentiated myoblasts. There is evidence of changes in the level of expression of LAP2β during development. Studies by Lang *et al.* (2000) demonstrated for the first time the developmentally regulated expression of an INMP during early embryogenesis: they identified XLAP2β, a homologue of mammalian LAP2β but it is found in *Xenopus*. This protein is expressed in *Xenopus* somatic cells, but it is not detectable in oocytes and early embryos before the beginning of the gastrula stage. Another member of the LAP2β family is of 84 KDa and is found in oocytes and early embryo, however its amount decreases during embryogenesis. The data presented here strongly suggests that antigens at the nuclear periphery are developmentally

regulated. The reasons behind the changes in the levels of expression of these proteins are not known. However, it is known that LAPs, emerin and LBR interact with nuclear lamins (Foisner and Gerace 1993; Harel *et al.* 1989; Maison et al. 1997; Schuler *et al.* 1994; Ye and Worman, 1996). These proteins may play a role in mediating interactions among the nuclear membrane, lamina proteins and chromatin. These interactions are essential for keeping the structure of the NM-chromatin organization during interphase and for the disassembly and reassembly of the nuclear envelope at the end mitosis (Nigg, 1992). But, differentiated skeletal muscle cells are non-dividing as demonstrated by Western blotting using anti-PCNA: the level of expression of this protein decreases in differentiated cells. The nuclear membrane in those cells may be expected to offer structural stability to the nucleus over a long period of time. It is a possibility that, since division ceases, INMP and nuclear lamins change to accommodate a different, possibly "protective" role towards the nuclear periphery.

My data by immunofluorescence microscopy demonstrated that the distribution of emerin, although it maintains its peripheral location changes from a uniform labeling in undifferentiated cells to a dot-like labeling at the nuclear periphery in differentiated ones. This change in organization was never reported in the literature. Lattanzi *et al.* (2000) used differentiated C2C12 mouse cells into skeletal muscle but did not observe any changes in the organization of emerin. It is possible that different cell lines have cell-specific protein responses following differentiation.

Interestingly, nuclear lamins have been shown to have a role in chromatin dynamics and functions. Lourim and Lin (1989) have used primary cultures and tissue samples of chicken embryonic muscle to demonstrate by quantitative immunoblotting that the expression of lamin A increases during myoblast differentiation and its expression precedes that of many muscle-specific such as MHC. In undifferentiated samples, lamin A was barely detectable. Their data predicted that lamin A may have a role in regulating the myogenic differentiation program, possibly by mediating the interactions nuclear lamina – chromatin. The results presented in this thesis showed that the expression of lamins A/C at the protein level decreases after 9 days of L6E9 cellular differentiation into muscle fibers. Further studies by Chaly *et al.* (1996) have shown that lamin A expression starts increasing 3 days after initiation of differentiation. However these authors adjusted their sample concentration using equal amount of DNA. The results of their Western blots are based on DNA concentration, while mine are based on protein concentration. They also observed by immunofluorescence microscopy that lamins stain the nuclear periphery more crisply as the differentiation process develops. Such qualitative analysis is very difficult to assess using this method.

A recent study by Muralikrishna *et al.* (2001) demonstrated by Western blotting that the abundance or the migration of lamins A/C did not change in differentiating C2C12 myoblasts. However, they studied the distribution of lamins A/C by immunofluorescence microscopy and observed changes. They focused on lamin speckles that associated with RNA splicing factor speckles in C2C12

myoblasts and myotubes: they observed that lamin speckles exist in dividing myoblasts but start disappearing early during differentiation and were absent in myotubes and muscle fibers. It is possible that different cellular systems possess divergent responses in the expression and the localization of their proteins.

Manilal *et al.* (1999) showed that cardiac muscle expresses lamins A/C and lamin B2 but not lamin B1. In their article they mentioned that lamin B1 is not detected in skeletal muscle either. However, they did not show any data about the expression of lamin B1 in skeletal muscle cells. My data showed by immunofluorescence microscopy and immunoblotting that lamin B1 is expressed in undifferentiated L6E9 myoblasts and in differentiated myotubes. The presence of lamins A/C and lamin B1 in differentiated cells may provide a protective role in maintaining the integrity of nuclear structure. It is known that LAP2β binds B-type lamins and chromatin (Foisner and Gerace, 1993; Furukawa *et al.* 1998); lamin B1 also binds chromatin, type-A lamins and LBR (Gerace and Foisner, 1994; Georgatos *et al.* 1994; Cowin and Burke, 1996; Ye and Worman, 1996). It is possible that LAPs and lamin B1 are involved in chromatin reorganization that occurs during differentiation. As mentioned by Chaly *et al.* (1996) condensed chromatin seems to gain a more peripheral organization in myotubes. Maybe the interactions chromatin-nuclear envelope may contribute to creating a non-random cell-specific chromatin distribution.

The data presented in this thesis indicated that the 1B4 antigen, associated with splicing factors reorganized in 9 days post-differentiated cultures. The distribution of this protein metamorphoses from a speckled distribution in

control cells and spreads within the nucleoplasm of multinucleated myotubes. A study by Luus (M.Sc. thesis, 1998) contradicts this result: 1B4 maintains its speckled distribution in L6E9 myotubes. However, the differentiation medium that was used contained 2% FBS and not horse serum as done in this study. Also, cell density was allowed to increase for three days only prior to observations – this is the time required to start observing cell fusion (Yaffe, 1968). In the data presented here, a different system for differentiation was used; also cells were observed 9 days post-differentiation. By this time, at least 90% of the cells were fused into multinucleated myotubes. It is possible that at the beginning of cell fusion, 1B4 maintains its speckled distribution and it changes during the latter stages of differentiation due to changes in cellular functions. It would be interesting to conduct a kinetic analysis to assess the exact timing of the changes in 1B4 distribution. To my knowledge, this is the first data indicating change in internal nuclear proteins in the L6E9 differentiating muscle system.

Chaly and Munro (1996) used immunofluorescence microscopy as a tool to demonstrate that centromeres of rat L6E9 cells reposition to the nuclear periphery during differentiation (with anti-centromere serum). They also used electron microscopy and observed that condensed chromatin became more prominent at the myotube nuclear envelope. Their purpose was to establish a parallel between nuclear organization and nuclear function. When a centromere repositions, the chromosome arms to which it is attached are repositioned as well. Thus the spatial order of the genome in these cells is deeply affected. This may be needed to help the expression of certain genes and not others. Also, the

fact that condensed chromatin is found to be more peripheral might indicate that gene expression is affected by altering DNA organization or by sequestering heterochromatin (Lourim and Lin, 1989). These changes in nuclear genome architecture might help explain the distribution of the 1B4 antigen in differentiated myoblasts. If genome organization is modified, it is not surprising that splicing sites undergo a change in their distribution; it could be in order to facilitate the splicing of certain genes or to repress others from being expressed. There is evidence that differentiated myotubes continue to synthesize mRNA and proteins at pre-fusion levels (Krauter et al., 1979; Benoff and Nadal-Ginard, 1980).

The differentiation of L6E9 cells into multinucleated myotubes is accompanied by reduced expression of protein located at the nuclear periphery. An interesting aspect would be to conduct a kinetic analysis in order to assess the exact timing of these changes. It would be interesting to know for example, if these changes occur early or late during the process of differentiation. This would help clarify the role of these proteins in muscle cell formation. The results obtained with 1B4 suggest that splicing in differentiating cells may take a different form, but is not necessarily arrested. Unfortunately, there is not a lot of studies relating changes in the localization and the expression of internal nuclear proteins in this cellular system. More studies on the expression of other internal nuclear proteins may provide a better understanding as to the structural and functional changes that happen during differentiation.

APPENDIX 1

Del-Pino E.M., Saenz F.E., Perez O.D., Brown F.D., Avila M-E., Barragan V.A., Haddad N., Paulin-Levasseur M., and Krohne G. (2002) Lamina-Associated Polypeptide 2 (LAP2) expression in fish and amphibians. Int. J. Dev. Biol. 46 :227-234.

I contributed entirely to the research performed on rainbow trout.

Int. J. Dev. Biol. 46: 227-234 (2002)

Original Article

Lamina-Associated Polypeptide 2 (LAP2) expression in fish and amphibians

EUGENIA M. DEL-PINO*, FABIÁN E. SÁENZ, OSCAR D. PÉREZ, FEDERICO D. BROWN, MARÍA-EUGENIA ÁVILA, VERÓNICA A. BARRAGÁN, NISRINE HADDAD[1], MICHELINE PAULIN-LEVASSEUR[1] and GEORG KROHNE[2]

Departamento de Ciencias Biológicas, Pontificia Universidad Católica del Ecuador, Quito, Ecuador, [1]Department of Biology, University of Ottawa, Ontario, Canada and [2]Division of Electron Microscopy, Biocenter of the University, Wuerzburg, Germany

ABSTRACT Somatic and germinal cells of 15 fish and 33 amphibian species were examined by SDS-PAGE followed by immunoblotting to determine the expression of LAP2 (lamina-associated polypeptide 2). LAP2 expression in frogs, salamanders and fish does not vary with the mode of reproduction. In fish and frog cells, a rim-like LAP2 positive region was detected around the nucleus by indirect immunofluorescence microscopy. The cell distribution and expression patterns of LAP2 in fish, frogs and salamanders are comparable with those found in *Xenopus* and zebrafish. The mammalian somatic cell pattern, which may also occur in gymnophione amphibians, includes LAP2α, β and γ as major isoforms, whereas LAP2α does not occur in cells of fish, frogs and salamanders. In fish, LAP2γ is the major isoform of somatic cells, suggesting that LAP2γ may be ancestral. However, in the rainbow trout, as in frogs and salamanders, LAP2β was the major somatic isoform. Fish and frog sperm only express low molecular weight polypeptides. In contrast, fish and frog oocytes express an oocyte-specific LAP2 isoform of high molecular weight. In the toad *Bufo marinus* this isoform becomes upregulated in pre-vitellogenic oocytes of 150-200 μm in diameter. The absence of LAP2α and the differential expression of LAP2 isoforms in somatic and germ cells, as found in fish and frogs, may be ancestral vertebrate characters. In spite of differences in developmental time, the LAP2 isoforms of somatic cells are upregulated during gastrulation, suggesting that LAP2 may be implicated in the early development of fish and frog.

KEY WORDS: *LAP2, somatic cell, germ cell, zebrafish, Xenopus*

Introduction

From the time of their discovery by Foisner and Gerace (1993), the functions of LAP2 (lamina-associated polypeptide 2) in nuclear dynamics and architecture, disease, and development have been gradually elucidated (reviewed in Dechat *et al.*, 2000; Gruenbaum *et al.*, 2000; Wilson, 2000). Six isoforms of LAP2 (LAP2α, β, ε, δ, γ and ξ) occur in mammals. These isoforms are generated by alternative splicing of the same transcript, and all of them, with the exception of LAP2α and LAP2ξ, are type II integral membrane proteins (IMPs) of the inner nuclear membrane (reviewed in Dechat *et al.*, 2000). LAP2 isoforms bind to the nuclear lamina, are involved in postmitotic nuclear reassembly, may stabilize chromatin structure, and may target membranes to the chromosomes (reviewed in Dechat *et al.*, 2000). In addition, LAP2 isoforms are implicated in autoimmune diseases (Konstantinov *et al.*, 1995; Paulin-Levasseur *et al.*, 1996) and LAP2-related proteins are involved in the Emery-Dreifuss muscular dystrophy (Wilson, 2000). The differential expression and the regulation of LAP2 isoforms during *Xenopus* development suggest that these polypeptides may play a role in development (Lang *et al.*, 1999).

LAP2β has an N-terminal nucleoplasmic domain, a transmembrane domain, and a C-terminal domain located between inner and outer nuclear membranes (reviewed in Dechat *et al.*, 2000). The nucleoplasmic domain includes a lamina binding region (to lamin B1/B2 residues) and a 187 amino acid long N-terminal region that interacts with the chromatin. LAP2 isoforms share the LEM domain in the N-terminal region with the related proteins, emerin and MAN1 (Lin *et al.*, 2000). The LEM domain interacts with the chromosomal barrier of autointegration factor (BAF),

Abbreviations used in this paper: A6, *Xenopus* kidney cells; BAF, barrier of autointegration factor; BCIP, 5-bromo-4-chloro-3-indolyl phosphate; IMP, integral membrane protein; kDa, kilodaltons; LAP2, lamina-associated polypeptide 2; LEM, LAP2-Emerin-MAN1 domain; NBT, nitro blue tetrazolium; P_{200}, *Xenopus* egg membranes; PBS, phosphate buffered saline; SDS-PAGE, sodium dodecyl sulfate-polyacrylamide gel electrophoresis; TBST, Tris buffered saline-tween; XLAP2β, *Xenopus* homologue of LAP2β.

***Address correspondence to:** Dr. Eugenia M. del Pino. Pontificia Universidad Católica del Ecuador, Departamento de Ciencias Biológicas, Avenida 12 de Octubre y Patria, Apartado 17-01-2184, Quito, Ecuador. Fax: +593-2-256-7117. e-mail: edelpino@puceuio.puce.edu.ec

0214-6282/2002/$25.00

Printed in Spain
www.ijdb.ehu.es

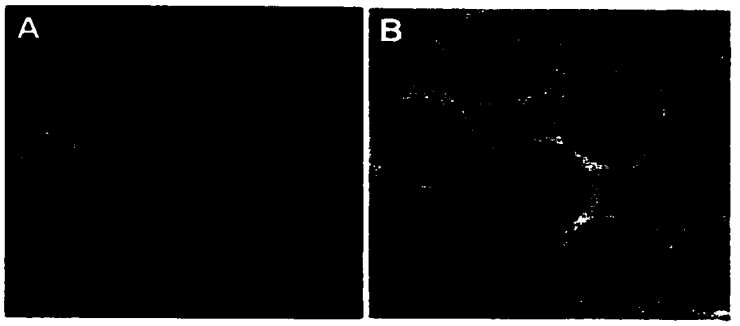

Fig. 1. LAP2 distribution in fish cells. (A) *Indirect immunofluorescence microscopy of rainbow trout hepatocytes with the MAN serum.* **(B)** *Phase contrast microscopy of the cells shown in (A). The average hepatocyte cell diameter is 14 μm.*

which seems to participate in the binding of LAP2 to the chromatin (Furukawa, 1999). LAP2 ε, δ, and γ are structurally similar to LAP2β, and lack only short regions of the LAP2β nucleoplasmic domain. In contrast, LAP2α only shares the N-terminus 187 amino acids with other LAP2 isoforms (Dechat *et al.*, 2000). It is postulated that the divergent LAP2α may contribute to stabilize higher order chromosome structure, whereas LAP2β may influence chromatin structure in ways that could modulate replication and possibly the competence for transcription (Gant *et al.*, 1999; Dechat *et al.*, 2000).

Two patterns of LAP2 expression have been detected, one in mammals (Harris *et al.*, 1994; Alsheimer *et al.*, 1998), and the other in *Xenopus* (Lang *et al.*, 1999). In mammals, the major LAP2 isoforms of somatic cells are LAP2α, β, and γ (Harris *et al.*, 1994; Alsheimer *et al.*, 1998; Goldberg *et al.*, 1999). In contrast, LAP2α has not been detected in *Xenopus* (Lang *et al.*, 1999). *Xenopus* somatic cells express one major LAP2 polypeptide (XLAP2: renamed XLAP2β), which is the homologue of the mammalian LAP2β (Gant *et al.*, 1999; Lang *et al.*, 1999), but it is unknown whether *Xenopus* expresses LAP2γ. In *Xenopus* oocytes and early embryos, XLAP2β is absent, and instead, an oocyte-specific LAP2 isoform has been found, whose cDNA has not been cloned. This isoform is down regulated after the gastrula stage, and becomes gradually replaced during development by XLAP2β, the isoform typical of somatic cells. The oocyte-specific LAP2 isoform has a higher molecular weight than XLAP2β, has a transmembrane domain, and therefore differs from the mammalian LAP2α (Lang *et al.*, 1999). In the zebrafish, somatic and oocyte-specific LAP2 isoforms have been found, with differential expression during development (Schoft *et al.*, unpublished). In contrast with *Xenopus*, LAP2γ is the major LAP2 isoform in zebrafish somatic cells and LAP2β is less abundant. The zebrafish LAP2β, γ, and oocyte-specific isoforms have been cloned (Schoft *et al.*, unpublished). Sequence information excludes the possibility that the zebrafish oocyte-specific LAP2 isoform is a homologue of the mammalian LAP2α (Schoft *et al.*, unpublished). As in *Xenopus*, LAP2α has not been detected in the zebrafish.

LAP2 expression patterns in fish and amphibians are of interest because these vertebrates display many distinct reproductive and developmental adaptations (Ballard, 1981; Wourms and Whitt, 1981; Duellman and Trueb, 1986; Harvey *et al.*, 1999). Taking advantage of the biodiversity of Ecuador, we have investigated the LAP2 expression in native fish and amphibians with modified modes of reproduction. The non-native fish studied are the swordfish (*Xiphophorus helleri*, and X. *maculatus*), the carp (*Cyprinus carpio*), the zebrafish (*Danio rerio*), and the rainbow trout (*Onchorhynchus mykiss*). The LAP2 expression in the small viviparous teleost *Priapichthys panamensis* was compared to 14 additional oviparous and viviparous teleost fish. Females of *P. panamensis* carry embryos of several developmental stages in the ovary (Sáenz *et al.*, unpublished), a condition known as superfetation (Haynes, 1995). Among the frogs, 17 species deposit their eggs in the water, such as the toad, *Bufo marinus*, and 13 species have terrestrial reproduction (amphibian reproductive modes are according to Duellman and Trueb, 1986). Frogs with terrestrial reproduction include frogs with direct development of the genus *Eleutherodactylus*, and the marsupial frogs of the genus *Gastrotheca* that brood the embryos inside a maternal pouch. In addition, the LAP2 expression of dendrobatid frogs was studied. Eggs of dendrobatid frogs are deposited on land, and when the tadpoles hatch, one of the adults transports them on its back to the water. Besides anurans, the comparison was extended to the lungless salamander *Bolitoglossa equatoriana* (Plethodontidae). *Bolitoglossa* eggs are terrestrial and undergo direct development. Two species of the limbless and tailless gymnophione amphibians genus *Caecilia* were also studied. Our comparative analysis of diverse fish and amphibian species suggests that LAP2 isoforms are important, not only within the cell, but also in development and evolution.

Results

LAP2 Expression in Somatic Cells

The human serum MAN (Paulin-Levasseur *et al.*, 1996) and the ZLAP2-serum1 (Schoft *et al.*, unpublished) reacted, albeit weakly in some cases, with fish LAP2 polypeptides. The MAN serum gave a stronger signal in amphibian cells. These tools allowed us to analyze LAP2 expression in fish and amphibians. The electrophoretically estimated molecular weights of the LAP2 isoforms varied among species of fish, frogs and salamanders (Tables 1, 2). The LAP2 signal, detected by immunofluorescence with the MAN antiserum, was located around the nuclear membrane in hepatocytes (Fig. 1 A,B), erythrocytes, brain, and white muscle cells (not shown) of the oviparous fish *Onchorhynchus mykiss* (rainbow trout). A similar LAP2 distribution was observed in the liver and testis of the viviparous fish *P. panamensis*, the toad *B. marinus* and the frog without tadpoles *Eleutherodactylus achatinus* (not shown). These patterns are equivalent to the LAP2 distribution seen in cells of *Xenopus* (Lang *et al.*, 1999).

The somatic LAP2 expression of oviparous and viviparous fish included LAP2β and LAP2γ polypeptides as major isoforms (Table 1). In fish, the expression levels of LAP2β and LAP2γ varied in different somatic tissues and species. LAP2γ was significantly more abundant than LAP2β in somatic cells of the zebrafish (Schoft *et al.*, unpublished) and most other fish, as illustrated by the LAP2 expression pattern in the heart of the viviparous fish, *P. panamensis* (Fig. 2A). LAP2γ was the only detected LAP2 isoform of certain tissues, such as the liver, heart, and spleen of the oviparous fish, *Moenkhausia* (Fig. 2B).

An exception to the fish somatic pattern was found in the rainbow trout. LAP2β was the major isoform of somatic cells. However the levels of LAP2β and LAP2γ expression varied in different cells (Fig. 2 C,D). For example, LAP2β was the major isoform found in the gills, brain, and heart cells (Fig. 2C), as well as

Fig. 2. LAP2 expression in fish. *Western blot analysis of fish polypeptides. Proteins were separated by SDS-PAGE with 11% acrylamide in (A), 10% acrylamide in (B), and 12% acrylamide in (C,D), and immunoblotted with the MAN serum.* **(A)** *LAP2 expression in an adult male of the viviparous fish* P. panamensis. *LAP2 expression in this fish (lanes 1 and 4-6) is compared to that in rat (lane 2) and Xenopus (lanes 3 and 7).* **(B)** *LAP2 expression in the oviparous fish* Moenkhausia. *LAP2β was not detected in liver, heart and spleen of this fish (lanes 1, 4 and 5, respectively). However it is abundant in the somatic cells of the ovary (compare lanes 6 and 8). Lane 6 corresponds to an oocyte-enriched fraction, contaminated with somatic cells.* **(C)** *LAP2 expression in the oviparous rainbow trout* (Onchorhynchus mykiss). *LAP2β was detected in the gills, brain and heart of this fish. A low expression level of LAP2γ occurred in the heart (lane 3).* **(D)** *LAP2 expression in hepatocytes and erythrocytes of the rainbow trout. The white dots in lane 2 of (A) and 3 of (B) indicate the rat LAP2α (78 kDa), LAP2β (58 kDa), and LAP2γ (40 kDa) isoforms. The white dots in lane 3 of (C) and lane 1 of (D) indicate LAP2β (65 kDa) and LAP2γ (40 kDa). Molecular masses of reference proteins are given (in kDa). In this and the following Figures, A6 corresponds to* Xenopus *kidney cells and P200 are* Xenopus *egg membranes. Erythr, erythrocytes; Hepat, hepatocytes; RV, rat somatic proteins; Spcytes, spermatocytes.*

in the spleen, kidney, white and red muscle cells (not shown). LAP2γ was not detected in most tissues. However low expression levels of LAP2γ were found in the heart (Fig. 2C), and spleen (not shown). The levels of LAP2γ expression were higher in some cases, such as in hepatocytes and erythrocytes (Fig. 2D). In hepatocytes, LAP2β and LAP2γ had similar levels of expression, whereas LAP2γ was the only LAP2 isoform of rainbow trout erythrocytes (Fig. 2D).

As in *Xenopus*, LAP2β was the major isoform found in somatic cells of frogs and salamanders (Table 2). This pattern is illustrated for the frog without tadpoles, *Eleutherodactylus unistrigatus* (Fig. 3A), the toad *B. marinus* (Fig. 3A), and the tree frog *Hyla lanciformis* (Fig. 3B). A small polypeptide was frequently found in frog spleen (Fig. 3A). All of the examined somatic tissues of *Osteocephalus yasuni* expressed a small polypeptide of about 40 kDa (not shown). Poeciliid fish somatic cells express a smaller polypeptide (Fig. 2A). However, the small polypeptides found in fish and frog cells cannot be regarded as LAP2 isoforms, because the MAN serum detects a small LAP2-unrelated polypeptide in *Xenopus* (Lang *et al.*, 1999).

LAP2α was not found in cells of the fish and amphibians analyzed. However in somatic cells of the gymnophione amphibian *Caecilia*, an immunoreactive polypeptide was detected with mobility on SDS-PAGE similar to the mammalian LAP2α (Fig. 3C; Table 2). Presently we do not know whether this large immunoreactive polypeptide has biochemical similarities with LAP2α. Moreover, *Caecilia* somatic cells express in addition two LAP2 isoforms, with electrophoretic mobilities that resemble the mammalian LAP2β and γ (Fig. 3C; Table 2). This pattern differs from the LAP2 expression pattern of fish and frog somatic cells and resembles the pattern of rat somatic cells.

LAP2 Expression in Sperm and Testis

The sperm of fish and frogs lacks the LAP2 isoforms that are typical of somatic cells (LAP2β and γ in fish and LAP2β in frogs). Instead, one or two small polypeptides were characteristically found in fish and frog sperm cells (Table 1, 2), as shown for the viviparous fish *P. panamensis* (Fig. 2A), and the tree frog *H. lanciformis* (Fig. 3B). Two sperm-specific small polypeptides were usually found in the testis of hylid frogs, whereas in other frog and fish species, usually only one small sperm-specific polypeptide was detected (Table 2). Fish and frog spermatocytes expressed the sperm-specific polypep-

TABLE 1

APPARENT MOLECULAR SIZE (kDa) OF LAP2 ISOFORMS IN FISH WITH DIFFERENT REPRODUCTIVE MODES

Fish species	LAP2 isoforms				Small polypeptide (<40 kDa)	
	α	β	γ	Oocyte	Sperm	Oocyte
Viviparous fish						
CYPRINODONTIFORMES: POECILIIDAE						
Priapichthys panamensis	No	64	46	87	Yes	Yes
Xiphophorus helleri	No	58	48	88	Yes	Yes
X. maculatus	No	60	48	81	Yes	Yes
Oviparous fish						
CHARACIFORMES: CHARACIDAE						
Aphyocharax sp.	No	Nd	45	84	Nd	Nd
Bryconamericus caucanus	No	62	44	80	Yes	Yes
Moenkhausia oligolepis	No	Nd	46	84	Yes	Yes
Moenkhausia sp.	No	59	48	84	Nd	Yes
Rhoadsia altipinna	No	Nd	46	76	Yes	Yes
CHARACIFORMES: CURIMATIDAE						
CURIMATIDAE sp.	No	Nd	46	Nd	Nd	Nd
CYPRINIFORMES: CYPRINIDAE						
Cyprinus carpio	No	68	47	Nd	Yes	Yes
Danio rerio (zebrafish)[1]	No	63	45	84	Yes[2]	Nd
PERCIFORMES: CICHLIDAE						
Aequidens rivulatus	No	Nd	52	78	Nd	Yes
PERCIFORMES: ELEOTRIDAE						
Dormitator latifrons	No	Nd	50	Nd	Yes	Yes
SALMONIFORMES: SALMONIDAE						
Onchorhynchus mykiss	No	65	40	Nd	Nd	Nd
SILURIFORMES: LORICARIIDAE						
Ancistrus sp.	No	Nd	45	Nd	Nd	Yes

[1]Schoft *et al.*, unpublished. [2]This work, not shown. Nd, not determined; No, not present; Yes, present

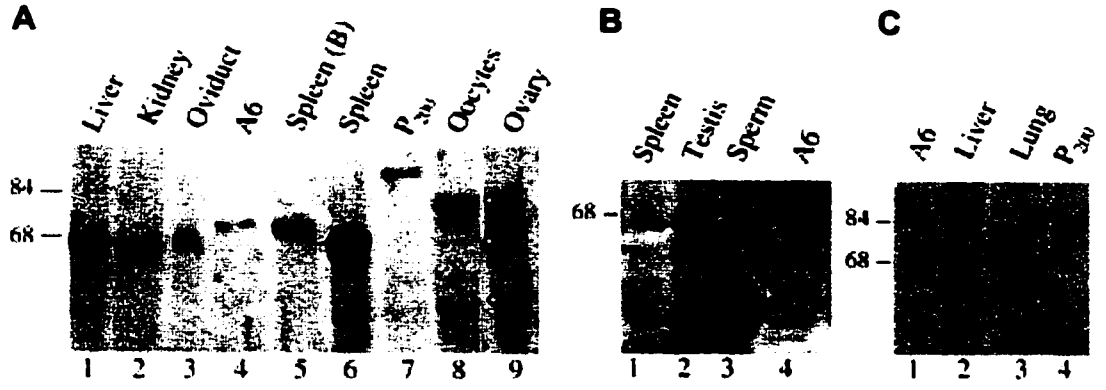

Fig. 3. LAP2 expression in Amphibia. *Proteins were separated by SDS-PAGE with 10% acrylamide and immunoblotted with the MAN serum.* **(A)** *LAP2 expression in* Eleutherodactylus unistrigatus, *a frog with direct development, in comparison to* Bufo marinus *and* Xenopus, *frogs with aquatic reproduction. LAP2 expression in* E. unistrigatus *(lanes 1-3, 6, 8, and 9), and in the spleen of* B. marinus *(spleen B, lane 5) is compared to that of* Xenopus *(lanes 4 and 7). Somatic tissues of* E. unistrigatus *and* B. marinus *(lanes 1-3, and 5-6) express LAP2β.* E. unistrigatus *oocytes (lane 8) express the oocyte-specific LAP2 isoform and a small polypeptide which is also found in the spleen of this frog. In the ovary (lane 9), follicle cell LAP2β was found in addition to the oocyte specific LAP2 polypeptides (seen in lane 8). The white dots indicate the oocyte-specific isoform (73 kDa), follicle cell LAP2β (58 kDa) and a small oocyte-specific polypeptide (<40 kDa).* **(B)** *LAP2 expression in a male* Hyla lanciformis, *a frog with aquatic reproduction. LAP2 expression in this frog (lanes 1-3) is compared to that of* Xenopus *(lane 4). LAP2β was detected in the spleen and testis (lanes 1-2). However sperm only express two small polypeptides of about 33 and 26 kDa, which are also seen in the testis (indicated by white dots in lane 2).* **(C)** *LAP2 expression in the gymnophione amphibian* Caecilia orientalis *(lanes 2-3) is compared to that observed in* Xenopus *(lanes 1 and 4). The samples were derived from an aquatic* C. orientalis *larvae at hatching. The white dots in lane 2 indicate the three polypeptides of* C. orientalis *(about 90, 68 and 43 kDa, respectively) which crossreacted with LAP2 antibodies of the MAN serum. Molecular masses of reference proteins are given (in kDa).*

tides and the LAP2 isoforms typical of somatic cells (Fig. 2A). The testes in fish, frogs, and salamanders contain somatic, spermatogenic and sperm cells and expressed the LAP2 isoforms of somatic cells and the sperm-specific polypeptides. This pattern is seen in the fish *P. panamensis* and the frog *H. lanciformis* (Figs. 2A, 3B). In the carp (*Cyprinus carpio*) similar amounts of LAP2β and LAP2γ were found in testes and spermatocytes. Carp somatic cells, in contrast, expressed higher amounts of LAP2γ than of LAP2β, as seen in somatic cells of most other fish. No sperm-specific polypeptide was detected in the carp testis (not shown).

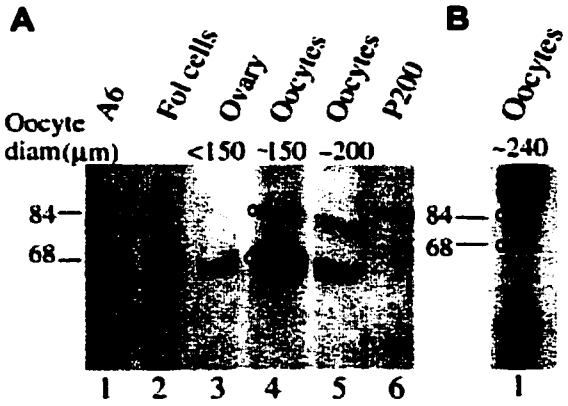

Fig. 4. LAP2 expression during oogenesis in *Bufo marinus*. *Proteins were separated by SDS-PAGE with 10% acrylamide and immunoblotted with the MAN serum. The size of the oocytes analyzed is comparable to that of* Xenopus *stage I oocytes (Dumont, 1972).* **(A)** *LAP2 expression in follicle cells, a juvenile ovary and previtellogenic oocytes of up to approximately 200 μm in diameter. LAP2 expression in Bufo (lanes 2-5) is compared to that in* Xenopus *(lanes 1 and 6).* **(B)** *LAP2 expression in oocytes of up to approximately 240 μm in diameter. The oocyte diameters given in (A) and (B) are the maximum diameter of oocytes found in each ovarian sample. The 68 kDa band in oocyte samples comes from small oocytes and possible contamination with follicle cells. The white dots in lane 4 of (A) and lane 1 of (B) signal the oocyte-specific LAP2 (84 kDa) and LAP2β (68 kDa). Molecular masses of reference proteins are given (in kDa). Fol cells, follicle cells.*

LAP2 Expression in Ovary and Oocytes

Fish, frog, and salamander oocytes expressed an oocyte-specific LAP2 isoform, whose apparent molecular weight is higher than that of LAP2β (Table 1, 2). The LAP2 isoforms, characteristic of somatic cells (LAP2β and LAP2γ in fish, and LAP2β in frogs and salamanders), were not found in oocytes, as shown for the oviparous fish *Moenkhausia* (Fig. 2B) and the frog with direct development *E. unistrigatus* (Fig. 3A). The LAP2β band seen in *Moenkhausia* oocytes (Fig. 2B) comes from contamination with follicle cells. A small polypeptide was sometimes found in fish and frog oocytes (Table 1, 2), as seen for *E. unistrigatus* (Fig. 3A), and *Xenopus* (Lang *et al.*, 1999).

In contrast with oocytes, fish ovary expressed three LAP2 isoforms, which are the LAP2β and γ isoforms of follicle cells, and the oocyte-specific LAP2 polypeptide (Fig. 2B). This pattern is different from that of mammalian cells, because LAP2α did not occur in fish. In frog ovaries, the two polypeptides detected are LAP2β of follicle cells and the high molecular weight oocyte-specific LAP2 polypeptide. Additionally, in ovaries of some frogs, a small polypeptide was also present (Fig. 3A).

The onset of expression for the oocyte-specific LAP2 isoform was determined in juvenile ovaries of *B. marinus*. In ovaries containing oocytes of up to 150 μm in diameter, only LAP2β was detected, whereas the oocyte-specific LAP2 isoform became detectable in oocytes of 150-240 μm in diameter (Fig. 4 A,B). Thereafter, the oocyte-specific LAP2 was the major isoform found in oocytes throughout *Bufo* oogenesis (not shown). *Bufo* oocytes of 200 μm in diameter were previtellogenic, translucent, and with a large germinal vesicle that contains numerous nucleoli. In sections, the oocyte chromosomes resembled lampbrush chromosomes (not shown). This observation suggests that the upregulation of the oocyte-specific LAP2 isoform occurs in oocytes that may have reached the diplotene stage.

LAP2 Expression During Development

The gradual replacement of the oocyte-specific LAP2 by the isoforms typical of somatic cells starts during gastrulation in *Xenopus* and in the zebrafish (Lang *et al.*, 1999; Schoft *et al.*,

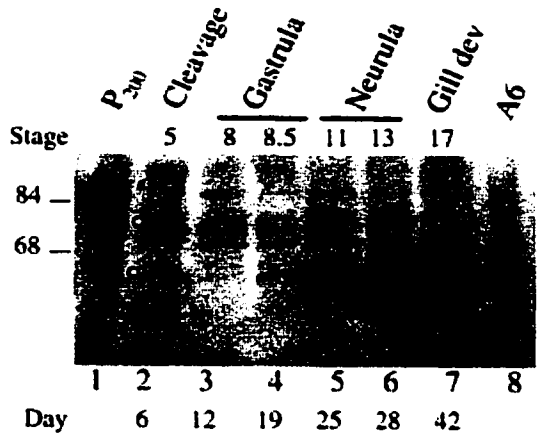

Fig. 5. LAP2 expression during development of the marsupial frog *Gastrotheca riobambae*. *Proteins were separated by SDS-PAGE with 10% acrylamide and immunoblotted with the MAN serum. Each lane contains proteins from one embryo. LAP2 expression in Gastrotheca embryos (lanes 2-7) is compared to that in* Xenopus *(lanes 1 and 8). The oocyte-specific LAP2 (74 kDa) and LAP2β (62 kDa) are signaled by dots in lane 2. The intermediate size polypeptide may correspond to a degradation product of the oocyte-specific LAP2, as in* Xenopus *(Lang et al., 1999). Molecular masses of reference proteins are given (in kDa). Gill dev, gill development.*

unpublished). Similarly, the switch of LAP2 expression from oocyte-specific to the somatic pattern occurred during gastrulation in the frogs *Gastrotheca* (Fig. 5), and *Colostethus machalilla*, and in the viviparous fish *P. panamensis* (not shown). In embryos of the marsupial frog *Gastrotheca*, the oocyte-specific LAP2 polypeptide was the major LAP2 isoform of cleavage stage embryos. LAP2β became upregulated in the advanced gastrula, and gradually replaced the maternal oocyte-specific LAP2 during development (Fig. 5). The main difference found among species was in the timing of developmental events. Whereas *Xenopus* embryos require 13.25 hours to reach the late gastrula (stage 12 of Nieuwkoop and Faber, 1994), *C. machalilla* takes 3 days (Ávila, *et al.*, unpublished), and *Gastrotheca* (Fig. 5) requires 19 days (del Pino and Escobar, 1981). In *Gastrotheca*, low levels of LAP2β may be expressed during cleavage, as suggested by the faint LAP2β band seen in cleavage and early gastrula embryos (Fig. 5). The time to reach the gastrula stage is unknown for the viviparous fish *P. panamensis*.

Discussion

Three patterns of LAP2 expression (Table 3) are found in the vertebrates, exemplified by the zebrafish, *Xenopus*, and the rat (Alsheimer *et al.*, 1998; Lang *et al.*, 1999; Schoft *et al.*, unpublished). The major LAP2 isoforms of fish somatic cells are LAP2β and γ, with varying levels of expression in different tissues and species (Table 3). The prevalent pattern is the abundance of LAP2γ in fish somatic cells, such as it occurs in the zebrafish (Schoft *et al.*, unpublished). However, in the rainbow trout LAP2β is the major isoform of somatic cells. Similarly, LAP2β is the major isoform of somatic cells in frogs and salamanders. In contrast, somatic cells of gymnophione amphibians express three LAP2 isoforms with mobilities similar to the mammalian α, β and γ polypeptides (Fig. 3C; Table 3). Presently we do not know whether the large immunoreactive polypeptide of gymnophione amphibians represents a LAP2 isoform that possesses biochemical properties comparable with that of the mammalian α-polypeptide or a membrane bound polypeptide like LAP2β. So far, the presence of three major LAP2 isoforms (LAP2α, β, and γ) in somatic cells appears as characteristic of the mammals (Table 3). LAP2γ may represent an ancestral isoform, as it is predominant among fish (Table 1). LAP2β and LAP2α may be derived isoforms, given their presence in fish and frog cells and in mammalian cells, respectively (Tables 1, 2).

The germ cell LAP2 expression differs from the somatic patterns. Rat sperm expresses LAP2α (Alsheimer *et al.*, 1998). However fish and frog sperm cells express only small LAP2-related polypeptides (Table 3). An oocyte-specific LAP2 isoform is characteristic of fish and frog oocytes and early embryos, whereas, in the mammals this LAP2 isoform has not been detected (Table 3). We found the presence of LAP2α, β, and γ in the mouse ovary, as in somatic cells (not shown). However the large proportion of somatic cells may hinder the detection of an oocyte-specific LAP2 isoform in the mouse ovary. LAP2 expression may be linked to the characteristics of differentiated cells, such as the different lamin types or to the chromatin structure. In fact, cells with different functions, such as sperm, oocytes and early embryos, express different LAP2 isoforms (Table 3) and different lamins (Benavente and Krohne, 1985; Stick, 1988; Alsheimer *et al.*, 1998; Lang *et al.*, 1999). Moreover, the peculiarities of chromatin structure in the highly modified sperm, oocytes and embryonic cells may require the expression of different isoforms of LAP2.

This comparative analysis suggests that the different reproductive modes found in fish and amphibians are not related to the patterns of LAP2 expression (Tables 1, 2). We expected to find a wide variety of LAP2 expression patterns in the fish, given that they represent the most diverse vertebrate group. The analyzed fish (Table 1) are classified into eight families, representing five teleost orders according to Froese and Pauly (2000). However, an unvarying pattern was observed in the zebrafish, and in oviparous and viviparous teleost fish (Table 1). The major deviation from the fish common pattern occurs in the rainbow trout (Table 1), whose somatic cell LAP2 expression resembles the frogs rather than the fish. However, the reproductive mode of the rainbow trout provides no indication of its deviant mode of LAP2 expression. The rainbow trout LAP2 pattern may be shared by other Salmonidae, and therefore, it is important to analyze the LAP2 pattern in other members of this group. Similarly, representatives of other fish taxa should be analyzed to determine whether further LAP2 deviation exists among fish.

The analyzed frogs and salamanders (Table 2) have several modes of reproduction and represent six different anuran families, and one urodele family (Duellman and Trueb, 1986). However, the LAP2 expression pattern does not deviate from *Xenopus* (Table 2). Surprisingly, the somatic cell pattern of gymnophione amphibians differs from the other amphibians and appears comparable to that of the mammals (Table 2). The deviant LAP2 expression of gymnophione amphibians correlates with other features of this group. In fact, the gymnophione are the most divergent amphibians, lacking limbs and tail (Duellman and Trueb, 1986). Moreover, the caecilian vertebral development has unique characters, differs from frogs, and in general resembles the mammals (Wake and Wake, 2000). The rainbow trout and gymnophiones deserve further analysis to determine the molecular affinities of their divergent LAP2 polypeptides.

LAP2α does not occur in cells of the zebrafish (Schoft *et al.*, unpublished), 14 additional teleost fish (Table 1), *Xenopus* (Lang *et al.*, 1999), 30 frog species, and a salamander (Table 2). These findings contrast with the abundance of LAP2α in mammalian cells (Lang *et al.*, 1999; Dechat, *et al.*, 2000). It is unknown whether LAP2α is expressed in somatic cells of gymnophione amphibians (Table 2). Fish, frogs and salamanders have differential expression of LAP2 in somatic and germ cells, whereas only sperm has differential LAP2 expression in the mammals (Table 3). The absence of LAP2α and the differential expression of LAP2 in somatic, germ cells, and during development are common among the lower vertebrates, and may correspond to ancestral vertebrate characters. Moreover, the transition of LAP2 expression from oocyte-specific to the somatic pattern occurs at gastrulation in the species analyzed, in spite of differences in the timing of developmental events. These observations signal the likely involvement of LAP2 in the early development of fish and frogs.

TABLE 2

APPARENT MOLECULAR SIZE (kDa) OF LAP2 ISOFORMS IN AMPHIBIANS

Species	LAP2 isoforms				Small polypeptide (<40 kDa)	
	α	β	γ	Oocyte	Sperm	Oocyte
ANURA						
A. Eggs deposited in water[1]						
BUFONIDAE						
Atelopus spumarius	No	68	Nd	Nd	Yes	Nd
Bufo haematiticus	No	68	Nd	84	Yes	Yes
B. margaritifer	No	68	Nd	84	Yes	Yes
B. marinus	No	68	Nd	84	Yes	Yes
Dendrophryniscus minutus	No	68	Nd	84	Nd	Yes
HYLIDAE						
Hyla bifurca	No	59	Nd	Nd	Yes	Nd
H. carcarata	No	64	Nd	79	Yes	Yes
H. granosa	No	62	Nd	Nd	Yes	Nd
H. lanciformis	No	64	Nd	79	Yes (2 bands)	Yes
H. pelucens	No	58	Nd	70	Yes (2 bands)	Yes
H. rosembergi	No	59	Nd	Nd	Yes (2 bands)	Nd
Osteocephalus yasuni	No	60	Nd	74	Yes (2 bands)	Yes
Scinax ruber	No	65	Nd	Nd	Nd	Nd
Scinax quinquefasciata	No	61	Nd	75	Nd	Yes
LEPTODACTYLIDAE						
Barycholos pulcher	No	58	Nd	73	Nd	Yes
Physalaemus sp.	No	58	Nd	Nd	Yes	Nd
PIPIDAE						
Xenopus laevis[2]	No	68	Nd	84	Nd	Nd
B. Eggs arboreal, tadpoles drop into water[1]						
CENTROLENIDAE						
Centrolene grandisone	No	64	Nd	Nd	Nd	Nd
C. Eggs terrestrial, tadpoles carried to water by an adult[1]						
DENDROBATIDAE						
Colostethus machalilla	No	62	Nd	75	Nd	Yes
C. infraguttatus	No	63	Nd	77	Nd	Yes
Epipedobates boulengeri	No	68	Nd	84	Nd	No
E. tricolor	No	68	Nd	84	Nd	Yes
D. Eggs terrestrial, direct development[1]						
LEPTODACTYLIDAE						
Eleutherodactylus achatinus	No	58	Nd	73	Yes	Nd
E. appendiculatus	No	58	Nd	73	Nd	Nd
E. eugeniae	No	58	Nd	73	Nd	Yes
E. longirostris	No	58	Nd	73	Nd	Yes
E. simonbolivari	No	58	Nd	73	Nd	No
E. unistrigatus	No	58	Nd	73	Yes	Yes
E. w-nigrum	No	58	Nd	Nd	Yes	Yes
E. Eggs carried in dorsal pouch of female, tadpoles aquatic[1]						
HYLIDAE						
Gastrotheca riobambae	No	62	Nd	74	No	Yes
G. pseustes	No	64	Nd	Nd	No	Nd
URODELA						
Eggs terrestrial, direct development[1]						
PLETHODONTIDAE						
Bolitoglossa equatoriana	No	59	Nd	Nd	Nd	No
GYMNOPHIONA						
Reproduction unknown[1]						
CAECILIIDAE						
Caecilia guntheri	87[3]	65[3]	40[3]	Nd	Nd	Nd
C. orientalis	90[3]	68[3]	43[3]	Nd	Nd	Nd
MAMMALIA						
Rattus rattus[2]	78	58	40	No[4]	Nd	Nd

[1]Reproductive modes according to Duellman and Trueb (1986). [2] According to Lang *et al.*, (1999). [3] It is unknown whether these polypeptides have biochemical similarities with the mammalian LAP2α, β and γ. [4] In the mouse (not shown). Nd, not determined; No, not present; Yes, present

Materials and Methods

LAP2 Standards of Zebrafish, Xenopus and Rat

The following *Xenopus* protein standards were used for comparison: A6 (total protein of kidney epithelial cells), P_{200} (total protein of egg membranes prepared according to Lang *et al.*, 1999). The molecular weight of XLAP2β, found in A6 cells is 68 kDa, and the oocyte-specific-specific XLAP2 found in P_{200} is 84 kDa (Lang *et al.*, 1999). In addition, the zebrafish ovary and rat somatic cells were used for comparison. The zebrafish LAP2β, γ, and oocyte-specific LAP2 have molecular weights of 63, 45, and 84 kDa, respectively (Schoft *et al.*, unpublished). Rat somatic cells (RV) contain three main LAP2 polypeptides: LAP2α of 78 kDa, LAP2β of 58 kDa and LAP2γ of 40 kDa (Lang *et al.*, 1999). Molecular weight protein standards of 205, 116, 97.4, 66, 45 and 29 kDa were used in SDS-PAGE.

Cells, Tissues and Embryos

From each animal, small pieces (of about 10 mm^3) of organs, such as the heart, spleen, liver, kidney, and the gonads were homogenized in sample buffer (Laemmli 1970). Sperm was isolated from spermatogenic and somatic cells by gently squeezing the testis in phosphate buffered saline (PBS: 137 mM NaCl, 3 mM KCl, 1.5 mM KH_2PO_4, 7 mM Na_2HPO_4, pH 7.4). The resulting liquid was transferred to a new tube and allowed to rest on ice for 10 min. The upper layer after this period was enriched in swimming mature sperm, whereas the sediment contained mostly round spermatocytes (microscopically detected). Each fraction was mixed with sample buffer. Oocyte enriched fractions were obtained by gently squeezing a piece of ovary in PBS, followed by centrifugation for 5 seconds at 15,000 g. The supernatant, enriched in oocytes, was mixed with sample buffer. The *Bufo* oocyte preparations included oocytes of several sizes, and the maximum oocyte diameter of each ovarian sample was recorded. To obtain follicle cells enriched preparations, an ovarian fragment was squeezed and washed several times in PBS to remove oocytes, the remaining tissue was homogenized and mixed with sample buffer. Individual embryos of the marsupial frog *Gastrotheca* were homogenized in PBS on ice and centrifuged at 15,000 g for 5 seconds. The supernatant was mixed with sample buffer. *Gastrotheca* embryos were staged according to del Pino and Escobar (1981). Rainbow trout hepatocytes were isolated as previously described (Mommsen *et al.*, 1994). Red blood cells were obtained from the caudal vein and mixed with heparin to prevent the formation of cell aggregates. They were separated from leucocytes in a washing solution (10 mM Tris-HCl, 147 mM NaCl, 15 mM Na_3Citrate, pH 7.5) by low speed centrifugation. Both cell types were solubilized in sample buffer. The rainbow trout analyzed, weighed around 250 g, and were kindly supplied by Dr. Thomas Moon (Department of Biology, University of Ottawa).

Antibodies

The following primary antibodies were used: The human antiserum designated MAN (Paulin-Levasseur *et al.*, 1996), and the guinea pig polyclonal antibody against the zebrafish amino terminal region present in all zebrafish LAP2 isoforms (ZLAP2-serum1; Schoft *et al.*, unpublished). Antibodies of both sera react with the common aminoterminal domain of LAP2 isoforms. The MAN antiserum was diluted 1:10,000 to 1:20,000 for immunoblotting in Tris buffered saline-Tween buffer (TBST: 140 mM NaCl, 0.3% Tween-20, 10

TABLE 3

LAP2 EXPRESSION IN FISH, AMPHIBIANS AND MAMMALS[1]

Pattern	*Major LAP2 isoforms*				*SP*
	α	β	γ	O	
1. FISH					
SOMATIC[2]		■	■		
OOCYTE				■	
SPERM					■
2. FROGS AND SALAMANDERS					
SOMATIC		■			
OOCYTE				■	
SPERM					■
3. MAMMALS					
SOMATIC	■	■	■		
OVARY[3]	■	■	■		
SPERM	■				

[1]Each block indicates the occurrence of a LAP2 isoform. [2]The LAP2β and LAP2γ levels of expression vary among tissues and species. [3]According to our observations in the mouse. O, oocyte; SP, small polypeptide

mM Tris-HCl, pH 8.0), the ZLAP2-serum1 was diluted 1:2,000 to 1:3,000 in 5% non-fat dry milk in TBST. For microscopic immunolabelling the dilution of the MAN antiserum was of 1:5,000. The anti-human and anti-guinea pig antibodies conjugated to alkaline phosphatase (from Dianova) were used as secondary antibodies for immunoblotting in all species, except for the rainbow trout. The biotinylated secondary antibody used for immunoblotting of trout proteins was sheep anti-human IgG (whole antibody from Amersham Canada, Oakville, Ontario). The secondary antibody used for immunofluorescence was goat anti-human IgG conjugated to CY3 (Jackson Immunoresearch, West Grove, Pa.).

SDS-PAGE and Immunoblotting

Proteins were separated in 5% stacking and 10% to 12% resolving SDS-polyacrylamide gel electrophoresis (PAGE) as previously described (Laemmli 1970). The separated polypeptides were electrophoretically transferred from gels to nitrocellulose membranes, and processed for immunoblotting following the procedure given in Lang *et al.*, (1999). Blots of rainbow trout polypeptides were reacted with the appropriate biotinylated secondary antibody, followed by incubation with horseradish peroxidase-conjugated streptavidine (from Amersham Canada) at a dilution of 1:4,000 in PBS-Tween for 45 min. at 20°C. The blots were then developed using the chemiluminescence kit (Amersham Canada). The reactivity was visualized on hyperfilm ECL (Amersham Canada). For other species, the presence of the bound secondary antibodies was detected with NBT/BCIP (nitro blue tetrazolium, and 5-Bromo-4-chloro-3-indolyl Phosphate) color reaction. The nitrocellulose membrane was incubated in the dark with 66 µl NBT solution (50 mg/ml in 70% dimethylformamide) and 33 µl BCIP solution (50 mg/ml in 100% dimethylformamide) in 10 ml alkaline buffer (100 mM Tris, 100 mM NaCl, 50 mM $MgCl_2$, pH 9.5). Incubation was done inside a plastic bag to avoid bubbles of air, from hours to several days until the bands developed. The color reaction was stopped with 2% formalin in distilled water. The membranes were stored wet inside plastic bags, and scanned with a Hewlett Packard Scan Jet 4C using the Adobe Photoshop (Adobe Systems Inc.). Molecular weights of the LAP2 isoforms were estimated with Total Lab version 1.1 (Phoretix).

Tissue Sections

For immunolabelling, rainbow trout brain and liver were fixed in methacarn (60% methanol, 30% chloroform and 10% acetic acid) for 24 hours at 4°C as described previously by Dardick *et al.*, (1988). Rainbow trout white muscle remained unfixed. Methacarn-fixed tissues were cryoprotected by successive immersions, each for 2 h, in sterile 5, 10 and 15% sucrose/PBS. Fixed tissues were then stored in 15% sucrose/PBS at 4°C until used. Immediately after excision from the animal, small pieces of white muscle were placed in plastic molds, embedded in Shandon cryomatrix medium (Fisher Scientific, Ottawa, Canada) and frozen in dry ice. White muscle blocks were stored at -80°C until used. For sectioning, methacarn-fixed tissues were embedded in Shandon cryomatrix medium and frozen in 1,1,1,2-tetrafluoroethane (Histofreeze from Fisher Scientific, Ottawa, Canada). Freezing was allowed to conclude on dry ice. Frozen tissues, including white muscle, were placed in an Ames-cryostat and allowed to equilibrate with the cryostat chamber temperature. Sections of 8 µm in thickness were cut at –20°C and collected on 0.5% gelatin-coated slides. Slides were stored at -20°C until histochemical staining was performed.

Indirect Immunofluorescence Staining

Rainbow trout hepatocytes and erythrocytes were allowed to attach to coverslips coated with 0.01% poly-L-lysine. Samples were fixed, permeabilized and stained as previously described (Chaly *et al.*, 1984). Frozen sections of unfixed and fixed tissues were warmed to room temperature prior to staining. Sections were then incubated with the primary antibody for 1 hour, rinsed in PBS, treated with the secondary antibody for one hour, and extensively washed in PBS. Following reaction with antibodies, all cells and tissue preparations were stained for one minute in DNA-specific 4'-6-diamino-2-phenylindole (0.1 mg/ml diluted 1:3,000, Molecular Probes, Eugene, Oregon, US). All samples were rinsed extensively in PBS and mounted in PBS (pH 7.0) containing 0.1% *p*-phenylene diamine and 50% glycerol. For controls, all cells and tissues studied were incubated with PBS instead of the primary antibody. Conventional epifluorescence microscopy was carried out on a Zeiss Axiophot and observations were recorded on Ilford XP2-400 film.

Acknowledgments

We thank L. Coloma, and S. Ron for allowing us to participate in field collecting trips, for the permission to obtain tissue samples before specimen processing, and for amphibian identification. We thank R. Barriga for identifying fish species. The fish and amphibians used in this work have been deposited in the Zoology Museum of the Pontificia Universidad Católica del Ecuador. We thank I. Aveiga, R. Barriga, L. Coloma, and A. Narváez for equipment loans, and K.-H. Thierauch for the donation of equipment. Thanks are expressed to M. I. Aguinaga, and M. S. Benítez, for their valuable suggestions. We gratefully acknowledge the help of F. Ayala, M. Díaz, C. Funk, L. E. López, I. P. Muñoz, C. A. Ruiz, J. C. Santos, and I. Tapia for their help in the collection of fish, and amphibians. T. Moon kindly supplied rainbow trouts. We thank C. Lang for her aid in establishing the SDS-PAGE and Western Blot methods, and V. Schoft for sharing with us information about zebrafish LAP2 expression, prior to publication. We thank I. B. Dawid for critically reading the manuscript. Grants from the Natural Sciences and Engineering Research Council of Canada and the Pontificia Universidad Católica del Ecuador supported the work of M. Paulin-Levasseur and E. M. del Pino, respectively.

References

ALSHEIMER, M., FECHER, E. and BENAVENTE, R. (1998). Nuclear envelope remodelling during rat spermiogenesis: distribution and expression pattern of LAP2/thymopoietins. *J. Cell Sci.* 111: 2227-2234.

BALLARD, W.W. (1981). Morphogenetic movements and fate maps of vertebrates. *Am. Zool.* 21: 391-399.

BENAVENTE, R. and KROHNE, G. (1985). Change of karyoskeleton during spermatogenesis of *Xenopus*: Expression of lamin L_{IV}, a nuclear lamina protein specific for the male germ line. *Proc. Natl. Acad. Sci. USA.* 82: 6176-6180.

CHALY, N., LITTLE, J.E. and BROWN, D.L. (1984). Localization of nuclear antigens during preparation of nuclear matrix antigens during the mitotic cycle. *J. Cell Biol.* 99: 661-671.

DARDICK, I., PARKS, W.R., LITTLE, J. and BROWN, D.L. (1988). Characterization of cytoskeletal proteins in basal cells of human parotid salivary gland ducts. *Pathol. Anat. Histopathol.* 412: 525-532.

DECHAT, T., VLCEK, S. and FOISNER, R. (2000). Review: Lamina-associated polypeptide 2 isoforms and related proteins in cell cycle-dependent nuclear structure dynamics. *J. Struct. Biol.* 129: 335-345.

DEL PINO, E.M. and ESCOBAR, B. (1981). Embryonic stages of *Gastrotheca riobambae* (Fowler) during maternal incubation and comparison of development with that of other egg-brooding hylid frogs. *J. Morphol.* 167: 277-296.

DUELLMAN, W.E. and TRUEB, L. (1986). *Biology of Amphibians.* McGraw-Hill, New York.

DUMONT, J.N. (1972). Oogenesis in *Xenopus laevis* (Daudin). I. Stages of oocyte development in laboratory maintained animals. *J. Morphol.* 136: 153-180.

FOISNER, R. and GERACE, L. (1993). Integral membrane proteins of the nuclear envelope interact with lamins and chromosomes, and binding is modulated by mitotic phosphorilation. *Cell* 73: 1267-1279.

FROESE, R. and PAULY, D. (2000). *FishBase 2000: concepts, design and data sources.* ICLARM, Los Baños, Laguna, Philippines.

FURUKAWA, K. (1999). LAP2 binding protein 1 (L2BP1/BAF) is a candidate mediator of LAP2-chromatin interaction. *J. Cell Sci.* 112: 2485-2492.

GANT, T.M., HARRIS, C.A. and WILSON, K.L. (1999). Roles of LAP2 proteins in nuclear assembly and DNA replication: truncated LAP2 beta proteins alter lamina assembly, envelope formation, nuclear size, and DNA replication efficiency in *Xenopus laevis* extracts. *J. Cell Biol.* 144: 1083-1096.

GOLDBERG, M., NILI, E., COJOCARU G., TZUR, Y.B., BERGER, R., BRANDIES, M., RECHAVI, G., GRUENBAUM, Y. and SIMON, A.J. (1999). Functional organization of the nuclear lamina. *Gene Ther. Mol. Biol.* 4: 143-158.

GRUENBAUM, Y., WILSON, K.L., HAREL, A., GOLDBERG, M. and COHEN, M. (2000). Review: nuclear lamins—structural proteins with fundamental functions. *J. Struct. Biol.* 129: 313-323.

HARRIS, C.A., ANDRYUK, P.J., CLINE, S.C., NATARAJAN, A., SIEKIERKA, J.J. and GOLDSTEIN, G. (1994). Three distinct human thymopoietins are derived from alternatively spliced *Mr*NAs. *Proc. Natl. Acad. Sci. USA* 91: 6283-6287.

HARVEY, P.F., JANIS, C.M. and HEIDNER, J.B. (1999). *Vertebrate Life.* Prentice Hall, New Jersey, U.S.A.

HAYNES, J. (1995). Standarized Clasification of Poeciliid Development for Life-History Studies. *COPEIA* 1995: 147-154.

KONSTANTINOV, K., FOISNER, R., BYRD, D., LIU, F.T., TSAI, W.M., WIIK, A. and GERACE, L. (1995). Integral membrane proteins associated with the nuclear lamina are novel autoimmune antigens of the nuclear envelope. *Clin. Immunol. Immunopathol.* 74: 189-199.

LAEMMLI, U.K. (1970). Cleavage of structural proteins during the assembly of the head of bacteriophage T4. *Nature* 227: 680-685.

LANG, C., PAULIN-LEVASSEUR, M., GAJEWSKI, A., ALSHEIMER, M., BENAVENTE, R. and KROHNE, G. (1999). Molecular characterization and developmentally regulated expression of *Xenopus* lamina-associated polypeptide 2 (XLAP2). *J. Cell Sci.* 112: 749-59.

LIN, F., BLAKE, D.L., CALLEBAUT, I., SKERJANC, I., HOLMER, L., MCBURNEY, M., PAULIN-LEVASSEUR, M. and WORMAN, H.J. (2000). MAN1, an inner nuclear membrane protein that shares the LEM domain with lamina-associated polypeptide 2 and emerin. *J. Biol. Chem.* 275: 4840-4847.

MOMMSEN, T.P., MOON, T.W. and WALSH, P.J. (1994). Hepatocytes: isolation, maintenance and utilization. In *Biochemistry and molecular biology of fishes* (Eds. Hochachka, P.W. and Mommsen, T.P.). Elsevier, Amsterdam, vol. 3. pp. 355-373.

NIEUWKOOP, P.D. and FABER, J. (1994). *Normal Table of Xenopus laevis (Daudin).* Garland Publishing, New York, London.

PAULIN-LEVASSEUR, M., BLAKE, D.L., JULIEN, M.Y. and ROULEAU, L. (1996). The MAN antigens are non lamin constituents of the nuclear lamina in vertebrate cells. *Chromosoma* 104: 367-379.

STICK, R. (1988). cDNA cloning of the developmentally regulated lamin L_{III} of *Xenopus laevis*. *EMBO J.* 7: 3189-3197.

WAKE, M.H., and WAKE, D.B. (2000). Developmental morphology of early vertebrogenesis in Caecilians (Amphibia: Gymnophiona): Resegmentation and phylogenesis. *Zoology* 103: 68-88.

WILSON, K.L. (2000). The nuclear envelope, muscular dystrophy and gene expression. *Trends Cell Biol.* 10: 125-129.

WOURMS, J.P. and WHITT, G. (1981). Future directions of research on the Developmental Biology of fishes. *Am. Zool.* 21: 597-604.

Received: November 2001
Reviewed by Referees: December 2001
Modified by Authors and Accepted for Publication: January 2002

REFERENCES

Almendral J. M., Huebsch D., Blundell P. A., Macdonald-Bravo H., and Bravo R. (1987) Cloning and sequence of the human nuclear protein cyclin: homology with DNA-binding proteins. *Proc Natl Acad Sci U S A.* **84**, 1575-1579.

Baserga R. (1991) Growth regulation of the PCNA gene. *J Cell Sci.* **98**, 433-436.

Beckmann R. P., Mizzen L. E., and Welch W. J. (1990) Interaction of Hsp 70 with newly synthesized proteins: implications for protein folding and assembly. *Science.* **248**, 850-854.

Benavente R. and Krohne G. (1986) Involvement of nuclear lamins in postmitotic reorganization of chromatin as demonstrated by microinjection of lamin antibodies. *J Cell Biol.* **103**, 1847-1854.

Benoff S. and Nadal-Ginard B. (1979) Most myosin heavy chain mRNA in L6E9 rat myotubes has a short poly(A) tail. *Proc Natl Acad Sci U S A.* **76**, 1853-1857.

Benoff S. and Nadal-Ginard B. (1980) Transient induction of poly(A)-short myosin heavy chain messenger RNA during terminal differentiation of L6E9 myoblasts. *J Mol Biol.* **140**, 283-298.

Behrens S.E. and Luhrmann R. (1991) Immunoaffinity purification of a [U4/U6.U5] tri-snRNP from human cells.Genes Dev. **5(8)**:1439-52.

Berezney R. (1991) The nuclear matrix: a heuristic model for investigating genomic organization and function in the cell nucleus. *J Cell Biochem.* **47**, 109-123.

Berezney R. and Coffey D. S. (1974) Identification of a nuclear protein matrix. *Biochem Biophys Res Commun.* **60**, 1410-1417.

Berezney R. and Coffey D. S. (1975) Nuclear protein matrix: association with newly synthesized DNA. *Science.* **189**, 291-293.

Berezney R. and Coffey D. S. (1976) The nuclear protein matrix: isolation, structure, and functions. *Adv Enzyme Regul.* **14**, 63-100.

Berezney R. and Coffey D. S. (1977) Nuclear matrix. Isolation and characterization of a framework structure from rat liver nuclei. *J Cell Biol.* **73**, 616-637.

Blair O. C., Winward R. T., and Roti Roti J. L. (1979) The effect of hyperthermia on the protein content of HeLa cell nuclei: a flow cytometric analysis. *Radiat Res.* **78**, 474-484.

Bond U. (1988) Heat shock but not other stress inducers leads to the disruption of a sub-set of snRNPs and inhibition of in vitro splicing in HeLa cells. *Embo J.* **7**, 3509-3518.

Bond U. and Schlesinger M. J. (1986) The chicken ubiquitin gene contains a heat shock promoter and expresses an unstable mRNA in heat-shocked cells. *Mol Cell Biol.* **6**, 4602-4610.

Bonne G., Di Barletta M. R., Varnous S., Becane H. M., Hammouda E. H., Merlini L., Muntoni F., Greenberg C. R., Gary F., Urtizberea J. A., Duboc D., Fardeau M., Toniolo D., and Schwartz K. (1999) Mutations in the gene encoding lamin A/C cause autosomal dominant Emery- Dreifuss muscular dystrophy. *Nat Genet.* **21**, 285-288.

Borer R. A., Lehner C. F., Eppenberger H. M., and Nigg E. A. (1989) Major nucleolar proteins shuttle between nucleus and cytoplasm. *Cell.* **56**, 379-390.

Bosman F. T. (1999) The nuclear matrix in pathology. *Virchows Arch.* **435**, 391-399.

Bravo R. and Celis J. E. (1980) A search for differential polypeptide synthesis throughout the cell cycle of HeLa cells. *J Cell Biol.* **84**, 795-802.

Bravo R. and Celis J. E. (1985) Changes in the nuclear distribution of cyclin (PCNA) during S-phase are not triggered by post-translational modifications that are expected to moderately affect its charge. *FEBS Lett.* **182**, 435-440.

Bravo R., Fey S. J., Bellatin J., Larsen P. M., Arevalo J., and Celis J. E. (1981) Identification of a nuclear and of a cytoplasmic polypeptide whose relative proportions are sensitive to changes in the rate of cell proliferation. *Exp Cell Res.* **136**, 311-319.

Bravo R., Fey S. J., Bellatin J., Larsen P. M., and Celis J. E. (1982) Identification of a nuclear polypeptide ("cyclin") whose relative proportion is sensitive to changes in the rate of cell proliferation and to transformation. *Prog Clin Biol Res.* **85**, 235-248.

Caizergues-Ferrer M., Dousseau F., Gas N., Bouche G., Stevens B., and Amalric F. (1984) Induction of new proteins in the nuclear matrix of CHO cells by a heat shock: detection of a specific set in the nucleolar matrix. *Biochem Biophys Res Commun.* **118**, 444-450.

Cartegni L., di Barletta M. R., Barresi R., Squarzoni S., Sabatelli P., Maraldi N., Mora M., Di Blasi C., Cornelio F., Merlini L., Villa A., Cobianchi F., and Toniolo D. (1997) Heart-specific localization of emerin: new insights into Emery-Dreifuss muscular dystrophy. *Hum Mol Genet.* **6**, 2257-2264.

Celis J.E. (1994) Cell Biology, A Laboratory Handbook. Academic Press Limited, London, UK.

Chaly N., Bladon T., Setterfield G., Little J. E., Kaplan J. G., and Brown D. L. (1984) Changes in distribution of nuclear matrix antigens during the mitotic cell cycle. *J Cell Biol.* **99**, 661-671.

Chaly N., Little J. E., and Brown D. L. (1985) Localization of nuclear antigens during preparation of nuclear matrices in situ. *Can J Biochem Cell Biol.* **63**, 644-653.

Chaly N. and Munro S. B. (1996) Centromeres reposition to the nuclear periphery during L6E9 myogenesis in vitro. *Exp Cell Res.* **223**, 274-278.

Chaly N., Munro S. B., and Swallow M. A. (1996) Remodelling of the nuclear periphery during muscle cell differentiation in vitro. *J Cell Biochem.* **62**, 76-89.

Chaly N. and Stochaj U. (1999) Nonlamin components of the lamina: a paucity of proteins. *Biochem Cell Biol.* **77**, 311-319.

Chiodi I., Biggiogera M., Denegri M., Corioni M., Weighardt F., Cobianchi F., Riva S., and Biamonti G. (2000) Structure and dynamics of hnRNP-labelled nuclear bodies induced by stress treatments. *J Cell Sci.* **113**, 4043-4053.

Chu A., Rassadi R., and Stochaj U. (1998) Velcro in the nuclear envelope: LBR and LAPs. *FEBS Lett.* **441**, 165-169.

Connolly J. A., Sarabia V. E., Kelvin D. J., and Wang E. (1988) The disappearance of a cyclin-like protein and the appearance of statin is correlated with the onset of differentiation during myogenesis in vitro. *Exp Cell Res.* **174**, 461-471.

Cotto J. J. and Morimoto R. I. (1999) Stress-induced activation of the heat-shock response: cell and molecular biology of heat-shock factors. *Biochem Soc Symp.* **64**, 105-118.

Cowin P. and Burke B. (1996) Cytoskeleton-membrane interactions. *Curr Opin Cell Biol.*

8, 56-65.

Cross F. R. (1990) Cell cycle arrest caused by CLN gene deficiency in Saccharomyces cerevisiae resembles START-I arrest and is independent of the mating-pheromone signalling pathway. *Mol Cell Biol.* **10**, 6482-6490.

Dechat T., Gotzmann J., Stockinger A., Harris C. A., Talle M. A., Siekierka J. J., and Foisner R. (1998) Detergent-salt resistance of LAP2alpha in interphase nuclei and phosphorylation-dependent association with chromosomes early in nuclear assembly implies functions in nuclear structure dynamics. *Embo J.* **17**, 4887-4902.

de Graaf A., Meijne A. M., van Renswoude A. J., Humbel B. M., van Bergen en Henegouwen P. M., de Jong L., van Driel R., and Verkleij A. J. (1992) Heat shock-induced redistribution of a 160-kDa nuclear matrix protein. *Exp Cell Res.* **202**, 243-251.

De Maio A. (1999) Heat shock proteins: facts, thoughts, and dreams. *Shock.* **11**, 1-12.

Dessev G. N. (1992) Nuclear envelope structure. *Curr Opin Cell Biol.* **4**, 430-435.

DiDomenico B. J., Bugaisky G. E., and Lindquist S. (1982) The heat shock response is self-regulated at both the transcriptional and posttranscriptional levels. *Cell.* **31**, 593-603.

Drebot M. A., Barnes C. A., Singer R. A., and Johnston G. C. (1990) Genetic assessment of stationary phase for cells of the yeast Saccharomyces cerevisiae. *J Bacteriol.* **172**, 3584-3589.

Dreyfuss G., Matunis M. J., Pinol-Roma S., and Burd C. G. (1993) hnRNP proteins and the biogenesis of mRNA. *Annu Rev Biochem.* **62**, 289-321.

Duband-Goulet I., Courvalin J. C., and Buendia B. (1998) LBR, a chromatin and lamin binding protein from the inner nuclear membrane, is proteolyzed at late stages of apoptosis. *J Cell Sci.* **111**, 1441-1451.

Dundr M. and Misteli T. (2001) Functional architecture in the cell nucleus. *Biochem J.* **356**, 297-310.

Dynlacht J. R., Story M. D., Zhu W. G., and Danner J. (1999) Lamin B is a prompt heat shock protein. *J Cell Physiol.* **178**, 28-34.

Edington B. V., Whelan S. A., and Hightower L. E. (1989) Inhibition of heat shock (stress) protein induction by deuterium oxide and glycerol: additional support for the abnormal protein hypothesis of induction. *J Cell Physiol.* **139**, 219-228.

Ellis J. A., Craxton M., Yates J. R., and Kendrick-Jones J. (1998) Aberrant intracellular targeting and cell cycle-dependent phosphorylation of emerin contribute to the Emery-Dreifuss muscular dystrophy phenotype. *J Cell Sci.* **111**, 781-792.

Fidorra J., Mielke T., Booz J., and Feinendegen L. E. (1981) Cellular and nuclear volume of human cells during the cell cycle. *Radiat Environ Biophys.* **19**, 205-214.

Fisher D. Z., Chaudhary N., and Blobel G. (1986) cDNA sequencing of nuclear lamins A and C reveals primary and secondary structural homology to intermediate filament proteins. *Proc Natl Acad Sci U S A.* **83**, 6450-6454.

Foisner R. and Gerace L. (1993) Integral membrane proteins of the nuclear envelope interact with lamins and chromosomes, and binding is modulated by mitotic phosphorylation. *Cell.* **73**, 1267-1279.

Franke W. W. (1987) Nuclear lamins and cytoplasmic intermediate filament proteins: a growing multigene family. *Cell.* **48**, 3-4.

Furukawa K. (1999) LAP2 binding protein 1 (L2BP1/BAF) is a candidate mediator of LAP2- chromatin interaction. *J Cell Sci.* **112**, 2485-2492.

Furukawa K. and Hotta Y. (1993) cDNA cloning of a germ cell specific lamin B3 from mouse spermatocytes and analysis of its function by ectopic expression in somatic cells. *Embo J.* **12**, 97-106.

Furukawa K., Fritze C.E., and Gerace L. (1998) The major nuclear envelope targeting domain of LAP2 coincides with its lamin binding region but is distinct from its chromatin interaction domain. *J Biol Chem.* **273(7)**:4213-9.

Furukawa K., Inagaki H., and Hotta Y. (1994) Identification and cloning of an mRNA coding for a germ cell-specific A- type lamin in mice. *Exp Cell Res.* **212**, 426-430.

Furukawa K., Pante N., Aebi U., and Gerace L. (1995) Cloning of a cDNA for lamina-associated polypeptide 2 (LAP2) and identification of regions that specify targeting to the nuclear envelope. *Embo J.* **14**, 1626-1636.

Garrido C., Gurbuxani S., Ravagnan L., and Kroemer G. (2001) Heat shock proteins: endogenous modulators of apoptotic cell death. *Biochem Biophys Res Commun.* **286(3)**:433-42.

Georgatos S. D., Meier J., and Simos G. (1994) Lamins and lamin-associated proteins. *Curr Opin Cell Biol.* **6**, 347-353.

Gerace L. and Burke B. (1988) Functional organization of the nuclear envelope. *Annu Rev Cell Biol.* **4**, 335-374.

Gruenbaum Y., Wilson K. L., Harel A., Goldberg M., and Cohen M. (2000) Review: nuclear lamins--structural proteins with fundamental functions. *J Struct Biol.* **129**, 313-323.

Hadwiger J. A., Wittenberg C., Richardson H. E., de Barros Lopes M., and Reed S. I. (1989) A family of cyclin homologs that control the G1 phase in yeast. *Proc Natl Acad Sci U S A.* **86**, 6255-6259.

Harel J., Leibovitch M.P., Guillier M., Borycki A.G. and Leibovitch SA. (1989) Proto-oncogenes and differentiation versus transformation of striated muscle cells. Ann N Y Acad Sci. **567**:187-207.

Hightower L. E. (1991) Heat shock, stress proteins, chaperones, and proteotoxicity. *Cell.* **66**, 191-197.

Huang, S., Deerinck, T.J., Ellisman, M.H., Spector D.L. (1994) In vivo analysis of the stability and transport of nuclear poly(A)$^+$ RNA. J. Cell Biol. **126**:877-899.

Hughes J. H. and Cohen M. B. (1999) Nuclear matrix proteins and their potential applications to diagnostic pathology. *Am J Clin Pathol.* **111**, 267-27.

Johnston GC, Singer RA. (1980) Ribosomal precursor RNA metabolism and cell division in the yeast Saccharomyces cerevisiae. Mol Gen Genet. **178(2)**:357-60.

Jordan E. and Shaw P. (1995) The nucleolus. Ann. Rev. Cell Biol., 11:93-122.

Jonsson Z.O. and Hubscher U. (1997) Proliferating cell nuclear antigen: more than a clamp for DNA polymerases. bioessays. **19(11)**:967-75.

Kass S. Tyc K. Steitz J.A. and Sollner-Webb B. (1990) The U3 small nucleolar ribonucleoprotein functions in the first step of preribosomal RNA processing. *Cell.* **60**:897-908.

Kelman Z. and Hurwitz J. (1998) Protein-PCNA interactions: a DNA-scanning mechanism? *Trends Biochem Sci.* **23**, 236-238.

Khanuja P.S., Lehr J.E., Soule H.D., Gehani S.K., Noto A.C., Choudhury S., Chen R., and Pienta KJ. (1993) Nuclear matrix proteins in normal and breast cancer cells. *Cancer Res.* **53(14)**:3394-8.

Krauter K. S., Soeiro R., and Nadal-Ginard B. (1979) Transcriptional regulation of ribosomal RNA accumulation during L6E9 myoblast differentiation. *J Mol Biol.* **134**, 727-741.

Laemmli U. K. (1970) Cleavage of structural proteins during the assembly of the head of bacteriophage T4. *Nature.* **227**, 680-685.

Lamarre D., Talbot B., de Murcia G., Laplante C., Leduc Y., Mazen A., and Poirier G. G. (1988) Structural and functional analysis of poly(ADP ribose) polymerase: an immunological study. *Biochim Biophys Acta.* **950**, 147-160.

Lang C., Paulin-Levasseur M., Gajewski A., Alsheimer M., Benavente R., and Krohne G. (1999) Molecular characterization and developmentally regulated expression of Xenopus lamina-associated polypeptide 2 (XLAP2). *J Cell Sci.* **112**, 749-759.

la Thangue NB, Chan WL (1984) The characterization and purification of DNA binding proteins present within herpes simplex virus infected cells using monoclonal antibodies. Arch Virol.**79(1-2)**:13-33.

Lattanzi G., Ognibene A., Sabatelli P., Capanni C., Toniolo D., Columbaro M., Santi S., Riccio M., Merlini L., Maraldi N. M., and Squarzoni S. (2000) Emerin expression at the early stages of myogenic differentiation. *Differentiation.* **66**, 208-217.

Lavoie S. B., Albert A. L., Thibodeau A., and Vincent M. (1999) Heat shock-induced alterations in phosphorylation of the largest subunit of RNA polymerase II as revealed by monoclonal antibodies CC-3 and MPM-2. *Biochem Cell Biol.* **77**, 367-374.

Lawson M. A. and Purslow P. P. (2000) Differentiation of myoblasts in serum-free media: effects of modified media are cell line-specific. *Cells Tissues Organs.* **167**, 130-137.

Lee M. S. and Craigie R. (1994) Protection of retroviral DNA from autointegration: involvement of a cellular factor. *Proc Natl Acad Sci U S A.* **91**, 9823-9827.

Lee M. S. and Craigie R. (1998) A previously unidentified host protein protects retroviral DNA from autointegration. *Proc Natl Acad Sci U S A.* **95**, 1528-1533.

Lenz-Bohme B., Wismar J., Fuchs S., Reifegerste R., Buchner E., Betz H., and Schmitt B. (1997) Insertional mutation of the Drosophila nuclear lamin Dm0 gene results in defective nuclear envelopes, clustering of nuclear pore complexes, and accumulation of annulate lamellae. *J Cell Biol.* **137**, 1001-1016.

Leonhardt H., Rahn H. P., Weinzierl P., Sporbert A., Cremer T., Zink D., and Cardoso M. C. (2000) Dynamics of DNA replication factories in living cells. *J Cell Biol.* **149**, 271-280.

Lewis M.J. and Pelham H.R. (1985) Involvement of ATP in the nuclear and nucleolar functions of the 70 kd heat shock protein. **4(12)**:3137-43.

Li L., Shen G., and Li G. C. (1995) Effects of expressing human Hsp70 and its deletion derivatives on heat killing and on RNA and protein synthesis. *Exp Cell Res.* **217**, 460-468.

Lin F., Blake D. L., Callebaut I., Skerjanc I. S., Holmer L., McBurney M. W., Paulin-Levasseur M., and Worman H. J. (2000) MAN1, an inner nuclear membrane

protein that shares the LEM domain with lamina-associated polypeptide 2 and emerin. *J Biol Chem.* **275**, 4840-4847.

Lischwe M. A., Cook R. G., Ahn Y. S., Yeoman L. C., and Busch H. (1985) Clustering of glycine and NG,NG-dimethylarginine in nucleolar protein C23. *Biochemistry.* **24**, 6025-6028.

Lischwe M. A., Ochs R. L., Reddy R., Cook R. G., Yeoman L. C., Tan E. M., Reichlin M., and Busch H. (1985) Purification and partial characterization of a nucleolar scleroderma antigen (Mr = 34,000; pI, 8.5) rich in NG,NG-dimethylarginine. *J Biol Chem.* **260**, 14304-14310.

Liu X. D., Liu P. C., Santoro N., and Thiele D. J. (1997) Conservation of a stress response: human heat shock transcription factors functionally substitute for yeast HSF. *Embo J.* **16**, 6466-6477.

Lorincz A. T. and Reed S. I. (1984) Primary structure homology between the product of yeast cell division control gene CDC28 and vertebrate oncogenes. *Nature.* **307**, 183-185.

Lourim D. and Lin J. J. (1989) Expression of nuclear lamin A and muscle-specific proteins in differentiating muscle cells in ovo and in vitro. *J Cell Biol.* **109**, 495-504.

Lutz Y., Jacob M., and Fuchs J. P. (1988) The distribution of two hnRNP-associated proteins defined by a monoclonal antibody is altered in heat-shocked HeLa cells. *Exp Cell Res.* **175**, 109-124.

Luus L. (1998) Characterisation of the 1B4 Antigen. M.Sc. Thesis

Luus L. and Paulin-Levasseur, M., (1997) Characterization of the 1B4. *Molecular and Biology of the Cell.* **8**:217a.

Mahl P., Lutz Y., Puvion E., and Fuchs J. P. (1989) Rapid effect of heat shock on two heterogeneous nuclear ribonucleoprotein-associated antigens in HeLa cells. *J Cell Biol.* **109**, 1921-1935.

Maison C, Pyrpasopoulou A, Theodoropoulos PA, Georgatos SD. (1997) The inner nuclear membrane protein LAP1 forms a native complex with B-type lamins and partitions with spindle-associated mitotic vesicles. EMBO J. **(16)**:4839-50.

Manilal S., Nguyen T. M., Sewry C. A., and Morris G. E. (1996) The Emery-Dreifuss muscular dystrophy protein, emerin, is a nuclear membrane protein. *Hum Mol Genet.* **5**, 801-808.

Manilal S., Sewry C.A., Pereboev A., Man N., Gobbi P., Hawkes S., Love D.R., and Morris G.E. (1999) Distribution of emerin and lamins in the heart and implications for Emery-Dreifuss muscular dystrophy. Hum Mol Genet. **8(2)**:353-9.

Marshall W. F., Fung J. C., and Sedat J. W. (1997) Deconstructing the nucleus: global architecture from local interactions. *Curr Opin Genet Dev.* **7**, 259-263.

Martin L., Crimaudo C., and Gerace L. (1995) cDNA cloning and characterization of lamina-associated polypeptide 1C (LAP1C), an integral protein of the inner nuclear membrane. *J Biol Chem.* **270**, 8822-8828.

Matsumoto K., Moriuchi T., Koji T., and Nakane P. K. (1987) Molecular cloning of cDNA coding for rat proliferating cell nuclear antigen (PCNA)/cyclin. *Embo J.* **6**, 637-642.

McKeon F. (1991) Nuclear lamin proteins: domains required for nuclear targeting,

assembly, and cell-cycle-regulated dynamics. *Curr Opin Cell Biol.* **3**, 82-86.
McKeon F. D., Kirschner M. W., and Caput D. (1986) Homologies in both primary and secondary structure between nuclear envelope and intermediate filament proteins. *Nature.* **319**, 463-468.
Miyachi K., Fritzler M. J., and Tan E. M. (1978) Autoantibody to a nuclear antigen in proliferating cells. *J Immunol.* **121**, 2228-2234.
Moir RD, Yoon M, Khuon S, Goldman RD. (2000) Nuclear lamins A and B1: different pathways of assembly during nuclear envelope formation in living cells. J Cell Biol. **151(6)**:1155-68.
Muralikrishna B., Dhawan J., Rangaraj N., and Parnaik V. K. (2001) Distinct changes in intranuclear lamin A/C organization during myoblast differentiation. *J Cell Sci.* **114**, 4001-4011.
Nagano A, Koga R, Ogawa M, Kurano Y, Kawada J, Okada R, Hayashi YK, Tsukahara T, Arahata K. (1996) Emerin deficiency at the nuclear membrane in patients with Emery-Dreifuss muscular dystrophy. Nat Genet. **12(3)**:254-9.
Nakayasu H, Berezney R. (1991) Nuclear matrins: identification of the major nuclear matrix proteins. Proc Natl Acad Sci U S A. **88(22)**:10312-6.
Nakielny S. and Dreyfuss G. (1997) Nuclear export of proteins and RNAs. *Curr Opin Cell Biol.* **9**, 420-429.
Naya F.J. and Olson E. (1999) MEF2: a transcriptional target for signaling pathways controlling skeletal muscle growth and differentiation. *Curr. Opin. Cell Biol.* **11**:683-688.
Nelson W. G., Pienta K. J., Barrack E. R., and Coffey D. S. (1986) The role of the nuclear matrix in the organization and function of DNA. *Annu Rev Biophys Biophys Chem.* **15**, 457-475.
Newport J. W., Wilson K. L., and Dunphy W. G. (1990) A lamin-independent pathway for nuclear envelope assembly. *J Cell Biol.* **111**, 2247-2259.
Nickerson J. A. (1998) Nuclear dreams: the malignant alteration of nuclear architecture. *J Cell Biochem.* **70**, 172-180.
Nigg E. A. (1992) Assembly-disassembly of the nuclear lamina. *Curr Opin Cell Biol.* **4**, 105-109.
Ochs RL, Lischwe MA, Spohn WH, Busch H. (1985) Fibrillarin: a new protein of the nucleolus identified by autoimmune sera. Biol Cell. **54(2)**:123-33.
Ochs R. L. and Smetana K. (1991) Detection of fibrillarin in nucleolar remnants and the nucleolar matrix. *Exp Cell Res.* **197**, 183-190.
Ohtsuka K., Nakamura H., and Sato C. (1986) Intracellular distribution of 73,000 and 72,000 dalton heat shock proteins in HeLa cells. *Int J Hyperthermia.* **2**, 267-275.
O'Keefe R.T., Mayeda A., Sadowski C.L., Krainer A.R., and Spector D.L. (1994) Disruption of pre-mRNA splicing in vivo results in reorganization of splicing factors. J Cell Biol. 1994 Feb;**124(3)**:249-60.
Paine P. L., Moore L. C., and Horowitz S. B. (1975) Nuclear envelope permeability. *Nature.* **254**, 109-114.
Parker K.A. and Stitz J.A. (1990) Structural analysis of the human U3 ribonucleoprotein particle reveal a conserved sequence available for base pairing with pre-rRNA. *Mol. Cell. Biol.* 7:2899-2913.
Paulin-Levasseur M. and Julien M. (1999) Characterization of the 2A7 antigen as a 85-

kDa human nucleocytoplasmic shuttling protein. *Exp Cell Res.* **250**, 439-451.
Paulin-Levasseur M., Julien M., Horner M., and Chen G. (1995) Characterization of the 2H12 antigen as a nonshuttling human isoelectric variant of the nucleolar protein B23. *Exp Cell Res.* **219**, 514-526.
Pederson T. (1998) Thinking about a nuclear matrix. *J Mol Biol.* **277**, 147-159.
Pelham H. R. (1986) Speculations on the functions of the major heat shock and glucose-regulated proteins. *Cell.* **46**, 959-961.
Pellicciari C., Mangiarotti R., Bottone M. G., Danova M., and Wang E. (1995) Identification of resting cells by dual-parameter flow cytometry of statin expression and DNA content. *Cytometry.* **21**, 329-337.
Pinol-Roma S. and Dreyfuss G. (1991) Transcription-dependent and transcription-independent nuclear transport of hnRNP proteins. *Science.* **253**, 312-314.
Pinol-Roma S. and Dreyfuss G. (1993) Cell cycle-regulated phosphorylation of the pre-mRNA-binding (heterogeneous nuclear ribonucleoprotein) C proteins. *Mol Cell Biol.* **13**, 5762-5770.
Ritossa F. (1962) A new puffing pattern induced by temperature and DNAP in *Drosophila.* Experimentia **18**:571-573
Rowley A., Johnston G. C., Butler B., Werner-Washburne M., and Singer R. A. (1993) Heat shock-mediated cell cycle blockage and G1 cyclin expression in the yeast Saccharomyces cerevisiae. *Mol Cell Biol.* **13**, 1034-1041.
Saydam N., Georgiev O., Nakano M. Y., Greber U. F., and Schaffner W. (2001) Nucleo-cytoplasmic trafficking of metal-regulatory transcription factor 1 is regulated by diverse stress signals. *J Biol Chem.* **276**, 25487-25495.
Scheer U. and Benavente R. (1990) Functional and dynamic aspects of the mammalian nucleolus. *Bioessays.* **12**, 14-21.
Schneiter R., Kadowaki T., and Tartakoff A.M. (1995) mRNA transport in yeast: time to reinvestigate the functions of the nucleolus. Mol Biol Cell. **6(4)**:357-70.
Schuler E., Lin F., and Worman H.J. (1994) Characterization of the human gene encoding LBR, an integral protein of the nuclear envelope inner membrane. *J Biol Chem.* **269(15)**:11312-7.
Schwarzacher H. G. and Wachtler F. (1993) The nucleolus. *Anat Embryol (Berl).* **188:** 515-536.
Senior A., and Gerace L. (1988) Integral membrane proteins specific to the inner nuclear membrane and associated with the nuclear lamina. J Cell Biol. 107(6 Pt 1):2029-36.
Sharp F. R., Massa S. M., and Swanson R. A. (1999) Heat-shock protein protection. *Trends Neurosci.* **22**, 97-99.
Shin D.Y., Matsumoto K., Iida H., Uno I. and Ishikawa T. (1987) Heat shock response of Saccharomyces cerevisiae mutants altered in cyclic AMP-dependent protein phosphorylation. Mol Cell Biol. **7(1)**:244-50.
Sobell H. M. (1985) Actinomycin and DNA transcription. *Proc Natl Acad Sci U S A.* **82**, 5328-5331.
Staley J.P. and Guthrie C. (1998) Mechanical devices of the spliceosome: motors, clocks, springs and things. *Cell.* **92(3)**:315-26
Stevens A. and Maupin M. K. (1989) 5,6-Dichloro-1-beta-D-ribofuranosylbenzimidazole inhibits a HeLa protein kinase that phosphorylates an RNA polymerase II-derived

peptide. *Biochem Biophys Res Commun.* **159**, 508-515.
Stoffler D., Fahrenkrog B., and Aebi U. (1999) The nuclear pore complex: from molecular architecture to functional dynamics. *Curr Opin Cell Biol.* **11**, 391-401.
Sullivan T., Escalante-Alcalde D., Bhatt H., Anver M., Bhat N., Nagashima K., Stewart C. L., and Burke B. (1999) Loss of A-type lamin expression compromises nuclear envelope integrity leading to muscular dystrophy. *J Cell Biol.* **147**, 913-920.
Tani T., Derby R. J., Hiraoka Y., and Spector D. L. (1995) Nucleolar accumulation of poly (A)+ RNA in heat-shocked yeast cells: implication of nucleolar involvement in mRNA transport. *Mol Biol Cell.* **6**, 1515-1534.
Tinnemans M. M., Lenders M. H., ten Velde G. P., Ramaekers F. C., and Schutte B. (1995) Alterations in cytoskeletal and nuclear matrix-associated proteins during apoptosis. *Eur J Cell Biol.* **68**, 35-46.
Trotter E. W., Berenfeld L., Krause S. A., Petsko G. A., and Gray J. V. (2001) Protein misfolding and temperature up-shift cause G1 arrest via a common mechanism dependent on heat shock factor in Saccharomycescerevisiae. *Proc Natl Acad Sci U S A.* **98**, 7313-7318.
Ulitzur N., Harel A., Feinstein N., and Gruenbaum Y. (1992) Lamin activity is essential for nuclear envelope assembly in a Drosophila embryo cell-free extract. *J Cell Biol.* **119**, 17-25.
van Driel R., Wansink D. G., van Steensel B., Grande M. A., Schul W., and de Jong L. (1995) Nuclear domains and the nuclear matrix. *Int Rev Cytol*, 151-189.
Vester B., Smith A., Krohne G., and Benavente R. (1993) Presence of a nuclear lamina in pachytene spermatocytes of the rat. *J Cell Sci.* **104**, 557-563.
Wang E. and Krueger J. G. (1985) Application of a unique monoclonal antibody as a marker for nonproliferating subpopulations of cells of some tissue. *J Histochem Cytochem.* **33**, 587-594.
Wansink D. G., van Driel R., and de Jong L. (1994) Organization of (pre-)mRNA metabolism in the cell nucleus. *Mol Biol Rep.* **20**, 45-55.
Warner J.R., (1990) The nucleolus and ribosome formation. Curr Opin Cell Biol. 2(3):521-7.
Weighardt F., Cobianchi F., Cartegni L., Chiodi I., Villa A., Riva S., and Biamonti G. (1999) A novel hnRNP protein (HAP/SAF-B) enters a subset of hnRNP complexes and relocates in nuclear granules in response to heat shock. *J Cell Sci.* **112**, 1465-1476.
Welch W. J. and Feramisco J. R. (1984) Nuclear and nucleolar localization of the 72,000-dalton heat shock protein in heat-shocked mammalian cells. *J Biol Chem.* **259**, 4501-4513.
Welch W. J. and Mizzen L. A. (1988) Characterization of the thermotolerant cell. II. Effects on the intracellular distribution of heat-shock protein 70, intermediate filaments, and small nuclear ribonucleoprotein complexes. *J Cell Biol.* **106**, 1117-1130.
Welch WJ. (1992) Mammalian stress response: cell physiology, structure/function of stress proteins, and implications for medicine and disease. *Physiol Rev.* **72(4):**1063-81.
Welch W. J. and Suhan J. P. (1986) Cellular and biochemical events in mammalian cells during and after recovery from physiological stress. *J Cell Biol.* **103**, 2035-2052.

Wilson K. L. (2000) The nuclear envelope, muscular dystrophy and gene expression. *Trends Cell Biol.* **10**, 125-129.

Wittenberg C., Sugimoto K., and Reed S. I. (1990) G1-specific cyclins of S. cerevisiae: cell cycle periodicity, regulation by mating pheromone, and association with the p34CDC28 protein kinase. *Cell.* **62**, 225-237.

Worman H. J. and Courvalin J. C. (2000) The inner nuclear membrane. *J Membr Biol.* **177**, 1-11.

Wu B., Gu M. J., Heydari A. R., and Richardson A. (1993) The effect of age on the synthesis of two heat shock proteins in the hsp70 family. *J Gerontol.* **48**, B50-56.

Wyman C. and Botchan M. (1995) DNA replication. A familiar ring to DNA polymerase processivity. *Curr Biol.* **5**, 334-337.

Yaffe D. (1968) Retention of differentiation potentialities during prolonged cultivation of myogenic cells. *Proc Natl Acad Sci U S A.* **61**, 477-483.

Yang L., Guan T., and Gerace L. (1997) Lamin-binding fragment of LAP2 inhibits increase in nuclear volume during the cell cycle and progression into S phase. *J Cell Biol.* **139**, 1077-1087.

Ye Q. and Worman H. J. (1996) Interaction between an integral protein of the nuclear envelope inner membrane and human chromodomain proteins homologous to Drosophila HP1. *J Biol Chem.* **271**, 14653-14656.

Yen A. and Pardee A. B. (1979) Role of nuclear size in cell growth initiation. *Science.* **204**, 1315-1317.

Yost H. J. and Lindquist S. (1986) RNA splicing is interrupted by heat shock and is rescued by heat shock protein synthesis. *Cell.* **45**, 185-193.

Zhu W. G., Roberts Z. V., and Dynlacht J. R. (1999) Heat-induced modulation of lamin B content in two different cell lines. *J Cell Biochem.* **75**, 620-628.